UNIVERSITY OF THE WITWATERSRAND
JOHANNESBURG

THE GEOLOGY, PETROLOGY, AND GEOCHEMISTRY OF THE BUSHVELD GRANITES AND FELSITES IN THE POTGIETERSRUS TIN-FIELD

by

the late D.H. LENTHALL
(formerly Research Fellow, Economic Geology Research Unit)

and

D.R. HUNTER
(formerly Senior Research Fellow, Economic Geology Research Unit)

ECONOMIC GEOLOGY RESEARCH UNIT

INFORMATION CIRCULAR No. 110

May, 1977

THE GEOLOGY, PETROLOGY, AND GEOCHEMISTRY OF THE BUSHVELD GRANITES AND FELSITES IN THE POTGIETERSRUS TIN-FIELD

ABSTRACT

An area of 324 km^2 was selected for a pilot-study of the geochemical characteristics of the salic phase of the Bushveld Complex, based on the sampling of a regular grid of stations. Two hundred and sixty-nine sample sites were established. At ten of these sites, additional samples were collected to test the variance about sample stations.

Variances of La, Sc, and Zn, in particular, tend to be as great, or greater, on the local, as compared to the regional, scale. Despite these variances, it is valid to conclude that the distinctions in geochemistry between the stratiform granites, Bobbejaankop granites, and felsites are real in respect to the other elements.

Trace elements for which analytical data are available are Ba, Ce, Co, La, Li, Nb, Ni, Rb, Sc, Sn, Sr, Ti, Y, Zn, and Zr. The major elements Ca, Na, and K were also determined. Measurements of gamma-flux density in μr/hr were recorded in the field.

The stratiform granites in the Potgietersrus area have a mean concentration for these elements that compares closely with those in low-Ca granites. Differences exist in respect to Ce, La, Rb, Y, Zn, and Zr, which are relatively enriched, and to Sr which is impoverished. The apparently higher Ca content is due to the presence of fluorite. When corrections are made for Ca in this mineral, the stratiform and Bobbejaankop granites have a low Ca content available for the formation of feldspars and other primary minerals.

The felsites are distinguished from the stratiform granites by virtue of their higher concentrations of Ba, Co, Sc, Sr, Ti, and Zn and by their lower contents of La, Rb, Y, and K. The stanniferous Bobbejaankop granite is impoverished in Ba, Sr, Ti, Zn, and Zr, and considerably enriched in La, Nb, Rb, and Y. The median tin concentration in the felsites is <5 ppm, in the stratiform granites 6,5 ppm, and in the Bobbejaankop granite 9 ppm.

The stratiform granite sheet displays lithological variations from coarse-grained, mesocratic granite, at the base, through medium-grained, grey and red granites and fine-grained, red granophyric granites, to granophyre and feldspar porphyry, at the top. The stratiform granites intrude the Mafic Phase of the Bushveld Complex, below, and the Rooiberg felsites, above. Discordant stocks of Bobbejaankop granite intrude the stratiform granites.

It is considered that the red discoloration, the higher degree of Al/Si ordering in the alkali feldspars, the development of exsolution perthites, and the alteration of hornblende and biotite to chlorite in the stratiform granite close to the roof result from the presence of volatiles that carried with them any elements, e.g. Rb, Zn, Sn, incompatible within the lattices of crystallizing mineral phases, that accumulated with them. Where large volumes of volatiles collected in structural highs in the roof of the stratiform granite as a result of their migration down pressure and temperature gradients, the melting point of the magma was depressed below the ambient temperature, permitting re-mobilization and movement of the granite. The presence of excess volatiles did not permit the re-mobilized magma to move far vertically before the melting curve was re-crossed and the material solidified. The Bobbejaankop granite represents an example of such a concentration of volatiles. Where there was a lack of structural highs, the volatiles were more dispersed along the roof zone. Escape of the volatile phases took place where the roof-rocks were fractured, thereby giving rise to exogranitic mineralization.

* *

THE GEOLOGY, PETROLOGY, AND GEOCHEMISTRY OF THE BUSHVELD GRANITES AND FELSITES IN THE POTGIETERSRUS TIN-FIELD

Editorial Note

At the time of his death on 17 June, 1973, David H. Lenthall had completed the field and laboratory work that was to have provided the basis for his doctoral thesis. He had also prepared a draft outline of the thesis and had virtually finalized the major proportion of his conclusions. These had been briefly summarized in a paper he read at the Congress of the Geological Society of South Africa, held in April, 1973, in Bloemfontein. Using the analytical data, notes, and information contained in field-books, the editor has attempted to bring together the results of that part of the research carried out by Dave Lenthall in the Potgietersrus area, in keeping with the views he had expressed in personal discussions and in the draft of his thesis. Responsibility for the correctness of these conclusions and for any errors and omissions rests with the editor.

D.R. HUNTER

THE GEOLOGY, PETROLOGY, AND GEOCHEMISTRY OF THE BUSHVELD GRANITES AND FELSITES IN THE POTGIETERSRUS TIN-FIELD

CONTENTS

CONTENTS (Continued)

oOo

ISBN 0 85494 458 3

THE GEOLOGY, PETROLOGY, AND GEOCHEMISTRY OF THE BUSHVELD GRANITES AND FELSITES IN THE POTGIETERSRUS TIN-FIELD

INTRODUCTION

The Potgietersrus tin-field (see Figure 1) was selected as a suitable area for a pilot-study of the geochemistry of the Bushveld granites and the Rooiberg felsites. The area has been the subject of a number of geological investigations (Strauss and Truter, 1944; Söhnge, 1944; Strauss, 1954) that have provided a sound foundation for detailed study. Furthermore, within the 324 km^2 (27 km x 12 km) selected for the study, the felsic rocks outcrop prominently and display most of the range of textural variations that are found within the Bushveld Complex.

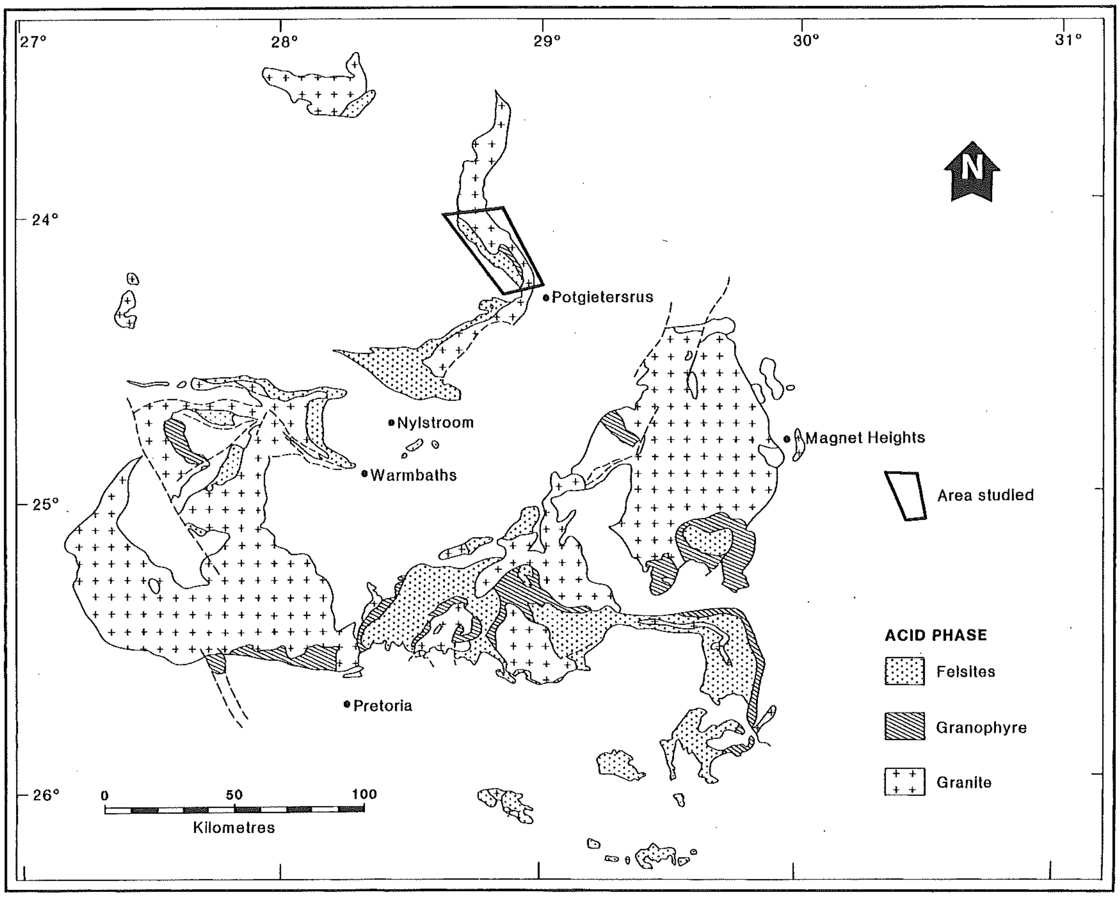

Figure 1 : *Location of area studied*

The Bushveld granites and Rooiberg felsites in the Potgietersrus tin-field form the Makapansberg which builds a northwesterly-trending escarpment overlooking an undulating plain, which is underlain by mafic rocks of the Bushveld Complex and Archean granites, over which the Magalakwena river flows. The Makapansberg attains its maximum elevation west of Potgietersrus, 10 km south of the studied area, where it rises 610 m above the Magalakwena plain. The elevation of the range decreases gradually towards the northwest until it is represented by a series of isolated hills north of the Sterk river, beyond the northern boundary of the area studied. Further to the northwest, these low hills merge into a sandy undulating plain where outcrops of the felsic rocks are infrequent.

Overlying the Rooiberg felsites are arenaceous and argillaceous rocks of the Waterberg Sequence, the base of which transgresses on to successively lower members of the felsite pile, until it rests on the Bushveld granites, and, finally, 50 km north of the Sterk river, on the mafic rocks of the Bushveld Complex. The Waterberg rocks build the eastern escarpment of the great Palala plateau, diversified in the Potgietersrus tin-field by long dip-slopes. All the rock units (i.e. the Bushveld Complex, the Rooiberg felsites, and the Waterberg sedimentary rocks) dip at low angles towards the west.

Four varieties of granite have been recognized in this area (Strauss and Truter, 1944; Strauss, 1954) :

1. Main granite,
2. Foothills granite,
3. Bobbejaankop granite, and
4. Lease granite.

The Main granite displays a number of textural variations which are, in general, transitional and gradational into each other. It was demonstrated (Strauss and Truter, 1944; Strauss, 1954) that these textural varieties have a crude, stratiform arrangement, forming a sheet, approximately 2 750 m thick, intruded more-or-less concordantly between the overlying felsites and the underlying layered mafic sequence. Discontinuous lenses of metamorphosed sedimentary rocks of presumed Transvaal age outcrop along the interface between the Main granite and the mafic rocks. Diabase sheets intrude the granite, particularly in the southern half of the mapped area, and dykes of the same composition, as well as dolerites of post-Karroo age, cut the whole sequence of rock-types. Most dykes strike north-eastwards, but some strike eastwards.

The Foothills granite consists of sheet-like, slightly younger intrusions that cut the stratiform Main granite, being most prominent along the foothills of the Makapansberg, immediately overlying the mafic layered sequence.

The Bobbejaankop granite and its marginal facies, the Lease granite, build a small, discordant pluton intrusive into the stratiform Main granite. The eastern contact of the pluton is close to vertical, but, on the western flank, where the Lease granite is developed, the contact dips at a low angle towards the west.

On the basis of the results of the present mapping (Figure 2), the felsic rocks were subdivided into the following units, which are compared with those recognized by Strauss (1954) :

	Present Study	Strauss (1954)
(x)	Rooiberg felsites	Rooiberg felsites
(ix)	Feldspar porphyry	Granite porphyry; facies of Main granite
(viii)	Sterk River granophyre	Bushveld granophyre, in part; facies of Main granite
(vii)	Granophyric granite	Facies of Main granite
(vi)	Groenfontein granophyre	Bushveld granophyre, in part; facies of Main granite
(v)	Welgevonden granophyre	Bushveld granophyre, in part; facies of Main granite
(iv)	Coarse-grained granite	Facies of Main granite
(iii)	Aplite and porphyritic aplite	Foothills granite
(ii)	Bobbejaankop granite, including its finer-grained marginal facies	Bobbejaankop and Lease granites
(i)	Blinkwater granophyre	Pseudo-granophyre

Units (iv) to (ix) constitute the stratiform granite sheet.

The terms introduced in this tabulation are intended to assist description and do not necessarily represent a terminology that may be applied to the felsic rocks of the Bushveld Complex generally. During the course of the mapping, it was found that granophyric textures were developed in response to a number of processes. It was necessary to identify these different granophyric facies in order to relate any subtle geochemical differences in the analytical data to the geology. The Sterk River granophyre is an integral part of the stratiform granite sheet, whereas the Groenfontein granophyre refers to the granophyric texture superimposed on the stratiform granite marginal to the Bobbejaankop granite, as a consequence of the intrusion of this pluton. The Welgevonden granophyre has acquired its superimposed granophyric texture from the intrusion of diabase sheets. The Blinkwater granophyre is that granophyre developed in association with the meta-sediments at the top of the mafic layered sequence.

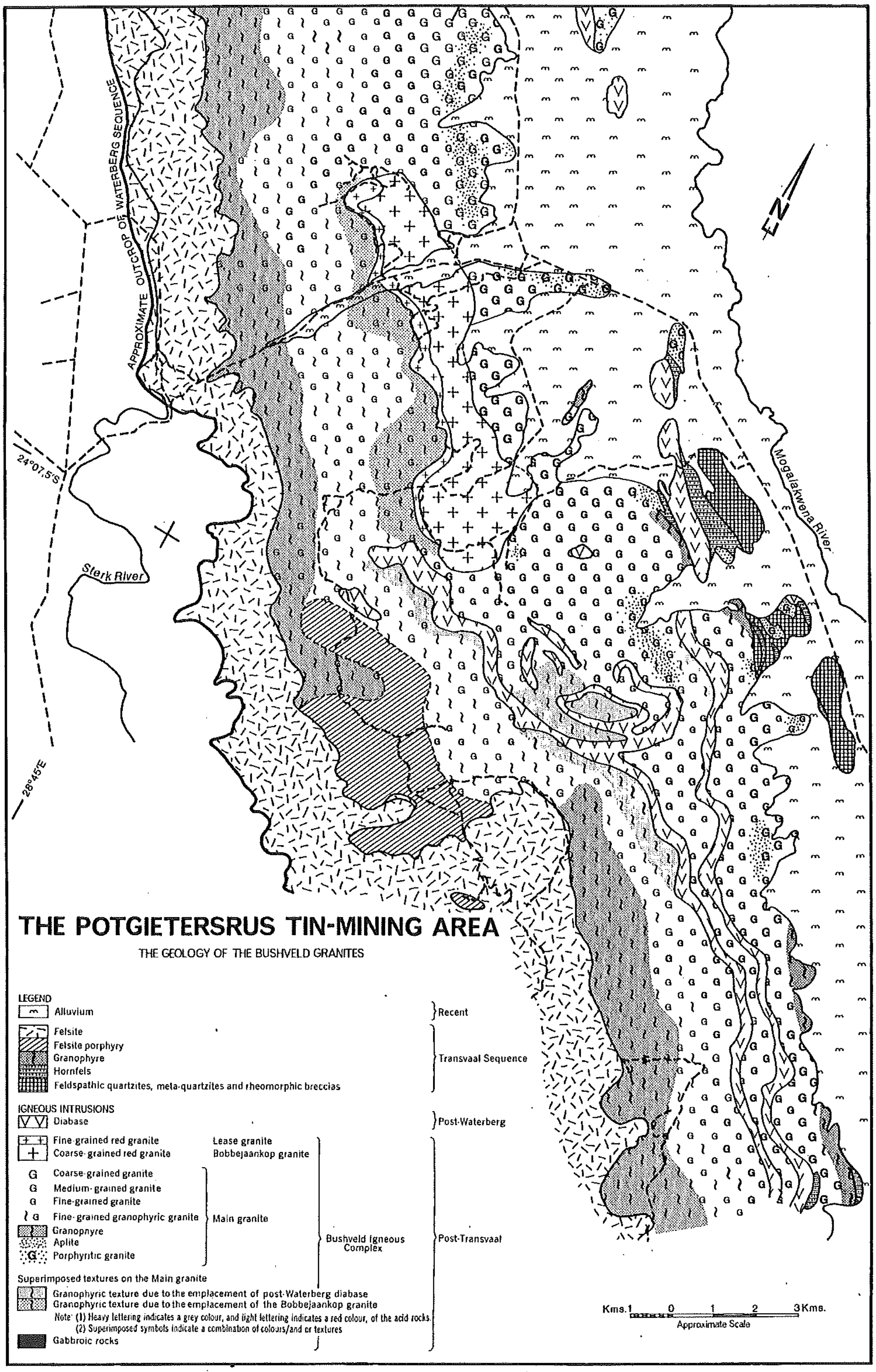

Figure 2 : *Generalized geological map of the Bushveld granites in the Potgietersrus-Zaaiplaats tin-mining area.*

PETROLOGY

(a) The Stratiform Granite

In the stratiform granite, the following unbroken transition of rock-types can be recognized from the base of the Makapansberg to the felsites :

1. coarse-grained, mesocratic, hornblende granite
2. medium- to coarse-grained, leucocratic, grey granite
3. leucocratic, equigranular, medium- to fine-grained, red granite
4. fine-grained, red, granophyric granite
5. granophyre (Sterk River-type) intrusive into the overlying felsites
6. feldspar porphyry forming a sheet between the granophyric granite and the felsites where the Sterk River granophyre is absent

In hand-specimen, the granite is devoid of any fabric and displays an equigranular, hypidiomorphic texture. Hornblende and biotite are abundant and constitute up to 15 per cent by volume of the granite in the coarser-grained varieties found at the base of the stratiform sheet. Feldspars are commonly euhedral and grey in colour, but isolated mantled feldspars, with cores of pink orthoclase rimmed by greenish-white albite, are encountered. In the more leucocratic, grey varieties of granite, the content of mafic minerals is less than 3 per cent by volume. Milky, grey quartz grains in both the lighter and darker granites are smaller in size and more anhedral than the feldspars in the same rock. On weathered surfaces, the quartz grains have a resinous, honey-brown colour that contrasts with the grey of the feldspars. At stratigraphically higher levels, the feldspars in the leucocratic granites gradually become brick-red in colour, imparting a reddish coloration to the rock as a whole. Concurrently, micropegmatitic intergrowths increase in abundance, thereby effecting the transition into granophyric granite. Where these intergrowths become the dominant constituent, the granophyric granite grades into granophyre. Mafic minerals in the granophyric granite and granite are extensively altered to chlorite.

In addition to the gradational textural changes described above, granophyric intergrowths are found in the leucocratic grey granite adjacent to the Bobbejaankop granite pluton and intrusive diabase sheets.

The characteristic feature in thin-sections of the coarse-grained granite is the ubiquitous presence of turbid feldspars; clear, unaltered plagioclase and orthoclase grains are exceptional. The typical granite is composed of quartz, microperthitic orthoclase, plagioclase, hornblende, and biotite. Accessory minerals are zircon, fluorite, apatite, sphene, epidote, hematite, and magnetite. Alteration of the primary minerals results in the formation of biotite, chlorite, saussurite, epidote, and fine aggregates of clay minerals.

Quartz, which forms approximately 25 per cent by volume of the granite, appears to have had a prolonged crystallization history. Early-formed quartz is found as equant, anhedral grains which interlock with one another in a complex manner. These grains usually display uniform extinction, although individual grains having undulose extinction are also present. Strained quartz grains occur randomly throughout the granite, and frequently they contain minute, crystallographically-controlled fractures that are occupied by secondary minerals. Strings of small, almost submicroscopic bubbles are common in quartz grains of the early generation. Similar bubbles are present also in later-formed quartz, but they are considerably less abundant.

Potassium feldspar embays the early-formed quartz grains, giving rise to complex mutual relationships. In extreme cases, isolated quartz grains in optical continuity with the parent quartz occur as remnants in the feldspar. The complexly-sutured boundaries between quartz and plagioclase (oligoclase) suggest that these two minerals crystallized simultaneously.

Quartz of a later generation appears to have crystallized together with the potassium feldspar, along the boundaries of, or within interstices between, earlier-formed minerals, giving rise to crude, granophyric intergrowths. Occasionally, quartz was observed as lens-shaped grains along the cleavage planes in biotite flakes. The position of this quartz in the crystallization history of the granite is uncertain.

Feldspars are the most important component of the granites, constituting between 60 and 70 per cent by volume. The feldspars are normally grey, but, in the vicinity of faults or in proximity to later intrusives, they become red due to the presence of fine hematitic dust. Orthoclase is consistently more abundant than plagioclase; however, subtle variations in the proportions of the two feldspars do exist. In the darker-coloured varieties of granite, plagioclase attains its maximum abundance, gradually decreasing in amount in the stratigraphically higher, more leucocratic granites. X-ray-diffraction studies of the potassium feldspars reveal that the most common type is poorly-ordered monoclinic orthoclase that has a tendency to better ordering towards the roof of the intrusive sheet.

Orthoclase of more than one generation can be recognized. Early-formed orthoclase occurs as subhedral to anhedral grains up to 5 mm in diameter. Without exception, early orthoclase is microperthitic. Delicate, film and coarser, vein perthite are both present, the clear albite of the perthites contrasting with the turbid orthoclase. The coarse, vein perthite tends to become more irregular in shape with increasing turbidity in the host.

Towards the final stages of crystallization, orthoclase and quartz were virtually the only minerals to form. Late orthoclase is found in replacement veinlets in plagioclase, within interstices, and as irregularly-shaped grains. In general, late orthoclase is less turbid and microperthitic than its earlier counterpart. Embayment and replacement of previously-crystallized minerals by late orthoclase produces the involved relationships described above. Plagioclase being replaced by orthoclase is often more saussuritized than that which is not affected by replacement. Narrow, clear, albitic rims may develop in association with the replacement.

Orthoclase of both early and late generations displays varying degrees of alteration. In extreme cases, the turbidity becomes so intense that the feldspar is nearly opaque. Before this stage is reached, small flakes of white mica in the orthoclase mark the onset of sericitization which precedes the exsolution of iron, the oxidation of which causes the turbid appearance of the feldspar.

Plagioclase grains are always subhedral to anhedral, having an average diameter of 3 mm. Complexly-sutured boundaries between plagioclase and the early generation of quartz and orthoclase become progressively more involved where embayment and replacement by later-crystallizing minerals (notably quartz and orthoclase) have taken place. Plagioclase grains are twinned, dominantly according to the albite and Carlsbad-albite laws; pericline twinning, although subordinate, is not uncommon. The composition of the plagioclase is consistent - and average An content of 28 was obtained in all thin-sections that were examined.

Saussuritization is common, particularly where later minerals are embaying and replacing the plagioclase, clear albite rims being developed in company with this alteration.

<u>Mafic minerals</u> are not abundant, except in the basal part of the stratiform granite sheet. Brown biotite and green hornblende are the most common, primary, mafic silicates; some pyroxene has, however, been observed in mesocratic varieties near the base of the sheet. Hornblende predominates in the darker-coloured granites, locally constituting up to 15 per cent by volume of the rock, but more commonly averaging between 5 and 6 per cent by volume. Biotite, subordinate in the mesocratic granites to hornblende, is the dominant mafic mineral in the lighter-coloured granites.

Anhedral-to-subhedral hornblende is found as irregularly-shaped laths and as more equant basal sections. The latter exhibit extreme pleochroism from dark bottle-green to straw-yellow, while pleochroism in prismatic sections ranges from bright bottle-green, parallel to the cleavage traces, to olive-green. Individual hornblende grains are small and often occupy the interstices between larger grains of quartz and feldspar.

Hornblende is altered, wholly or partially, to clay minerals, biotite, and chlorite. The initial alteration-product is a green mica with high birefringence colours. This mica is altered, in turn, to penninite that displays the characteristic Berlin-blue interference colours. Minute granules of magnetite and quartz released during the alteration are scattered either through the secondary chlorite or around the original grain-boundaries, together with minor amounts of epidote. The final stage of alteration causes the break-down of the penninite to a honey-brown, micaceous, clay mineral.

Biotite, forming less than 3 per cent by volume of the rock, occurs as anhedral-to-subhedral flakes that commonly display partial chloritization. Pleochroism ranges from dark red-brown to bright bottle-green. Lens-shaped quartz and magnetite grains occupy cleavage planes in the biotite, distorting these planes as a result of their growth. Brown biotite alters to a green variety, and, with progressive alteration, micaceous minerals intermediate between chlorite and biotite are formed. A brown, micaceous, clay mineral is the final alteration product, in which are preserved lens-shaped aggregates of magnetite and quartz.

Diopsidic augite, partially replaced by hornblende, is found sparingly in the mesocratic granite at the base of the granite sheet.

Of the <u>accessory minerals</u>, fluorite is the most abundant, being encountered in every thin-section examined. Generally, the fluorite has a close spatial relationship to the mafic minerals, but isolated grains within quartz and feldspar mosaics are not uncommon.

Epidote and sphene tend to be more abundant in proximity to mafic minerals, the former being found most commonly near partially-altered hornblende laths. Zircon is present in small prismatic crystals, almost invariably doubly-terminated by well-formed, pyramidal faces.

(b) <u>Granophyric Granite</u>

The granophyric granite is transitional into leucocratic granite, below, and the Sterk River granophyre, above. In the field, an arbitary boundary between leucocratic and granophyric granite was taken where the first granophyric intergrowths could be observed by means of a hand-lens. The upper boundary was taken where such intergrowths constitute the entire rock.

In general, the granophyric granite is a fine- to medium-grained rock possessing an hypidiomorphic, granular texture. It is usually red in colour, but not uncommonly grey. Mafic minerals, of which chlorite is the most abundant, constitute between 2 and 5 per cent by volume. Long, accicular needles of hornblende are present occasionally.

As might be expected, the granophyric granite exhibits, in thin-section, characteristics of both the leucocratic granite and the granophyre. Typically, it is composed of microperthitic orthoclase, quartz, varying amounts of micropegmatite, minor plagioclase, biotite, and hornblende, the mafic minerals being extremely altered to chlorite. Accessory minerals include fluorite, epidote, apatite, sphene, magnetite, and hematite. In addition to chlorite, alteration-products are represented by saussurite, epidote, and micaceous, clay minerals.

Plagioclase grains are highly saussuritized and usually almost completely opaque, except for rims of clear albite. Individual grains may be lath-like or have complexly-sutured margins as a result of the interlocking mosaic with other minerals or of their embayment by orthoclase and quartz.

Orthoclase is found as subhedral grains and is granophyrically intergrown with quartz. Early-formed orthoclase commonly displays Carlsbad-twinning and is embayed by a later generation of quartz and orthoclase. In the initial stages of granophyric development, the quartz is irregular, both in shape and distribution, but becomes more regular as the abundance of micropegmatite increases. Fine intergrowths of quartz and orthoclase also develop around insets and, in the more granophyric granites, in isolation from the insets. The presence of fine, hematitic dust imparts a distinctive red coloration to the orthoclase, which is altered to sericite and, more infrequently, to a matt composed of micaceous, clay minerals.

The mafic minerals exhibit varying degrees of alteration. Remnant cores of hornblende are set in a chloritic matt. The pleochroism of hornblende is from light bottle-green to straw-yellow, the intensity of the colours being distinctly less than in the underlying, leucocratic, grey granite. Shredded flakes of biotite, pleochroic from pale-green to straw-yellow, are altered along the cleavage planes to chlorite with high birefringence colours. Penninite and matts of micaceous, clay minerals are the products of complete alteration of the mafic minerals. Some epidote is formed during the alteration of hornblende.

Fluorite is not as abundant in the granophyric granites as in the grey granites.

(c) Sterk River Granophyre and Feldspar Porphyry

Red, fine- to medium-grained granophyre or, locally, feldspar porphyry are found at the interface between the granitic rocks and the roof of felsites. Chloritization has bleached the red colour to buff in some places.

The granophyre exhibits a well-developed intergrowth between quartz and orthoclase throughout, with sparsely-distributed insets of quartz and feldspar. The former are fringed by radiating micropegmatitic intergrowths, and the plagioclase insets are so turbid that difficulty is experienced in determining their composition, which is probably close to oligoclase.

Intergrowths between quartz and orthoclase constitute between 90 and 95 per cent by volume of the rock. They develop as a result of, either the simultaneous crystallization of the two minerals, or the embayment of oligoclase by quartz. Hour-glass texture develops as a result of changes in the orientation of the intergrowths at the intersection of crystal faces normal to which the intergrowths are developed. Close to insets, the micropegmatite is fine-grained, often plumose, but it becomes progressively coarser-grained until, at the margin, the quartz forms bulbous heads. Where quartz builds the inset, the quartz of both the inset and the intergrowth are in optical continuity.

Micropegmatite formed by replacement of orthoclase by quartz is less abundant than that developed by simultaneous crystallization. Quartz has an irregular, cuneiform shape, and individual blebs of quartz within a particular intergrowth are usually in optical continuity.

Granophyric intergrowths are normally finer in the immediate contact zone and become progressively coarser in grain-size in the stratigraphically-lower granophyres.

Biotite and hornblende, together constituting less than 1 per cent by volume of the granophyre, are found as occasional remnants set in a chloritic and micaceous, phyllosilicate matt. Rosettes of penninite form irregular aggregates, sometimes with shreds of biotite preserved. Accessory minerals are not abundant in the granophyre; fluorite, sphene, apatite, and zircon are found sparingly, and clusters of magnetite grains are spread evenly through the rock.

The feldspar porphyry is a fine-grained rock with prominent insets of quartz and feldspar set in a dense, almost felsitic matrix that is red or greenish-grey in colour. The euhedral insets of quartz and turbid feldspar, largely oligoclase, are surrounded by spherulitic mantles of orthoclase arranged in fan-shapes around the insets which are embayed by the enclosing orthoclase. The fine-grained matrix is composed of quartz, feldspar, magnetite, and chlorite, the last-mentioned being most abundant in the darker-coloured porphyries.

(d) Aplitic and Porphyritic Aplitic Granite

Aplitic phases within the stratiform granite belong to two types. Irregular, nebulitic, aplitic patches contrast with those aplitic granites that build sharply-defined, sill- or dyke-like bodies, which, in general, dip conformably with the layering of the stratiform granite. In thin-section, the aplites resemble closely the medium- and coarse-grained granites, except in grain-size.

(e) Superimposed Granophyric Textures

Granophyric textures are developed in the leucocratic, medium-to-coarse-grained granites adjacent to intrusive plutons of Bobbejaankop granite and sheets of diabase. The abundance of granophyric intergrowths is greatest in the immediate contact zones of these intrusives and decreases gradually so that there is a progressive transition into normal granite. As a result of this gradation, an arbitrary limit to the extent of the superimposed Groenfontein and Welgevonden granophyric facies was made where no granophyric intergrowths could be observed with the aid of a hand-lens. The Groenfontein granophyre is confined to the upper, shallow-dipping contact of the Bobbejaankop granite, and, on the basis defined above, extends for distances ranging from several hundred to 1 500 metres from the contact. Maximum development of superimposed granophyric intergrowth in the stratiform granite coincides approximately with areas of economic tin mineralization in the Bobbejaankop granite. The Welgevonden granophyre is more restricted in its extent, due partly to the smaller size of the diabase sheets and to the fact that the sheets are found mainly along the steepest portion of the Makapansberg escarpment. Granophyric intergrowths of this type are developed both above and below the diabase sheets.

The micropegmatitic intergrowths result almost exclusively from the replacement of the feldspars by quartz, which forms irregular elongate and vermicular blebs or crudely-cuneiform shapes. Individual grains of quartz within a particular intergrowth are rarely in optical continuity.

(f) Blinkwater Granophyre

Outcrops of granophyre are associated with the metamorphosed sedimentary and/or volcanic rocks that occupy the interface between the granites and the layered mafic rocks. This granophyre has been described by Strauss (1954) and interpreted by him as the product of the complete reconstitution of quartzo-feldspathic sediments. It is still uncertain in the Potgietersrus tin-field whether the Blinkwater granophyre was formed as a response to the intrusion of the granites or of the layered mafic rocks. The fact that the granites have almost invariably sharp contacts with the Blinkwater granophyre does not necessarily prove that it did not develop as a result of emplacement of the granite.

(g) Bobbejaankop Granite

Strauss (1954) recognized three outcrops of this granite in the Potgietersrus tin-field, but only the southernmost and economically most important of these falls within the area covered by the present study. The largest outcrop of Bobbejaankop granite is the most northerly and is associated with deposits of cassiterite and molybdenite which are no longer being actively exploited.

The elongate body of Bobbejaankop granite that outcrops within the area of this study intrudes the coarse-grained, stratiform granites. Along its eastern margin, the contact with these granites is vertical or steeply inclined towards the northeast. This contact is not always clear in the field, as the leucocratic granites often take on a reddish hue, but, from a distance, the bald domes of Bobbejaankop granite contrast with the piles of scattered boulders that are more typical of the leucocratic granites. Coarse pegmatite is developed along the western contact of the Bobbejaankop pluton.

The Bobbejaankop granite is a coarse-grained, red rock composed of quartz and feldspars with variable amounts of chlorite and, less frequently, biotite. The Bobbejaankop granite can be distinguished from red varieties of the stratiform granites by virtue of its texture and the dull, earthy appearance of its feldspars. Mairolitic cavities and small clusters of tourmaline crystals are prominent in many outcrops, but it is the strings of quartz grains, prominent on weathered surfaces, that serve to distinguish the Bobbejaankop granite. Whereas in the stratiform granites, the quartz and feldspar form a complexly-interlocking mosaic, the quartz grains in the Bobbejaankop granite tend to coalesce to build discrete strings of grains. This feature is confirmed in those sections where it can be seen that the quartz grains are segregated from the turbid feldspars that are usually replaced by chlorite. Larger flakes of chlorite derived from the alteration of biotite are also present. Accessory minerals include fluorite, magnetite, and zircon.

The Bobbejaankop granite along the western flank of the pluton includes pegmatitic phases associated with a finer-grained granite. Alternations of layers of quartz and microcline impart a banded appearance that is enhanced by elongated vugs parallel to the layering. Sulphides and quartz and carbonate crystals line some of these vugs.

X-RAY-DIFFRACTION STUDIES OF THE ALKALI FELDSPARS

The separation of the 131 and $1\bar{3}1$ reflections was measured on forty-eight potassium feldspars, using filtered copper radiation.

Vorma (1971) tentatively recognized eight reflection or structural types as follows :

I. Orthoclase only

I/II. Orthoclase with subordinate high microcline

II. Orthoclase with high microcline, or only high microcline

II/III. Orthoclase with subordinate intermediate microcline

III. Orthoclase with intermediate microclinic (single unresolved peak)

IV. Orthoclase with intermediate microcline (three peaks)

III/V. Nearly maximum microcline or intermediate microcline with subordinate orthoclase or high microcline

V. Intermediate microcline or maximum microcline only

The patterns obtained from the granitic rocks in the Potgietersrus tin-field can be related to those classified by Vorma (1971). The results are summarized in Table I.

The following features are apparent from the distribution of the various structural types :

(i) The coarse-grained granites at the base of the stratiform sheet are characterized by orthoclase with intermediate microcline reflecting a moderately high thermal state.

(ii) There is a tendency for the alkali feldspar in the granites to achieve higher-order states at stratigraphically-higher levels.

(iii) The granophyric granites are characterized by intermediate microcline with subordinate orthoclase, i.e. a low or moderately low thermal state.

(iv) Whereas the alkali feldspar in the granophyre adjacent to the Bobbejaankop granite has a low thermal state, that in the Welgevonden granophyre adjacent to the diabase sheets apparently has a higher thermal state.

(v) The alkali feldspars in the Bobbejaankop granite are intermediate or maximum microcline only.

Obliquity values of potassium feldspars are influenced by temperature, the amount of Ab in solid solution, volatile content, stress, post-magmatic hydrothermal solutions, cooling rate, and the structural state of the associated feldspars. The obliquity values obtained from the finer-grained and, hence presumably, more rapidly-cooled granitic rocks can be attributed most probably to the presence of a higher content of volatiles in the roof of the intrusion, as reflected by the high fluorine content of the granophyric granites. In the absence of additional data concerning the amount of Ab in solid solution and of evidence for deformation, it is concluded that the presence of volatiles, a slower cooling rate, and possibly lower temperature influenced the higher degree of ordering in the alkali feldspars of the Bobbejaankop granite.

JOINT AND FRACTURE DENSITY

The relative frequencies of joint directions, based on measurements recorded at sample stations in the studied area, are shown in Figure 3. Three groups of directions dominate the pattern :

Group I	(a)	N 20°
	(b)	N 35°
Group II	(a)	N 95°
	(b)	N115°
Group III	(a)	N150°
	(b)	N160°

Less abundant joint directions trend N 0°, N 45°, and N 70°. The ten main joint trends are listed below, together with the features that are coincident with these directions, both in the Zaaiplaats area and within the Bushveld Complex as a whole.

TABLE I : Structural States and Obliquities of Potassium Feldspars

Sample No.	*Structural State*	*Obliquity Values*
	Coarse-grained Grey Granite	
A2	III	-
C2	III and IV	-
G2	III	-
H1	III	-
H3	III/V	0,754
I6	III/V	0,658
J2	III	-
J8	III/V	0,651
J11	III	-
M12	III/V	0,534
O1	III	-
O2	III	-
O3	III	-
O4	IV	0,606
T7	V	0,730
U3	V	0,771
	Granophyric Granite	
B5	V	0,830
D9	V	0,774
G6	V	0,771
M11	III/V	0,653
N9	III/V	0,675
N11	V	0,725
O6	III	-
R6	III/V	0,701
F8	III/V	0,723
F9	III/V	0,794
	Granophyre Beneath Felsites (Sterk-River-Type)	
B8	III/V	-
F10	III/V	0,735
F11	V	0,734
K12	V	0,775
K13	III/V	0,627
N8	V	0,705
O7	III	-
S8	III/V	0,676
	Granophyre Adjacent to Bobbejaankop Granite (Groenfontein-Type)	
F6	V	0,806
F7	V	0,845
	Granophyre Adjacent to Diabase Sheet (Welgevonden-Type)	
O5	III	-

TABLE I : Structural States and Obliquities of Potassium Felspars (Continued)

Sample No.	*Structural State*	*Obliquity Values*
	Aplitic Granite	
A3	III	-
E4	III	-
F1	III	-
K5	III	-
O2A	III/V	0,775
	Bobbejaankop Granite	
D4	V	0,771
D5	V	0,871
I10	V	0,801
J10A	V	0,730
F4	V	0,876
	Felsite	
O8	III	-

N 0° : minor post-Waterberg dyke direction; direction of elongation of northern (Appingamdam) stock of Bobbejaankop granite.

N 20° : post-Karroo dyke direction in granitic basement east of Zaaiplaats; ALNS stope fissure direction at Zaaiplaats mine.

N 35° : minor post-Karroo dyke direction; Dam fissure at Zaaiplaats mine strikes between N 30° and N 65°.

N 45° : prominent direction on satellite imagery; post-Karroo fault direction in Springbok Flats.

N 55° : prominent dyke direction in map area.

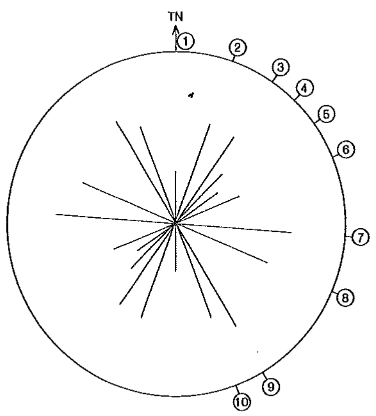

Figure 3 : *Frequency plot of joint directions in all rock-types*

N 70° : parallel to Murchison trend; strike of fold axes in Transvaal Supergroup rocks in Mhlapitsi fold-belt, axes of flexure of strike of Waterberg beds adjacent to map-area; post-Karroo fault direction in Springbok Flats.

N 95° : strike of monoclinal fold axes in Waterberg beds along southern margin of Palala plateau.

N 115° : direction of post-Waterberg dykes and faults on Palala plateau; ore shoots at Zaaiplaats mine plunge N 285°-290°.

N 150° : direction of elongation of Bobbejaankop granite outcrop in map-area; prominent direction on satellite imagery, particularly on Sekhukhuni plateau; direction of Adit fissure at Zaaiplaats mine; strike of Rustenburg fault.

N 160° : prominent joint direction in map-area; close to prominent joint direction (N 163°) in Bushveld rocks west of Pilanesberg, western Bushveld.

In the Zebedelia area, lying to the southeast of Zaaiplaats, Pretorius (1970) reported the dominant joint directions, in order of decreasing abundance, to be N 155°, N 70°, N 100°, N 45°, and N 20°. At the Union tin mine, joints striking N 22°, N 60°, and N 154° are prominent (Menge, 1963). The joint directions recorded in the map-area are coincident with those reported regionally throughout the Bushveld Complex.

In Figure 4, fracture density is recorded. The Bobbejaankop granite stock is approximately defined by the greatest density of fractures, but it is noteworthy that the main locus of mineralization (i.e. the Zaaiplaats mine) lies on the flank of the peak concentration. Scattered Zn and Sn, near to which are found higher concentrations of Li and La, are found in the area of higher fracture density south of the Bobbejaankop granite stock. The data are not sufficient to demonstrate that these abherrant values are directly related to fracturing, but it is suggested that concentration of fractures may provide targets for exploration. It would appear, however, that there is a lack of consistent association between fracture density and mineralization. No unusually high contents of elements that might be expected to be associated with volatiles have been reported from the extreme southern part of the map-area, despite a high fracture density.

GEOCHEMISTRY

(a) Sampling Method and Sample Preparation

The granites, granophyres, and felsites in the study area were sampled at approximately 0,75 km intervals along 21 traverse lines spaced about 1 km apart, with the result that 269 samples were collected. Traverse lines were oriented at right-angles to the general strike of the stratiform granite sheet and the overlying felsites (for key to sample stations see Figure 56 in Appendix II).

At each sample station, the following were measured in the field :

(i) total gamma flux density, using a portable scintillometer of Type NE 148A,

(ii) average grain-size of the feldspar, using a transparent graduated grid,

(iii) the proportion of mafic minerals, estimated visually, and

(iv) the barometric height in metres above the base-station established at the farmhouse immediately south of Sample Station I 1.

Duplicate samples were collected at six sample stations (A2, B9, D4, G13, N11, and S2) and submitted as hidden duplicates, for the purpose of checking analytical precision. Thus, the total number of samples analyzed amounted to 275. At each of six sample stations (C6, E4, H5, J10A, J17, and K14), suites comprising ten additional samples were collected at a radius of 5 m from the original sample station (except stations C6 and H5, where nine samples were collected about each station). Fresh material was collected at each sample station, but microscopic examination revealed that all the samples displayed varying degrees of alteration, such as saussuritization and/or sericitization. Primary crushing of the original samples, which weighed between 4 and 6 kg after the removal of any weathered material, was carried out in a jaw crusher and was followed by fine-grinding to -200 mesh in two stages, using a Siebtechnick pulverising apparatus with an agate-lined vessel and rings.

General Superintendence Co. (S.A.) (Pty.) Ltd. prepared pressed powder pellets for X-ray fluorescence determination of Ba, Ca, Co, La, Sc, Sn, Ti, Zn, and Zr. These pellets were subsequently also used for the determination of K_2O, Rb, and Sr. The National Institute of Metallurgy, Johannesburg, prepared a second set of pressed powder pellets for the determination of Na_2O.

The pressed powder pellets were made by General Superintendence Co. (S.A.) (Pty.) Ltd. from ten grams of sample powder mixed with 5 ml of a 3 per cent solution of perspex in acetone. The powder

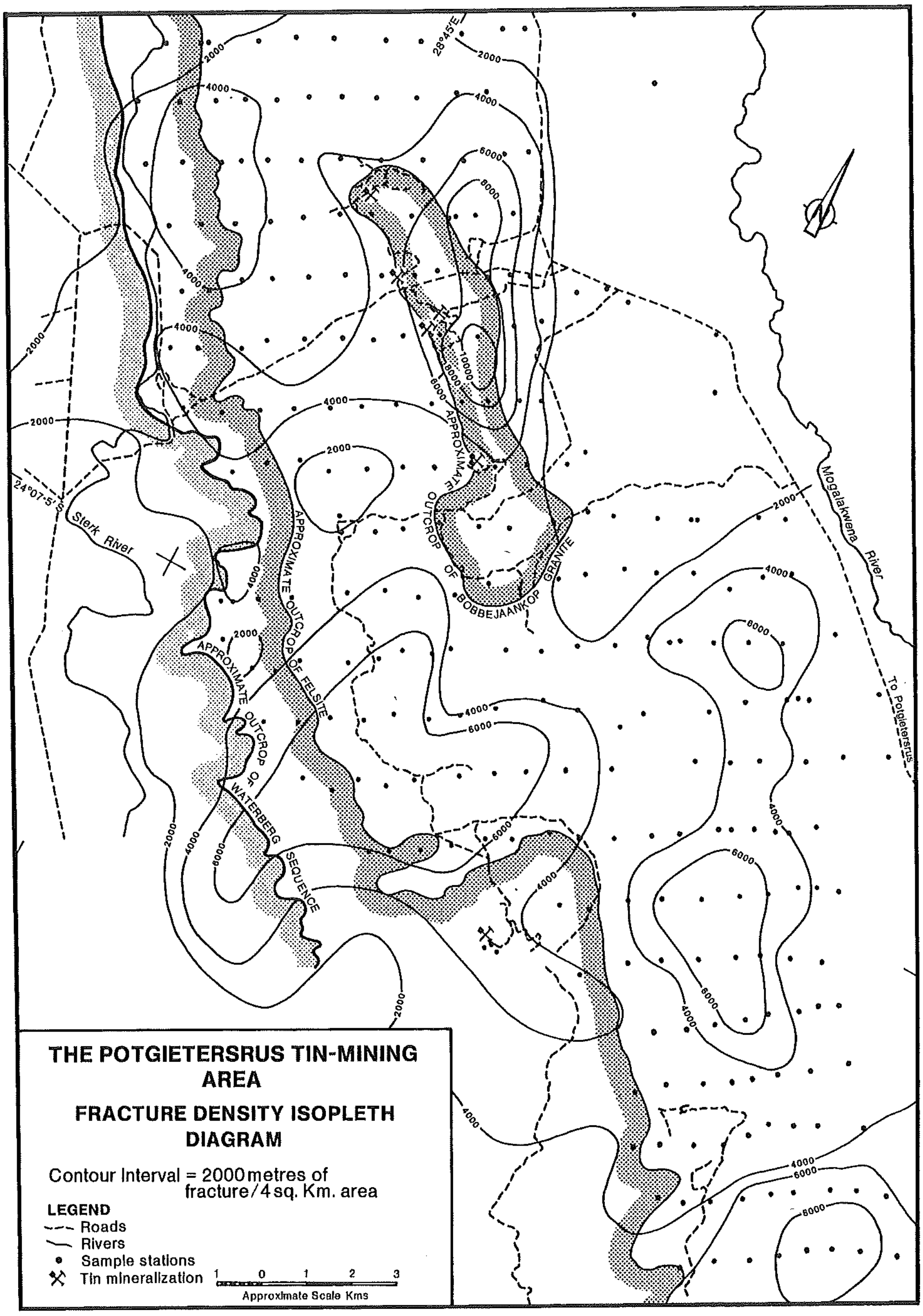

Figure 4 : *Isopleth map of fracture densities in all rock-types.*

was allowed to dry and then pressed in an aluminium cup at 15 x 10^3 kg pressure. The sample powders supplied to the National Institute of Metallurgy were re-milled in a Siebtechnick pulverizing apparatux, with a stainless steel vessel and rings, to -325 mesh. The bonding agent was a 5 per cent solution of ethyl cellulose in acetone, and, thereafter, the powder was pressed in the same manner.

The suites of samples collected about the 6 sample stations, together with a portion of the sample from the original station, were submitted to Dr. G. Hornung of the University of Leeds, who determined the contents of Ba, Ce, Co, La, Ni, Nb, Rb, Sc, Sn, Sr, Ti, Y, Zn, and Zr in each of the samples (see Appendix III). Duplicates from 21 sample stations were also analyzed by Dr. Hornung for the same elements (see Appendix IV).

Dr. D. M. Bibby, of the Nuclear Physics Research Unit of the University of the Witwatersrand, employed neutron activation analytical techniques to determine the fluorine content of twenty samples, but the results of these analyses must be regarded as provisional at this stage (see Appendix V).

Details of the instrumental conditions and standards used are given in Appendix I.

(b) Analytical Precision

Through the cooperation of Dr. G. Hornung, it was possible to obtain additional analytical data on selected samples. Dr. Hornung also analyzed these samples for elements that had been determined by General Superintendence Co. (S.A.) (Pty.) Ltd. It should be emphasized that submission of the duplicates to Dr. Hornung was not primarily intended as a test of analytical precision.

In Table II, the arithmetic mean contents of the common elements determined in three laboratories are compared. With the exception of Co, the results demonstrate a high degree of concordance.

Fourie (1969) analyzed samples of felsite and granite from the Potgietersrus tin-field using neutron activation techniques, and in Table III his mean values are compared with those obtained in Johannesburg and Leeds. Two factors must be remembered in making comparisons; firstly, the considerably greater number of samples analyzed in Johannesburg, and, secondly, the majority of Fourie's samples of stratiform granite were collected from the immediate vicinity of Bobbejaankop granite plutons. Despite these constraints, the mean values are in close accord, with the exception of Ce and Zn. Both these elements have highly erratic distributions, which might account for the differences, although the discordance between the Ce values cannot be wholly attributed to this factor. Ba, Sn, and Nb contents in the Bobbejaankop granite show moderately large differences between the different laboratories. This granite is distinguished by the very erratic behavior of these elements, and the differences reported in Table III are considered to be a reflection of the problems of sampling. The closer correspondence of the Co analyses reported by Fourie (1969) and Leeds implies that the Johannesburg results are an order of magnitude too high.

The close agreement that is evident in Table II and III, derived as they are from separate laboratories, using different techniques, supports the contention that the reported elemental contents reflect an accurate measure of their distribution in the various acid rocks and that conclusions drawn from these data are valid.

(c) Variation about Sample Stations

In order to test the validity of any differences in geochemistry that might exist between the various granites and felsites, additional samples were collected about selected sample stations on the original grid. It follows that, if significant variation is found about a sample station, the regional variation could be accounted for by sample inhomogeneity. In Table IV, the mean values, standard deviations, and the coefficients of variance, expressed as a percentage are given, and compared to the same parameters derived from the regional sampling.

Sampling about a sample station within the granite and its various granophyric modifications reveals that La, Sc, and Zn can vary locally to an equal or greater degree than the regional variance. The feldspar porphyry reflects a similar variation in respect to Ba, Co, and Sr, in addition to La, Sc, and Zn. It is worth noting that, because the sizes of the sample populations on both local and regional scales are closely similar, in the case of the feldspar porphyry, comparisons of local and regional variation are more valid than in the other rock-types. The felsites likewise display considerable local variations in Co, Sc, and Sn, whereas on a regional scale, Rb, Sr, and Zn also show considerable variance.

Despite the variances noted in Table IV, it is, however, valid to conclude that the distinctions in geochemistry between the stratiform granites, the Bobbejaankop granite, and the felsites are real in respect to Ba, Rb, Sr, Ti, and Zn and that they are not the result of sample inhomogeneity. This confirms the results previously obtained from applying discriminatory and cluster

TABLE II : Comparison of Analytical Results on Duplicate Samples

(a) *Coarse- to medium-grained granites (mean of 5 samples)*

	Ba	Co	La	Rb	Sc	Sn	Sr	Zn	Zr
L	850	3	81	226	1,4	7	36	96	382
J	867	12,5	103	206	3	6	35	94	435

(b) *Granophyric granites (mean of 4 samples)*

	Ba	Co	La	Rb	Sc	Sn	Sr	Zn	Zr
L	809	2	87,5	244	1,5	12,5	19	107	401
J	822	12	108	227	2	11	19,5	99	412

(c) *Sterk River granophyre (1 sample)*

	Ba	Co	La	Rb	Sc	Sn	Sr	Zn	Zr
L	654	3	111	237	0	7	18	145	301
J	720	13	149	233	2	5	18	153	371

(d) *Feldspar porphyry (mean of 2 samples)*

	Ba	Co	La	Rb	Sc	Sn	Sr	Zn	Zr
L	950	3	112	244	0,5	10	22	91	416
J	876	11	178	214	3	6	22	70	453

(e) *Bobbejaankop granite (mean of 5 samples)*

	Ba	Co	La	Rb	Sc	Sn	Sr	Zn	Zr
L	208	2	75	422	3	262	6	36	306
J	259	8	86	403	5	376	8	30	316

(f) *Felsite (mean of 4 samples)*

	Ba	Co	La	Rb	Sc	Sn	Sr	Zn	Zr
L	1017	4	69	228	6	9	67	135	435
J	1063	27	89	228	9	7	69	121	429

L = University of Leeds; J = General Superintendence Co. (Pty.) Ltd., and the writer.

analysis to the data (Lenthall, 1972). In this connection, it should be noted that the Ba contents given here differ from those in Lenthall (1972). The original analytical results were re-checked and found to give values that were significantly too high. The corrected means for the thirteen clustered families are given below :

Cluster	Mean Ba (ppm)	Cluster	Mean Ba (ppm)
1	1 281	8	2 269,5
2	813	9	1 120
3	734	10	1 067
4	733	11	1 054
5	222	12	621,5
6	220	13	279
7	381		

Clusters 1 to 4, 8, and 12 comprise the stratiform granite and its textural varieties; clusters 5 to 7 comprise the Bobbejaaniop granite; and clusters 9, 10, 11, and 13 comprise felsites, of which only one sample, depleted in both Na and K, constitutes cluster 13.

Despite the limited number of samples collected regionally from the Groenfontein and Welgevonden granophyres, which results in the regional sample population being smaller than that from about the sample stations, the variance is greater on a regional scale than it is about the individual stations. Only La in the Welgevonden granophyre is more variably distributed on the local scale than it is regionally.

The comparison of the variance in the aplitic and porphyritic aplitic granites on local and regional scales is included in Table IV. The known separation of these rock-types into at least two distinct groups militates against direct comparison between local and regional variance. The samples

TABLE III : Comparison of Mean Compositions of Felsites and Granites

	Felsites			Stratiform Granites			Bobbejaankop Granite		
	F	L	J	F	L	J	F	L	J
Ba	1 145	1 002	1 105	796	776	896	338	198	220
Ca	5 779	-	7 366	4 053	-	5 113	7 848	-	8 686
Ce	104	236	-	135	269	-	153	256	-
Co	4	5.7	28	1	2	11	1	2	9
La	57	70	72	80.5	83	100	92	91	118
Nb	18	18	-	23	24	-	48	83	-
Rb	231	233	176	278	243	225	523	434	408
Sc	7	6	10	1	1	3	1	2	3
Sn	10	9	7	18	9	8.5	23	131	123
Sr	60	69	70	35	26	39	6	6	7
Ti	2 155	-	2 337	1 132	-	1 173	399	-	393
Zn	334	131	175	114	99	91	62	33	26
Zr	381	437	395	362	365	433	260	289	328
K_2O%	4.16	-	4.49	4.98	-	4.91	4.85	-	4.86
Na_2O%	2.83	-	2.47	2.90	-	3.05	2.87	-	2.87
No. of Samples	5	4	37	10	16	209	17	5	17

F = Fourie (1969); L = University of Leeds; J = General Superintendence Co. (Pty.) Ltd., the writer, and National Institute for Metallurgy.

The stratiform granites include granites, granophyric granites and feldspar porphyry.

---

about Station E4 reflect the local variances of the more fractionated variety of porphyritic granites. These variances are of the same order of magnitude as in the other rock-types. It is concluded that the known sample inhomogeneity accounts for the large regional variance and that there is, within the aplitic and porphyritic aplitic granites, populations that have significantly distinct geochemical characteristics.

(d) The Geochemical Data

Goldschmidt (1937 , 1944) made important contributions to the recognition of laws that govern abundances and distributions of elements in rocks and minerals. He recognized that, in general terms,

(i) 'camouflage' will occur between two elements similar in size with the same valency,

(ii) 'capture' of a trace element in a major element lattice site occurs when the trace element is smaller in size but of higher valency, and

(iii) 'admission' is the reverse effect of capture.

Subsequent investigations confirm the general correctness of Goldschmidt's Rules, but, as more data became available, an increasing number of anomalies were revealed. The nature of the chemical bond was considered to be an additional factor that influenced the behavior of elements. More recently, the relative abundances and distributions of trace elements have been discussed in terms of partitioning theory, which has the advantage of testing quantitatively the validity of theories of magma generation and evolution. A lack of data on distribution coefficients in different phases of acid rocks places a constraint on the application of partitioning theory to these rocks at present. For ease

TABLE IV : Variance about Sample Stations Compared to the Regional Variance

(a) *Leucocratic coarse- to medium-grained granite*

(i) about station C6

	Ba	Co	La	Rb	Sc	Sn	Sr	Ti	Zn	Zr
$\bar{x}$	747	2,3	70	235	1,8	8	25	1276	122	371
σ	57,8	0,5	11,9	11,1	1,5	2,7	3,6	55,4	20,4	32,3
$\sigma/\bar{x}\%$	7,7	20,8	16,9	4,7	85,6	33,2	14,3	4,3	16,7	8,7

(ii) regional (88 samples)

	Ba	Co	La	Rb	Sc	Sn	Sr	Ti	Zn	Zr
$\bar{x}$	940	11	95	213,5	3,4	7	43	1165	89	428
σ	401,5	3,2	49,7	41,3	1,8	4,5	24,1	393,1	32,8	67,5
$\sigma/\bar{x}\%$	42	29	53	19	52	64	56	34	37	16

(b) *Granophyric granite*

(i) about station J14

	Ba	Co	La	Rb	Sc	Sn	Sr	Ti	Zn	Zr
$\bar{x}$	563	-	178	-	-	-	-	1126	42	357
σ	74,3	-	71,4	-	-	-	-	69,3	17,6	11,8
$\sigma/\bar{x}\%$	13,2	-	40,1	-	-	-	-	6,1	41,9	3,3

(ii) regional (43 samples)

	Ba	Co	La	Rb	Sc	Sn	Sr	Ti	Zn	Zr
$\bar{x}$	816	-	107	-	-	-	-	1142	97	417
σ	163,6	-	24,5	-	-	-	-	136,6	60,3	42,5
$\sigma/\bar{x}\%$	19	-	22	-	-	-	-	12	62	10

(c) *Sterk River granophyre*

(i) about station J16

	Ba	Co	La	Rb	Sc	Sn	Sr	Ti	Zn	Zr
$\bar{x}$	437	-	289	-	-	-	-	975	66	379
σ	77,2	-	296,8	-	-	-	-	29,2	22,8	20,2
$\sigma/\bar{x}\%$	15,3	-	102,7	-	-	-	-	3,3	34,5	5,3

(ii) regional (34 samples)

	Ba	Co	La	Rb	Sc	Sn	Sr	Ti	Zn	Zr
$\bar{x}$	899	-	112	-	-	-	-	1220	103	464
σ	269,8	-	30,3	-	-	-	-	227,5	44,1	57,6
$\sigma/\bar{x}\%$	30	-	27	-	-	-	-	19	43	12

(d) *Groenfontein granophyre*

(i) about station F6

	Ba	Co	La	Rb	Sc	Sn	Sr	Ti	Zn	Zr
$\bar{x}$	805	-	100	-	-	-	-	1246	144	416
σ	26,1	-	8,8	-	-	-	-	38,0	35,8	16,8
$\sigma/\bar{x}\%$	3,2	-	8,8	-	-	-	-	3,0	24,9	4,0

(ii) regional (7 samples)

	Ba	Co	La	Rb	Sc	Sn	Sr	Ti	Zn	Zr
$\bar{x}$	922	-	126	-	-	-	-	1208	81	449
σ	181,9	-	35,4	-	-	-	-	217,9	32,9	45,6
$\sigma/\bar{x}\%$	19,7	-	28,1	-	-	-	-	18,0	40,6	10,2

(e) Welgevonden granophyre

(i) about station K11

	Ba	Co	La	Rb	Sc	Sn	Sr	Ti	Zn	Zr
$\bar{x}$	892	-	118	-	-	-	-	1178	97	416
σ	23,4	-	16,1	-	-	-	-	50,5	15,4	16,8
$\sigma/\bar{x}\%$	2,6	-	13,6	-	-	-	-	4,2	15,9	4,0

(ii) regional (8 samples)

	Ba	Co	La	Rb	Sc	Sn	Sr	Ti	Zn	Zr
$\bar{x}$	1151	-	90	-	-	-	-	1328	97	512
σ	59,5	-	4,9	-	-	-	-	110,3	21,7	55,9
$\sigma/\bar{x}\%$	5,1	-	5,4	-	-	-	-	8,3	22,3	10,9

(f) Feldspar porphyry

(i) about station K14

	Ba	Co	La	Rb	Sc	Sn	Sr	Ti	Zn	Zr
$\bar{x}$	935	2,8	136	229	0,7	9,5	24	1256	118	389
σ	140,1	1,0	59,5	21,9	0,9	1,4	5,1	56,5	46,0	18,2
$\sigma/\bar{x}\%$	15	36,5	43,8	9,6	131,5	15,1	21,2	4,5	39,0	4,7

(ii) regional (12 samples)

	Ba	Co	La	Rb	Sc	Sn	Sr	Ti	Zn	Zr
$\bar{x}$	802	13,6	122	272	2,7	14,4	19,7	1146	66	428
σ	134,8	2,6	45,7	40,5	1,2	18,1	4,0	1192	16,8	28,7
$\sigma/\bar{x}\%$	16	19	46	15	44	126	20	10	26	7

(g) Aplitic and porphyritic aplitic granites

(i) about station E4

	Ba	Co	La	Rb	Sc	Sn	Sr	Ti	Zn	Zr
$\bar{x}$	138	1,5	80	278	0,6	5	13	925	108	321
σ	17,9	1,0	10,4	11,2	0,5	1,6	1,8	44,5	11,2	17,4
$\sigma/\bar{x}\%$	13	66	13	4	83	32	13,6	4,8	10,4	5,4

(ii) regional (17 samples)

	Ba	Co	La	Rb	Sc	Sn	Sr	Ti	Zn	Zr
$\bar{x}$	798	10,5	87	209	3,6	4,6	65	1122	87	399
σ	373,2	3,7	27,2	62,2	1,6	2,9	99,9	467,4	24,7	53,0
$\sigma/\bar{x}\%$	46	36	31	30	46	63	154	34	29	13

(h) Bobbejaankop granite

(i) about station H5

	Ba	Co	La	Rb	Sc	Sn	Sr	Ti	Zn	Zr
$\bar{x}$	235	0,1	70	361	2	222	10	-	25	298
σ	33,4	0,37	44,1	32,6	1,8	55,1	2,4	-	8,5	15,6
$\sigma/\bar{x}\%$	14,2	370	63,1	9	90	159,7	24	-	34,5	5,2

(ii) about station J10A

	Ba	Co	La	Rb	Sc	Sn	Sr	Ti	Zn	Zr
$\bar{x}$	94	2,3	94	429	1,8	13,8	6	568	40	247
σ	34,6	0,9	22,0	20,9	1,8	5,4	0,9	40,9	7,4	15,4
$\sigma/\bar{x}\%$	36,8	37,9	23,4	4,9	100,0	39,3	15,0	7,2	18,6	6,2

(iii) regional (17 samples)

	Ba	Co	La	Rb	Sc	Sn	Sr	Ti	Zn	Zr
$\bar{x}$	220	8,7	118	408	3	122	7	393	26	328
σ	90,8	3,6	78,5	66,7	2,3	311,1	2,5	122,5	16,2	48,3
$\sigma/\bar{x}\%$	41	41	67	16	68	255	36	31	62	15

(i) Felsite

(i) about station J17

	Ba	Co	La	Rb	Sc	Sn	Sr	Ti	Zn	Zr
$\bar{x}$	1090	8,5	65	169	7,2	3,6	105	2438	112	424
σ	66,6	3,3	4,2	14,3	2,3	1,2	14,1	82,1	13,0	14,1
$\sigma/\bar{x}\%$	6,1	38,1	6,5	8,5	31,8	33,8	13,4	3,4	11,6	3,3

(ii) regional (37 samples)

	Ba	Co	La	Rb	Sc	Sn	Sr	Ti	Zn	Zr
$\bar{x}$	1105	28	72	176	10	7	70	2337	174	395
σ	219,9	8,6	14,4	50,9	2,5	14,6	38,9	314,9	118,5	30,6
$\sigma/\bar{x}\%$	19	36	19	29	25	201	56	13	67	8

---

of reference, the ionic radius, electronegativity, and ionization potential of the elements considered in this study are listed in Table V.

(i) General Trace-Element Distribution in the Various Rock-Types

It has been shown (Lenthall, 1972) that statistical treatment of the analytical data permits the identification of three main components within the acid rocks of the Potgietersrus tin-field, namely, the stratiform granites and associated granophyres, the Bobbejaankop granite, and the felsites. Each of these groups can be further subdivided into a number of clusters of samples.

In Tables VI and VII, the mean concentrations and standard deviations for the various map units are given. There is evidence for a slight degree of fractionation from the base of the stratiform sheet to the feldspar porphyry beneath the felsite roof, while the felsites and the Bobbejaankop granite are, respectively, less and more fractionated than the stratiform granites. The Welgevonden granophyre, mapped in the field as a superimposed granophyric modification consequent upon the intrusion of diabase sheets, has concentrations of trace elements that place it intermediate in character between the felsites and the stratiform granites. The statistical treatment of the data revealed that a cluster of samples (cluster 1), that includes stratiform granites, forms a discrete zone immediately below the felsite in the southern part of the mapped area (see Lenthall, 1972, Figure 13). It is possible, therefore, that, in this part of the area, a portion of an early-crystallized roof of the granite is preserved, that has, in part, had a granophyric texture superimposed upon it by the intrusion of the diabase sheets. Alternatively, the presence of these sheets may have modified the chemistry of the granitic rocks.

The Bobbejaankop granite reflects a higher level of gamma radiation than do the other salic rocks, which can be attributed, in part, to the significantly higher contents of Th in this granite, as reported by Fourie (1969). The various subdivisions of the stratiform granite, in general, display only subtle differences in trace-element chemistry, a fact that has been established by the discriminant and cluster analyses of the data. The Bobbejaankop granite, however, is impoverished in Ba, Sr, Ti, and Zn and enriched in Ca, Rb, and Sn, in comparison to the stratiform granites. The enrichment in Ca is attributable to the greater volume of fluorine and carbonates in the Bobbejaankop granite. The mean value of 122,5 ppm Sn suggests a very substantial enrichment in this element in the Bobbejaankop granite. The standard deviation indicates a highly erratic distribution and the median value of 9 ppm Sn, compared to a median value of 6,5 ppm for the stratiform granites, more accurately reflects the general level of enrichment of this element in the Bobbejaankop granite. Similarly, the median Sn content in the felsites is less than 5 ppm. The felsites are enriched in Ba, Sr, Ti, and Zn, as compared to the stratiform granites, while Rb is impoverished.

The means, standard deviations, and coefficients of variance of the three main groups of salic rocks, based on the Johannesburg and Leeds analytical data, are given in Table VIII. This table illustrates the marked lack of variance in both K and Rb in the stratiform and Bobbejaankop granites, while Na is slightly more variable. K and Na display a greater variance in the felsites and may be, in part, due to the effects of devitrification. The table illustrates the generally higher degree of variance of all elements (except for K, Rb, and Zr) in the Bobbejaankop granite, in comparison to the stratiform granites and the felsites.

In Figures 5, 6, 7, 8, and 9, selected ratios are plotted. The K/Rb diagram illustrates graphically the lack of variation in the content of K in the granitic rocks, as compared to the felsites. The other diagrams demonstrate the overlap of the plots of the felsites into the granite field, the tendency of the felsites to occupy four distinct fields, the fractionation trend from felsite to

TABLE V : Ionic Radii, Electronegatives, Ionic Potentials, and Ionization Potentials of Elements Reported in This Study (from Taylor, 1965)

	Ionic Radius	Electro-negativity	Ionic Potential	Ionization Potential
Li^{+}	0,68	0,95	1,47	5,39
Ti^{4+}	0,68	1,6	5,88	6,82
Nb^{5+}	0,69	1,7	7,25	6,88
Sn^{4+}	0,71	1,8	5,63	7,34
Co^{2+}	0,72	1,7	2,78	7,86
Zn^{2+}	0,74	1,5	2,70	9,39
Zr^{4+}	0,79	1,5	6,40	6,84
Sc^{3+}	0,81	1,3	3,70	6,54
Y^{3+}	0,92	1,2	3,26	6,38
Ce^{4+}	0,94	1,1	4,26	6,54
Na^{+}	0,97	1,0	1,03	5,14
Ca^{2+}	0,99	1,04	2,02	6,11
La^{2+}	1,14	1,1	2,63	5,61
Sr^{2+}	1,18	1,0	1,69	5,69
K^{+}	1,33	0,8	0,75	4,34
Ba^{2+}	1,34	0,9	1,49	5,21
Rb^{+}	1,47	0,8	0,68	4,18

Bobbejaankop granite, and the grouping of the feldspar porphyry plots between the main concentrations of stratiform and Bobbejaankop granites. Some of the stratiform granite samples overlap the Bobbejaankop granite field, while others plot in positions offset from this field. Many of the samples of stratiform granite that lie in or close to the Bobbejaankop granite field are from aplitic bands.

Figure 10 illustrates the distribution of the K/Rb ratios, wherein it can be seen that, in general terms there is a zone of K/Rb values >200 along the foothills of the Makapansberg, where the base of the stratiform granite sheet crops out, overlain by an upper layer with K/Rb ratios <200, but within which patches with higher K/Rb ratios occur. The felsite roof is delineated very closely by the reappearance of the K/Rb = 200 contour along the western edge of the map. The Bobbejaankop granite is defined approximately by the K/Rb = 150 contour, but two other areas of low K/Rb ratios are also defined, both being approximately coincident with outcrops of feldspar porphyry.

(ii) Distribution Patterns of Individual Elements

Barium is log-normally distributed in the Bobbejaankop granite, but in the stratiform granites and the felsites there is a sharp inflection at about 20th percentile (Figure 11). However, the apparent double log-normality of the Ba distribution in the felsites depends on approximately 2 per cent of the samples having anomalously low values. This percentage is accounted for by only one sample that has anomalous chemistry in respect to Na and K as well. It is concluded that the felsites do, in fact, have a log-normal distribution of barium. This is illustrated by the histogram (Figure 12), which reflects an approximately unimodal distribution.

The histogram for Ba in the Bobbejaankop granite displays distinct positive skewness, but those for the stratiform granites have more complex, polymodal distribution patterns, with the exception of the Welgevonden granophyre. The Sterk River granophyre has a primary mode between 900 and 1 000 ppm, a secondary mode between 1 200 and 1 300 ppm, that is approximately coincident with the peak of the Welgevonden mode, and a tertiary mode between 500 and 600 ppm. This distribution pattern is confirmed by the statistical treatment of the data (Lenthall, 1972), wherein the samples of the Sterk River granophyre in the southern part of the map-area are included in cluster 1, while the remainder fall within cluster 3. The granophyric texture in the Welgevonden granophyre is considered to be a response to metamorphism induced by the intrusion of diabase sheets, and it might be concluded that

TABLE VIa : Means and Standard Deviations of the Trace and Major Elements in the Granites, Granophyres, and Felsites

	Granite		Granophyric Granite		Sterk River Granophyre		Feldspar Porphyry		Aplites and Porphyry Granites		Bobbejaankop Granite		Felsite	
	$\bar{x}$	σ	$\bar{x}$	σ	$\bar{x}$	σ	$\bar{x}$	σ	$\bar{x}$	σ	$\bar{x}$	σ	$\bar{x}$	σ
Ba	940,58	401,55	816,19	163,63	899,41	269,81	802,33	134,80	798,00	373,21	220,18	90,76	1104,67	219,90
Ca	5661,88	2072,41	4848,14	2446,08	4200,58	1614,53	4982,41	2493,15	5887,64	2073,44	8685,94	7399,20	7365,97	5075,67
Co	11,03	3,24	11,51	2,30	12,29	3,35	13,58	2,56	10,53	3,74	8,71	3,59	28,11	8,56
K_2O%	4,91	0,21	4,90	0,10	4,97	0,23	4,88	0,14	4,83	0,19	4,86	0,13	4,49	0,88
La	95,14	49,70	107,46	24,49	112,26	30,25	122,42	45,70	86,70	27,15	118,12	78,56	71,97	14,39
Li	34,78	58,08	31,84	6,27	33,32	7,01	35,17	6,16	35,94	6,34	35,35	6,72	40,86	8,42
Na_2O%	3,21	0,24	2,84	0,40	2,84	0,48	2,65	0,42	3,31	0,31	2,87	0,62	2,47	1,20
Rb	213,58	41,26	230,05	25,35	241,97	72,61	272,17	40,49	208,88	62,23	407,65	66,66	175,67	50,92
Sc	3,42	1,77	2,46	1,17	2,50	1,80	2,67	1,18	3,59	1,65	3,35	2,27	10,00	2,51
Sn	7,00	4,49	10,42	9,50	9,06	11,81	14,42	18,12	4,59	2,89	122,47	311,06	7,30	14,64
Sr	43,09	24,11	34,25	79,68	29,56	22,32	19,67	4,05	64,76	99,98	6,65	2,45	70,03	38,93
Ti	1164,89	393,10	1142,65	136,56	1220,41	227,52	1146,17	119,20	1122,47	467,38	392,94	122,47	2337,13	314,92
Zn	89,33	32,81	97,12	60,27	102,82	44,77	66,42	16,78	87,12	24,69	26,12	16,15	174,57	118,46
Zr	428,14	67,48	417,56	42,51	464,20	57,57	428,17	28,73	398,94	52,97	328,06	48,28	395,27	30,57
Gamma Flux Density	30,71	5,35	31,32	3,27	30,44	4,14	31,25	2,20	30,12	7,17	51,29	6,97	23,73	2,14
No. of Samples	88		43		34		12		17		17		37	

TABLE VIb : Coefficients of Variance as Percentages and Means of Granites, Granophyres, and Felsites

	Granite		Granophyric Granite		Sterk River Granophyre		Feldspar Porphyry		Aplitic Granite		Bobbejaankop Granite		Felsite	
	$\bar{x}$	$\sigma/\bar{x}\%$	$\bar{x}$	$\sigma/\bar{x}\%$	$\bar{x}$	$\sigma/\bar{x}\%$	$\bar{x}$	$\sigma/\bar{x}\%$	$\bar{x}$	$\sigma/\bar{x}\%$	$\bar{x}$	$\sigma/\bar{x}\%$	$\bar{x}$	$\sigma/\bar{x}\%$
Ba	940	42	816	19	899	30	802	16	798	46	220	41	1104	19
Ca	5662	27	4848	51	4982	38	4982	50	5888	35	8686	85	7366	69
Co	11	29	11	20	12	27	13	19	10	36	9	41	28	36
La	95	53	107	22	112	27	122	46	87	31	118	67	72	19
Li	35	23	32	19	33	21	35	17	36	17	35	20	41	20
Rb	213	19	230	9	242	30	272	15	209	30	408	16	176	29
Sc	3	52	2	47	2	72	3	44	3	46	3	68	10	63
Sn	7	64	10	91	9	130	14	126	4	63	122	255	7	201
Sr	43	56	34	235	29	73	20	20	65	154	7	29	70	56
Ti	1165	34	1143	12	1220	19	1146	10	1122	34	393	31	2337	13
Zn	89	37	97	62	103	43	66	26	87	29	26	62	174	67
Zr	428	16	417	10	464	12	428	7	399	13	328	15	395	8
K_2O %	4,91	4	4,90	2	4,97	5	4,88	3	4,83	4	4,86	3	4,49	20
Na_2O %	3,21	7	2,84	14	2,84	17	2,65	16	3,31	9	2,87	22	2,47	49
Gamma Flux Density	31	17	31	10	30	13	31	7	30	23	51	13	24	9

TABLE VIc : Means and Standard Deviations of Trace and Major Elements in the Groenfontein and Welgevonden Granophyres

	Groenfontein Granophyre			Welgevonden Granophyre		
	$\bar{X}$	σ	$\sigma/\bar{X}\%$	X	σ	$\sigma/\bar{X}\%$
Ba	922,57	181,9	19	1150,87	59,5	5
Ca	3723,14	1919,0	51	4145,00	1292,34	31
Co	10,43	2,1	21	11,62	1,73	15
La	125,86	35,36	29	90,00	4,95	5,5
Li	34,71	5,82	17	30,00	3,81	13
Rb	246,14	63,98	26	196,50	18,16	9
Sc	2,28	0,88	38	2,50	0,71	28
Sn	16,57	10,62	64	7,25	6,65	91
Sr	22,14	11,19	50	38,75	8,36	21
Ti	1208,14	217,88	18	1327,75	110,31	8
Zn	80,71	32,91	40	96,62	21,66	22
Zr	448,86	45,62	10	511,75	55,96	11
$K_2O\%$	4,82	0,16	3	4,83	0,21	4
$Na_2O\%$	2,92	0,45	15	3,11	0,28	8
Gamma Flux Density	31,28	1,83	6	28,12	3,82	13
No. of Samples	7			8		

TABLE VII : Ratios of Elements in Granites, Granophyres, and Felsites

	K/Rb	K/Ba	Ba/Sr	Ba/Rb	Ca/Sr	Ti/Zr	$Sc\times10^4/Ti$
Felsites	212	33,7	15,7	6,2	105	5,9	42,6
Welgevonden Granophyre	204	34,8	30	5,8	107	2,5	18,8
Granite	190	53	22	4,4	131	2,7	29,3
Granophyric Granite	177	49	23	3,5	141	2,7	21,5
Sterk River Granophyre	170	46	30	3,7	142	2,6	20,5
Groenfontein Granophyre	162	43	41,7	3,7	169	2,7	18,8
Feldspar Porphyry	150	50,5	41	2,9	253	2,7	23,3
Bobbejaankop Granite	98	183	33	0,5	1306	1,2	85,2

TABLE VIIIa : Means, Standard Deviations, and Coefficients of Variance of Measured Parameters in Stratiform Granite, Bobbejaankop Granite, and Felsite

	Felsites			Stratiform Granite			Bobbejaankop Granite		
	$\bar{x}$	σ	$\sigma/\bar{x}\%$	$\bar{x}$	σ	$\sigma/\bar{x}\%$	$\bar{x}$	σ	$\sigma/\bar{x}\%$
Ba	1105	219,90	19	896	322,56	36	220	90,76	41
Ca	7366	5076,67	69	5113	1840,68	36	8686	7399,20	85
Ce	236	13,74	6	269	55,92	20	256	63,83	25
Co	5,7	2,87	50	2	1,33	66	2	1,09	54
La	72	14,39	19	100	36,98	37	118	78,56	67
Li	41	8,42	20	34	10,07	30	35	6,72	20
Nb	18	3,81	21	24	7,17	29	83	27,07	32
Ni	0	0,43	-	1	1,32	132	1	0,99	99
Rb	176	50,92	29	225	33,75	15	408	66,66	16
Sc	10	2,51	63	3	1,57	52	3	2,27	68
Sn	7	14,64	201	8,5	7,23	85	122	311,06	255
Sr	70	38,93	56	39	56,92	146	7	2,45	29
Ti	2337	314,93	13	1173	281,49	24	393	122,47	31
Y	56,5	7,04	12	97	33,75	35	146	28,03	19
Zn	175	118,46	67	91	37,33	41	26	16,15	62
Zr	395	30,57	8	433	50,98	12	328	48,28	15
K_2O %	4,49	0,88	20	4,91	0,19	3	4,86	0,13	3
Na_2O%	2,47	1,20	49	3,05	0,32	11	2,87	0,62	22

Leeds analytical data used for Ce, Co, Nb, Ni, and Y; remaining analyses from Johannesburg data.

TABLE VIIIb : Mean Element Ratios in Stratiform Granite, Bobbejaankop Granite, and Felsite

	Felsite	Stratiform Granite	Bobbejaankop Granite
K/Rb	212	181	98
K/Ba	33,7	45,4	183
Ba/Rb	6,2	3,9	0,5
Ba/Sr	15,7	23	33
Ca/Sr	105,2	131	1306
Ti/Zr	5,9	2,7	1,2
$Sc \times 10^4/Ti$	42,8	25,5	85,2
Rb/Sr	2,5	5,7	58,3
Na/K	0,49	0,55	0,53
$Nb \times 10^3/Ti$	7,7	20,4	211
$Nb \times 10^3/Zr$	45,6	55,4	253

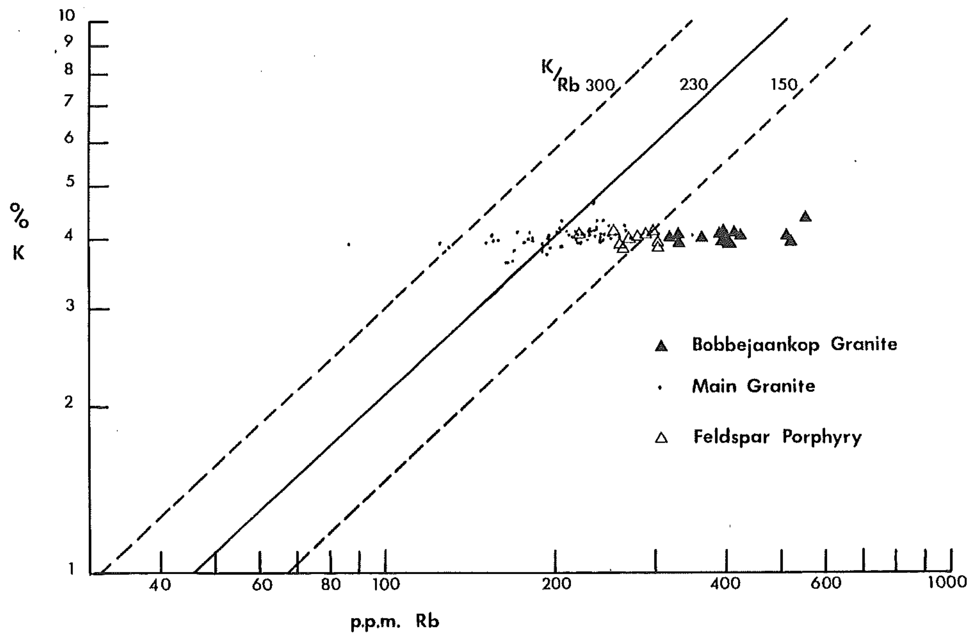

Figure 5 : *Scatter-diagram of K vs. Rb for the granitic rocks.*

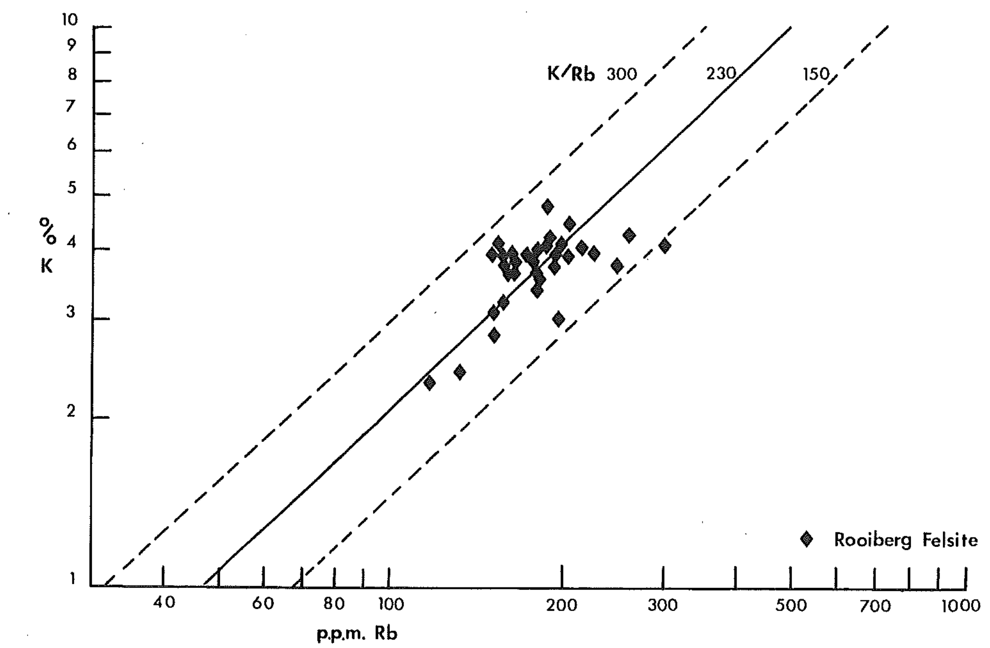

Figure 6 : *Scatter-diagram of K vs. Rb for the felsites.*

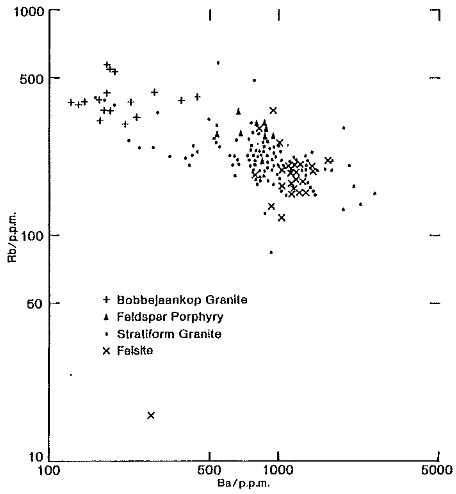

Figure 7 : *Scatter-diagram of Rb vs. Ba for the granitic rocks and felsites.*

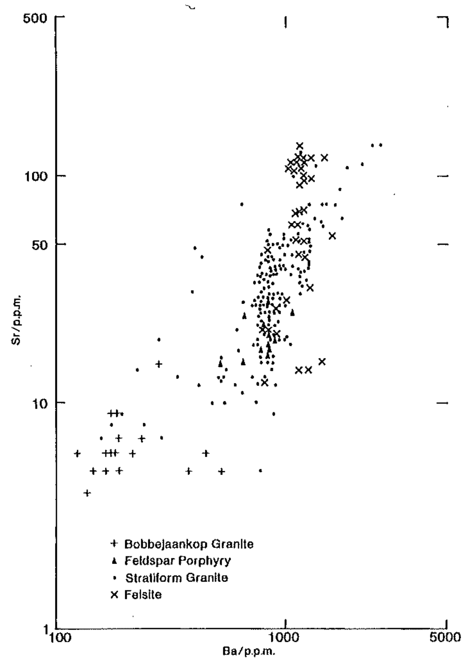

Figure 8 : *Scatter-diagram of Sr vs. Ba for the granitic rocks and felsites.*

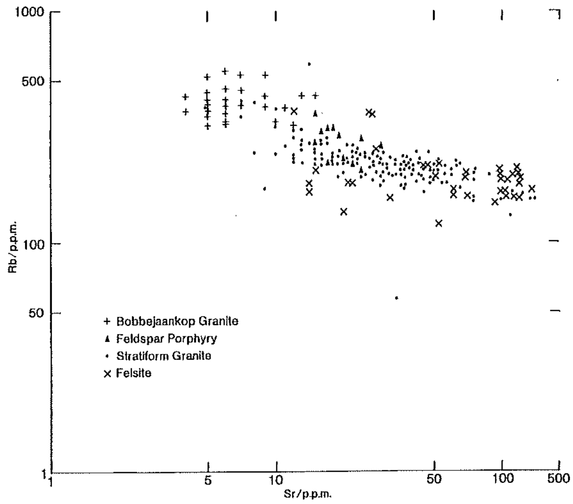

Figure 9 : *Scatter-diagram of Rb vs. Sr for the granitic rocks and felsites.*

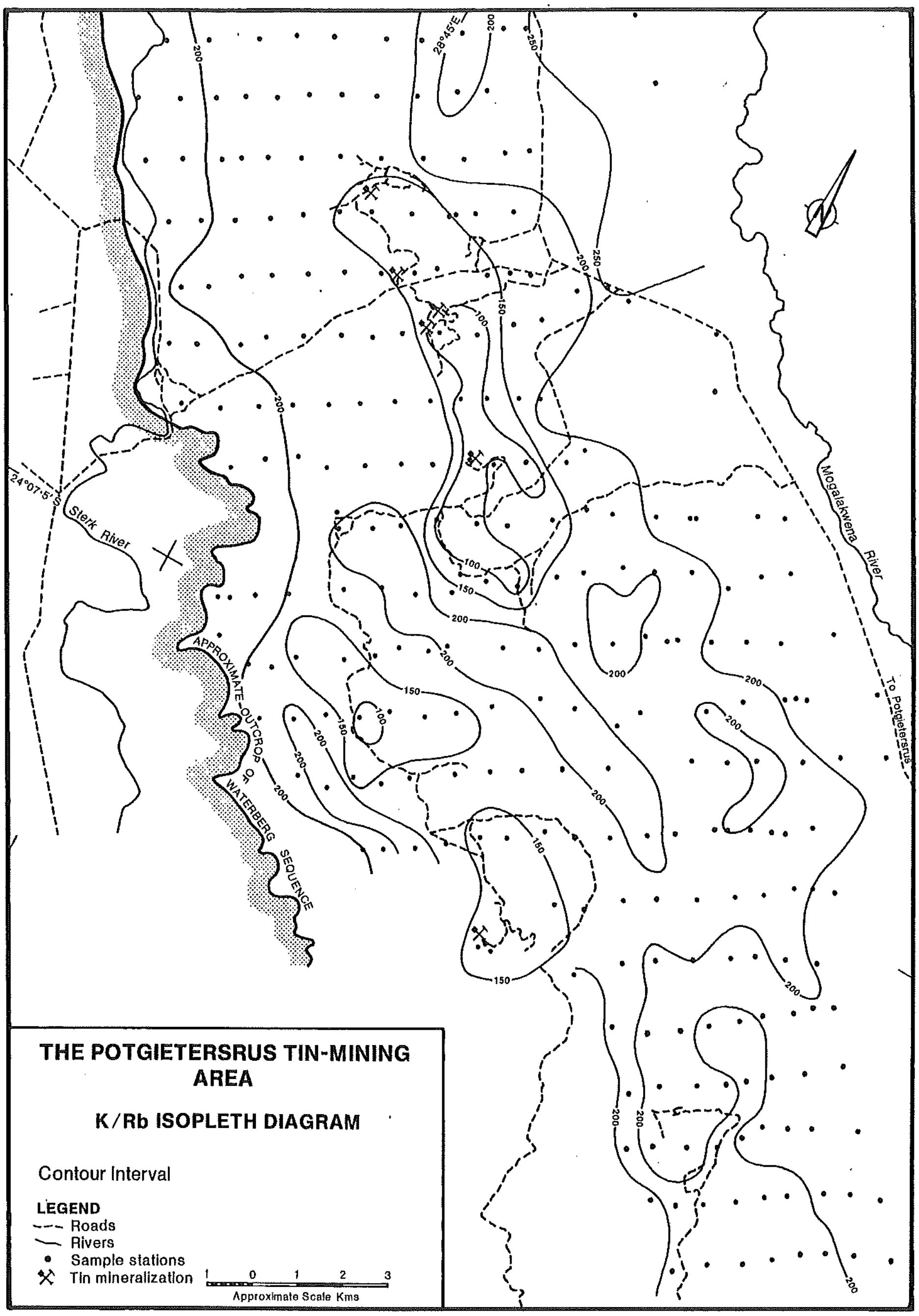

Figure 10 : *Isopleth map of K/Rb ratios in all rock-types.*

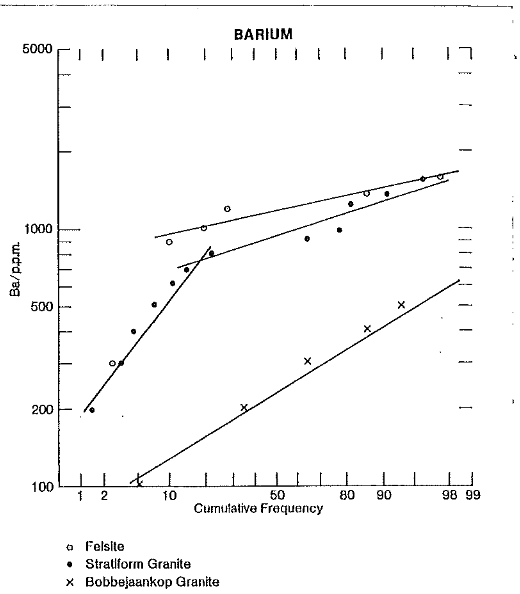

Figure 11 : *Cumulative frequency distribution (log-scale) of Ba in all rock-types.*

the barium distribution pattern could have arisen as a consequence of this metamorphism. However, the Groenfontein granophyre, the response to the thermal effects of the Bobbejaankop granites, has a distinct bimodal distribution pattern. The Sterk River granophyre histogram has a secondary mode between 1 200 and 1 300 ppm that is approximately coincident with the peak of the Welgevonden granophyre mode. All the Sterk River granophyre samples constituting the secondary mode were collected from the southern part of the map-area. The available evidence, therefore, suggests that the uppermost part of the stratiform granite in the south has an inherently higher Ba content than in the remainder of the map-area.

The aplitic granites display a prominent bimodal distribution pattern. In the field, it was found that aplitic granites occur as cross-cutting, sheeted bodies, typically with sharp contacts or in irregularly-shaped bodies, often with diffuse contacts. These field relations suggest two ages of aplitic granite crystallization, which may be the reason for the bimodality of the Ba distribution pattern. The primary mode, between 900 and 1 000 ppm is coincident with the primary mode in the Sterk River granophyre distribution pattern. The secondary mode between 200 and 300 ppm approaches the mode of the Bobbejaankop granite distribution pattern.

The coarse-grained and granophyric granites, together with the feldspar porphyry, have prominent modes between 800 and 900 ppm. The former rock-types have, in addition, a small percentage of samples with high (>1 600 ppm) Ba contents. The majority of these samples were collected at or near the base of the stratiform granite sheet.

The median Ba value of 845 ppm for the stratiform granites compares closely with the mean value of low-Ca granites (Turekian and Wedepohl, 1961) but differs considerably from the value of 420 ppm for African anorogenic acid intrusives that are also low in calcium (Rooke, 1971).

The contoured distribution of Ba (Figure 13) reveals that the outcrop pattern of the Bobbejaankop granite is clearly defined, and that, in the central and northern areas of the map, the 1 000 ppm Ba contour defines approximately the base of the felsite succession. In the south, the increase in Ba content of the granite does not permit the basal contact of the felsites to be identified, on the basis of the Ba data alone.

Barium substitutes only for potassium among the common cations. According to the data of Nockolds and Mitchell (1948), barium enters potassium feldspars more readily than biotites. The low Ba/Rb and K/Rb ratios in the Bobbejaankop granite are consistent with those expected during fractional crystallization. Fourie (1969) reported significant depletion in Eu in the Bobbejaankop granite. The parallel behavior of Eu, Ba, and Sr in the Bobbejaankop granite suggests that it is probably present as Eu^{2+}, intermediate in size between Ba^{2+} and Sr^{2+}, all three elements preferentially entering the K sites. The first crystallization products would then be expected to have higher K/Rb ratios and lower K/Sr, K/Ba, and K/Eu ratios than the melt. The residual liquid from which the Bobbejaankop granite crystallized would then be enriched in Rb and depleted in Ba, Sr, and Eu.

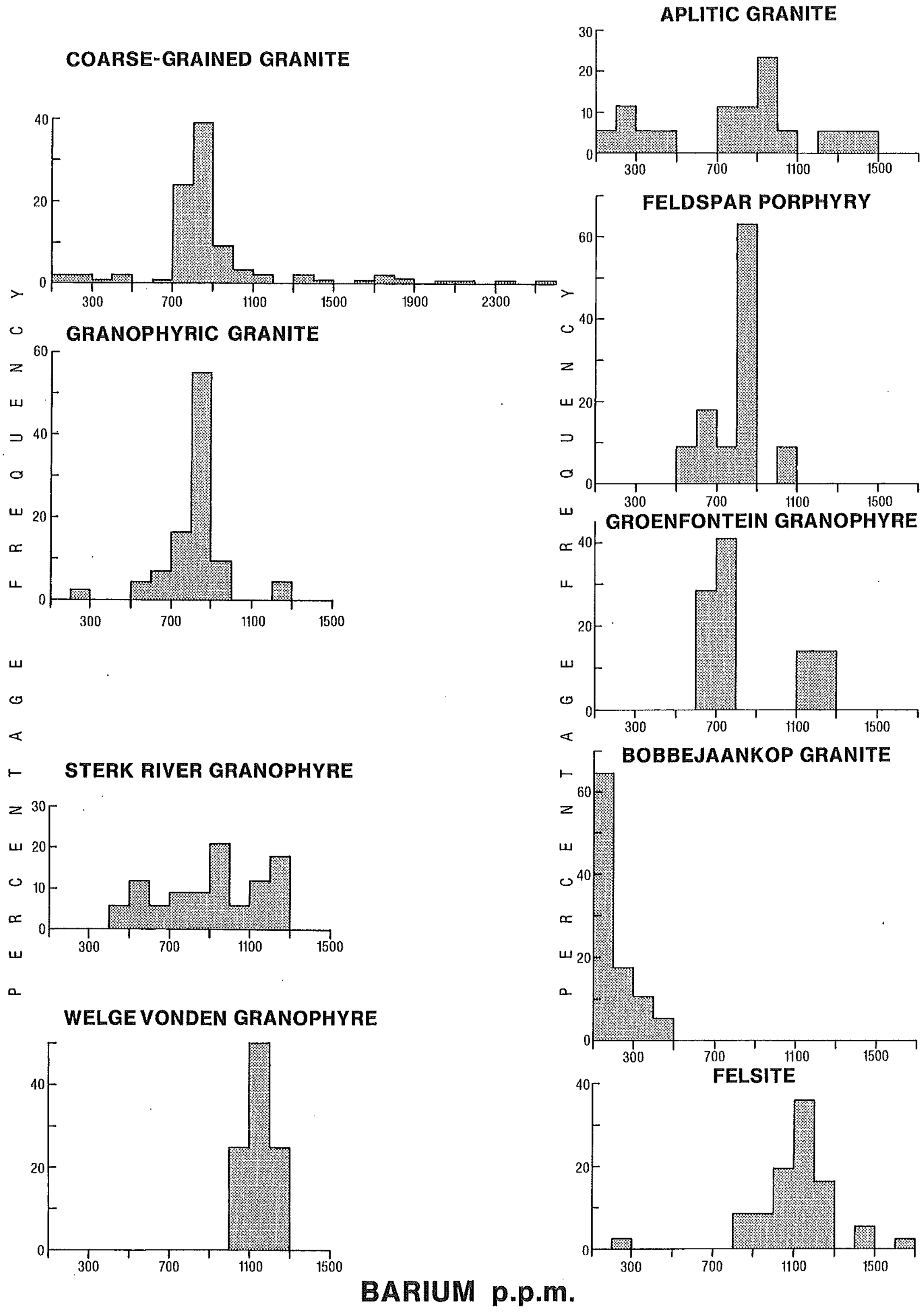

Figure 12 : *Histograms of Ba distribution in different rock-types.*

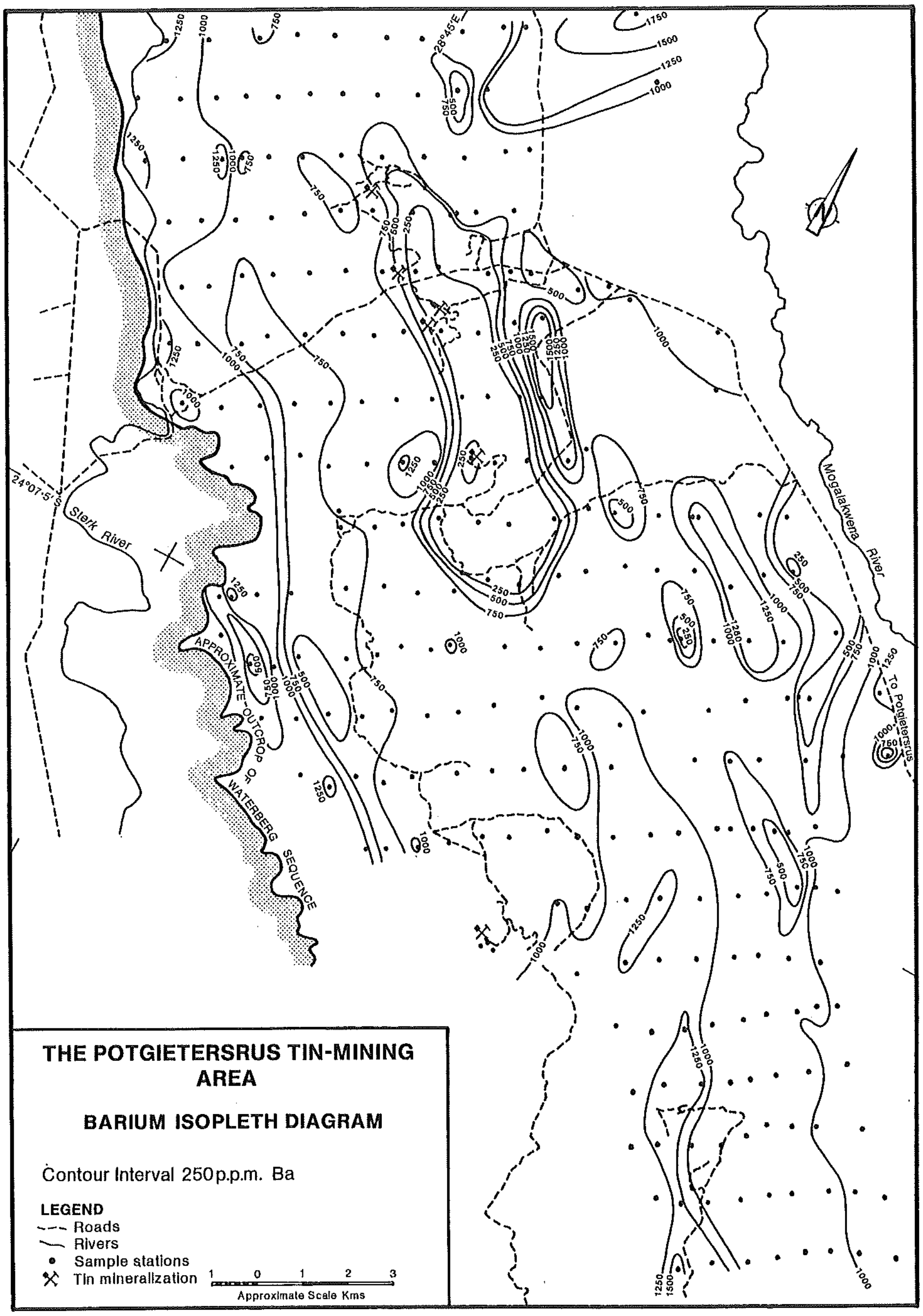

Figure 13 : *Isopleth map of Ba content of all rock-types.*

Calcium has an approximately log-normal distribution pattern in the coarse-grained granites and its granophyric modifications (Figure 14) that contrasts with the distribution patterns of the felsites and Bobbejaankop granite. In both these rock-types, there is an inflection of the distribution curves at about the 30th percentile. The contrasting patterns of the calcium distribution is emphasized in the histograms (Figure 15).

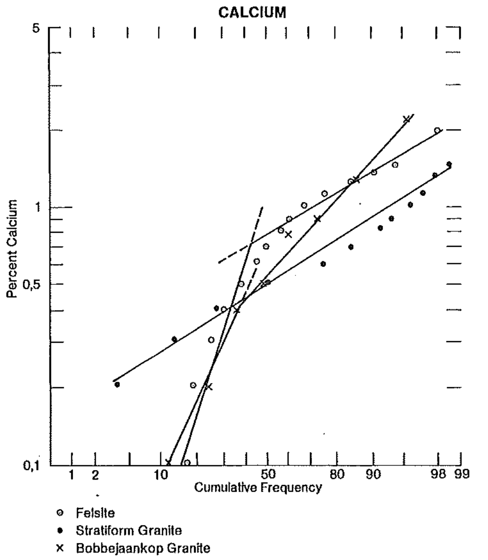

Figure 14 : *Cumulative frequency distribution (log-scale) of Ca in all rock-types.*

The calcium content of the Bobbejaankop granite is, at first appraisal, apparently anomalously high. The isopleth diagram (Figure 16) reflects the higher calcium contents of the Bobbejaankop granite samples. Petrographic study shows that the Bobbejaankop granite carries fluorite and carbonates in significant amounts. Preliminary fluorine analyses (using neutron activation techniques) by Dr. D. Bibby of the Nuclear Physics Research Unit, the University of the Witwatersrand, on twenty selected samples, give mean fluorine contents of 2 960 ppm and 5 500 ppm for the stratiform granites and the Bobbejaankop granite, respectively. If the calcium present in fluorite is deducted from the total calcium content, the stratiform granites carry 2 353 ppm and the Bobbejaankop granite 3 470 ppm Ca available for the formation of silicates. Strauss (1954) reported high contents of CO_2 in the mineralized granites, so that it is apparent that the calcium content of the Bobbejaankop granite available for silicates would be even further reduced. From Strauss's (1954) data, the stratiform granites have, after correction for carbonates and fluorite, a mean CaO-content of 0,72 per cent, as against a corrected calcium content of 0,65 per cent in the Bobbejaankop granites. The available data suggest that the stratiform and Bobbejaankop granites are comparable in their mean Ca-content to the low-Ca granites (Turekian and Wedepohl, 1961), but it is probable that they may be slightly impoverished in Ca, as compared to the world average of low-Ca granites, in the light of Dr. Bibby's preliminary results.

The felsites have a mean Ca-content of 0,70 per cent, that compares with the 0,69 per cent determined for African anorogenic acid extrusives (Rooke, 1971).

Cerium was determined in 46 samples by Dr. G. Hornung, of Leeds University, of which 32 samples were collected from three sample stations. The limited number of samples analyzed militates against the treatment of this data in a similar manner to that used for other elements. It is apparent that Ce is slightly enriched in the stratiform granites, as compared to the felsites, and that Ce is more erratically distributed in the stratiform and Bobbejaankop granites as compared to the felsites (Table VIIIa).

Variation in Ce-content about sample stations (Table IX) reflects maximum coefficients of variance in the marginal facies of the Bobbejaankop granite, wherein the highest fluorine contents are reported.

The Ce-contents reported here are significantly higher than those recorded by Fourie (1969). This is the only element where there is a lack of agreement in the analytical results obtained by different laboratories. Edge and Ahrens (1962) reported an analysis of Bobbejaankop granite, in which these authors determined 365 ppm, Ce which is of the same order of magnitude as the values given here.

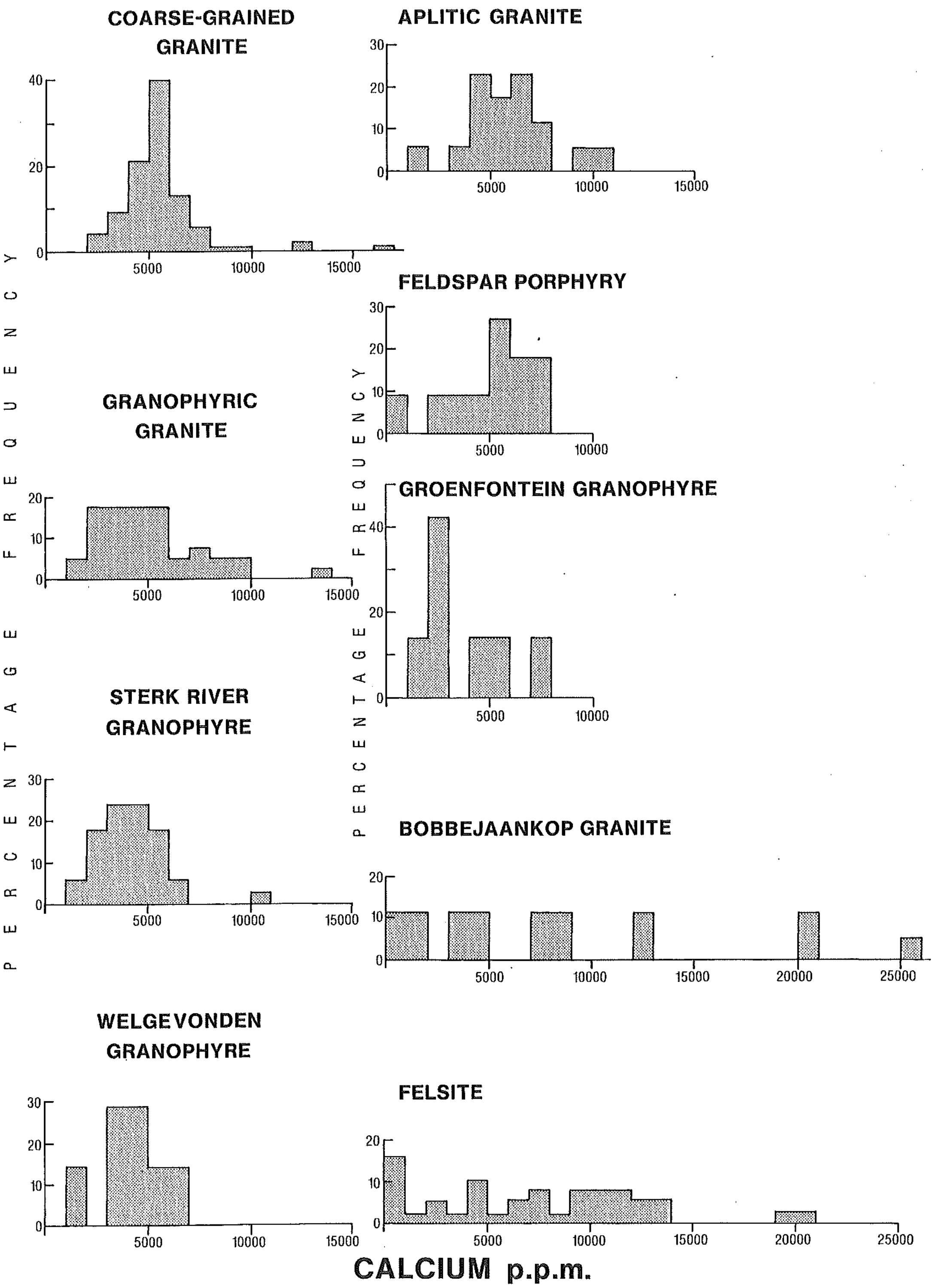

Figure 15 : *Histograms of Ca distribution in different rock-types.*

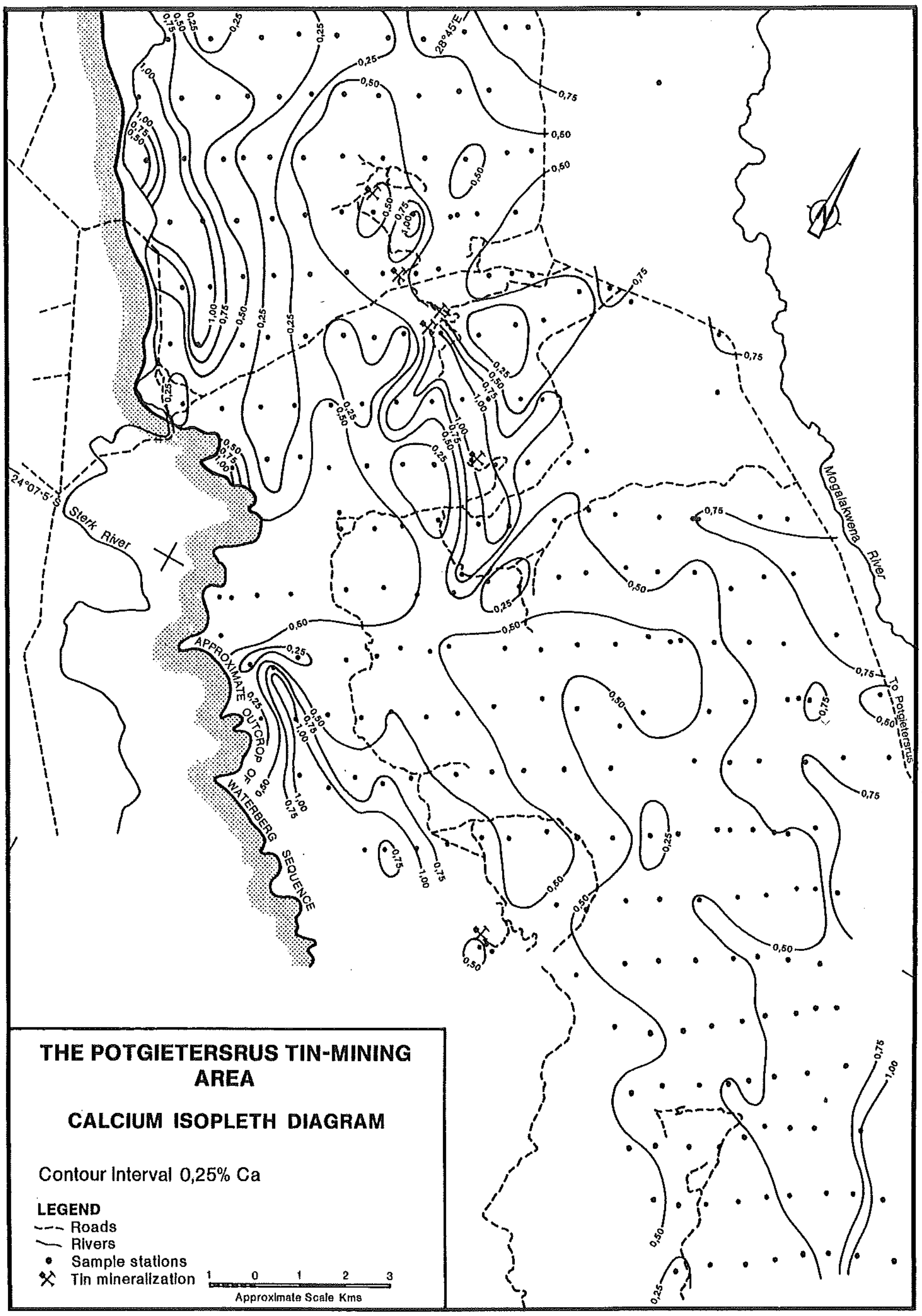

Figure 16 : *Isopleth map of Ca content of all rock-types.*

TABLE IX : Means and Standard Deviations of Ce-Content about Sample Stations

Rock-type	Mean $\bar{x}$	Standard Deviation σ	$\sigma/\bar{x}\%$
Coarse-grained granite (C6)	254	30,00	11,81
Aplitic granite (E4)	272	18,84	6,93
Feldspar porphyry (K14)	342	103,81	30,35
Bobbejaankop granite (J10A)	275	51,95	18,89
Bobbejaankop granite (H5)	185	105,03	56,77
Felsite (J17)	231	9,37	4,06

Cobalt values reported in the Johannesburg analyses are an order of magnitude greater than those given by Fourie (1969) and Dr. Hornung, the lower values being accepted here. The felsites carry three times the amount of Co that is present in the stratiform and Bobbejaankop granites. In all three rock-types, Co has an approximately log-normal distribution. In Figure 17, the Leeds data have also been plotted and show the same distribution pattern, but with lower concentrations. The Co isopleth diagram (Figure 18), based on the Johannesburg analyses, shows the increase in Co in the felsites, with the granites having isolated high values.

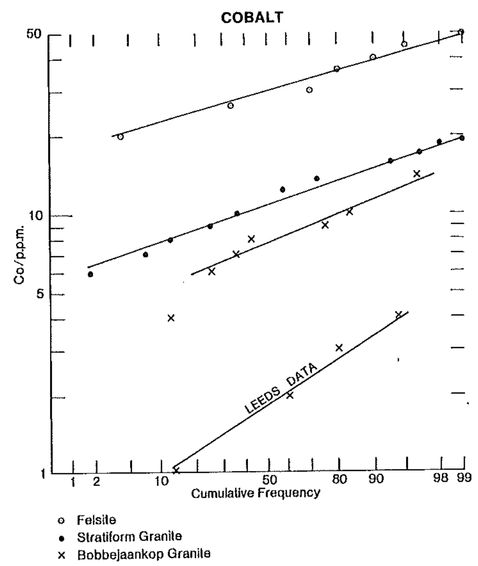

Figure 17 : *Cumulative frequency distribution (log-scale) of Co in all rock-types.*

Fourie's (1969) data suggest that the felsites and stratiform granites have slightly higher concentrations of Co relative to Mg than reported by Carr and Turekian (1961). A similar enrichment in Co was reported by Kolbe (1966) for the Cape granites. The Bobbejaankop granite displays an erratic relationship between Co and Mg.

Lanthanum contents increase from felsites to the Bobbejaankop granite, while the stratiform granites also display an increase in lanthanum content upwards from the base of the sheet. Lanthanum approaches a log-normal distribution in the felsites and the stratiform granites, but, in the Bobbejaankop granite there is a sharp inflection at the 40th percentile (Figure 19). With the exception of the Groenfontein granophyre, the constituent members of the stratiform granite sheet have approximately unimodal distribution patterns (Figure 20), with positive skewness in the granophyric granite, the Sterk River granophyre, and the feldspar porphyry. It is suggested that the tendency towards bi-modality in the Groenfontein granophyre stems from the fact that its recrystallization was accompanied by contamination from the Bobbejaankop granite. The isopleth diagram (Figure 21) illustrates the higher La-contents within the Bobbejaankop granite and the feldspar porphyry, both of which have high coefficients of variance (See Table VIb).

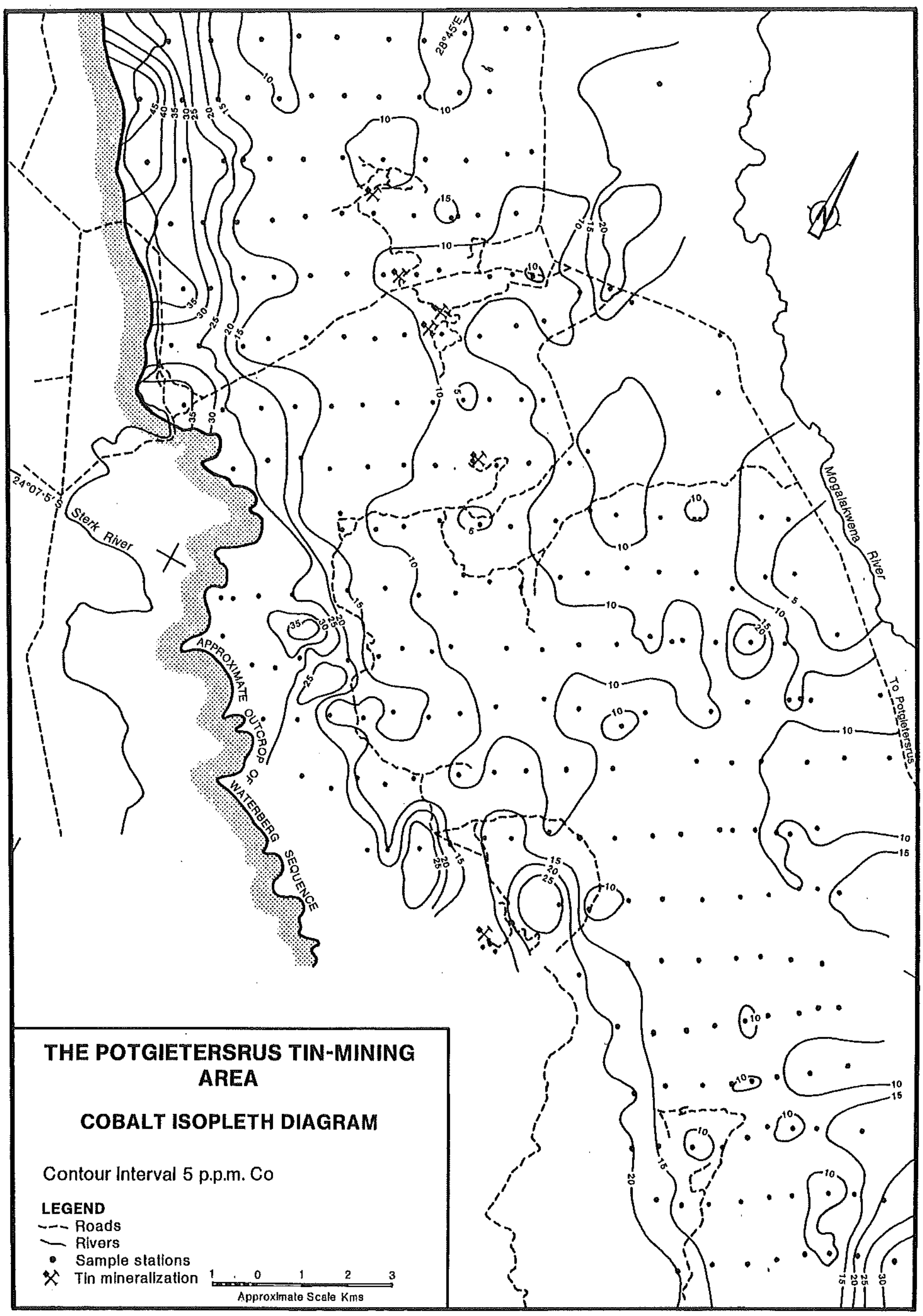

Figure 18 : *Isopleth map of Co content of all rock-types.*

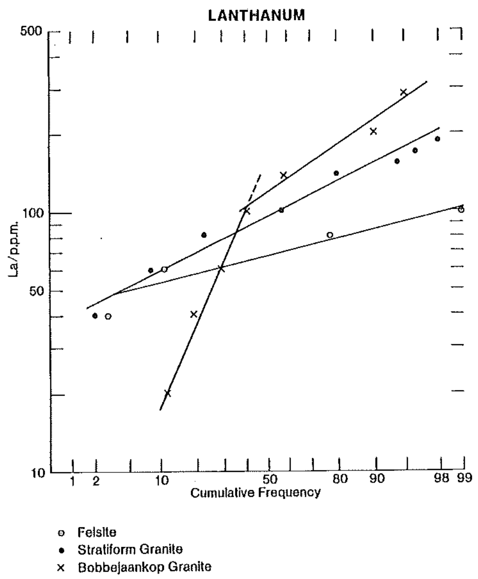

Figure 19 : *Cumulative frequency distribution (log-scale) of La in all rock-types.*

The behavior of the rare earth elements is complex and more data are required concerning their distribution within individual minerals. The increase in La cannot be related to the F-content in detail, although, in general terms, the Bobbejaankop contains higher concentrations of F than do the stratiform granites. The mean fluorine and lanthanum contents in the granites illustrate the crude relationship between these elements :

	Mean F ppm	Mean La ppm
Coarse-grained granite	2 457	95
Welgevonden granophyre	2 200	90
Granophyric granite	3 780	107
Bobbejaankop granite	5 500	118

It seems probable that the rare earth elements reflect a fractionation trend, on which has been superimposed additions accompanying the volatiles in the form of complex ions.

Lithium has a log-normal distribution in the three main rock-types, the concentrations in the Bobbejaankop and stratiform granites being identical (Figure 22), while the coefficients of variance in the different units are constant (see Tables VIb and c). The aplitic granites display a distinct bimodal character (Figure 23), that is less marked in the coarse-grained granites. Li^+, much smaller than the other alkali elements, is unable to occupy similar lattice positions and enters six-fold co-ordination positions, being thought to substitute for magnesium (Taylor, 1965). Lithium may be expected to concentrate in late-stage ferromagnesian minerals. High abundances of lithium are typical of extreme fractionation. It will be seen that the Li-content of the felsites and granites in the Potgietersrus tin-field is close to the world-wide mean for acid rocks.

Niobium has been determined in this study in 46 samples, of which 32 were collected around three sample stations. Whereas the mean contents in the felsites and stratiform granites of these analyses agree with those reported by Fourie (1969), the present study reflects a greater than three-fold increase in the Bobbejaankop granite, as compared with stratiform granites, with Fourie's (1969) data showing a two-fold increase. The coefficients of variance of Nb in the Bobbejaankop granite are greater than in the felsites and stratiform granites, which is also borne out by the variance about sample stations (Table X).

The mean Ti/Nb ratios calculated from the samples analysed for both Ti and Nb decrease from 140,5 in the felsites, to 63, in the stratiform granites, to 5,6, in the Bobbejaankop granites. The coarse-grained granites have a mean Ti/Nb ratio of 50, as compared to 54 for the granophyric granites and 47,5 for the feldspar porphyry. The aplitic granites have Ti/Nb ratios ranging from 8,4 to 85 and, if more samples had been analysed, it is probable that a bimodal distribution of Nb also would have been detected in this rock-type.

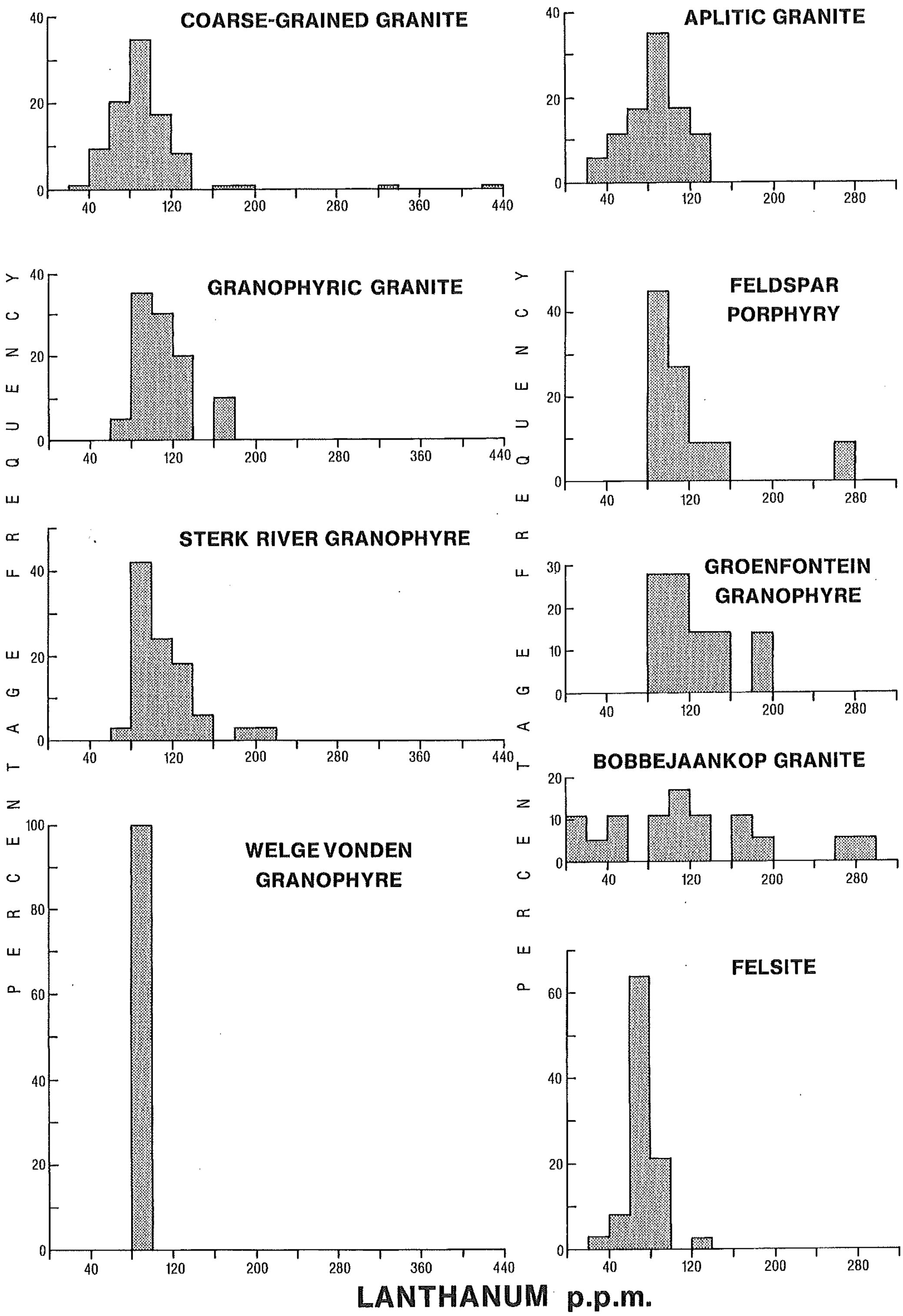

Figure 20 : *Histograms of La distribution in different rock-types.*

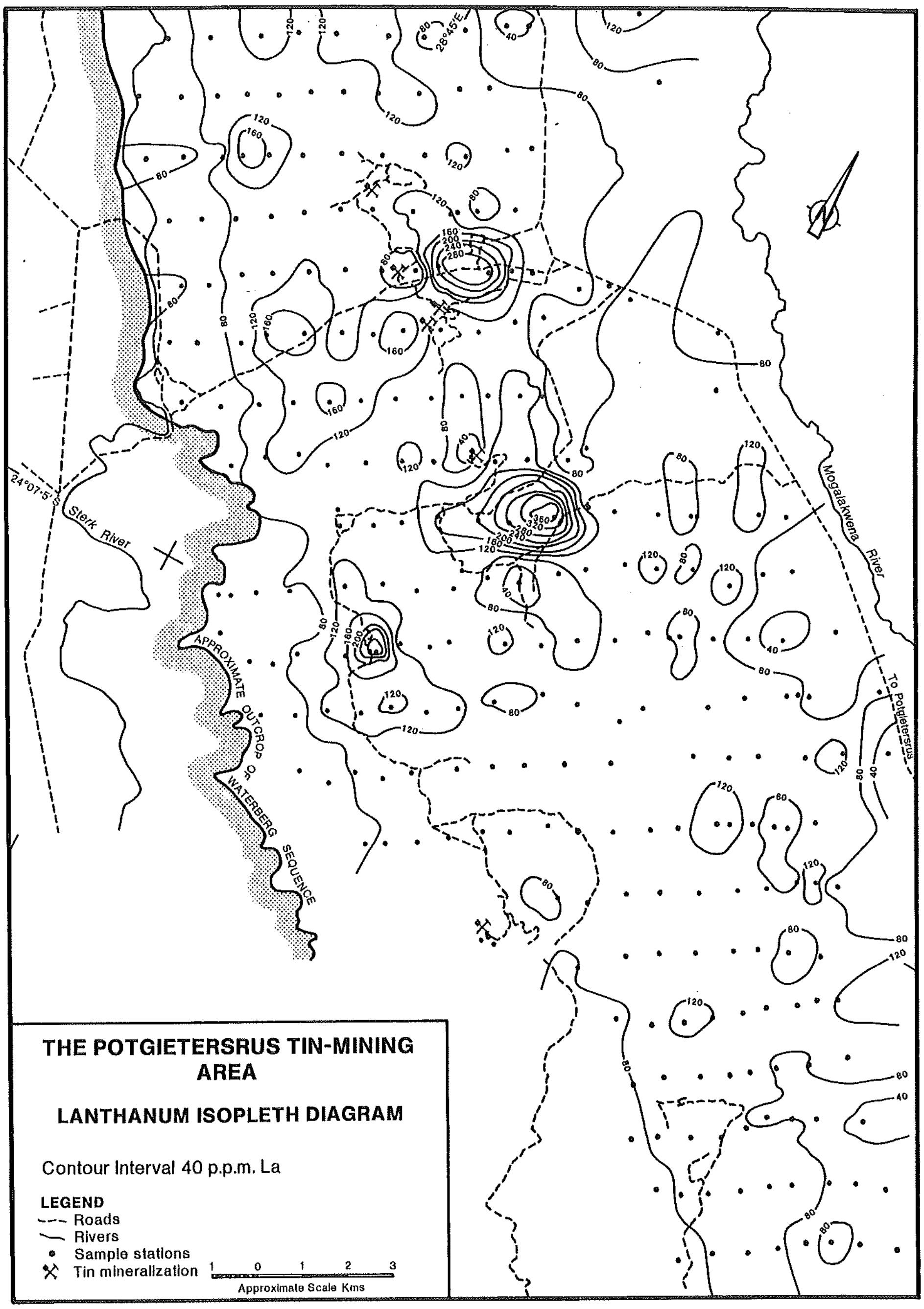

Figure 21 : *Isopleth map of La content of all rock-types.*

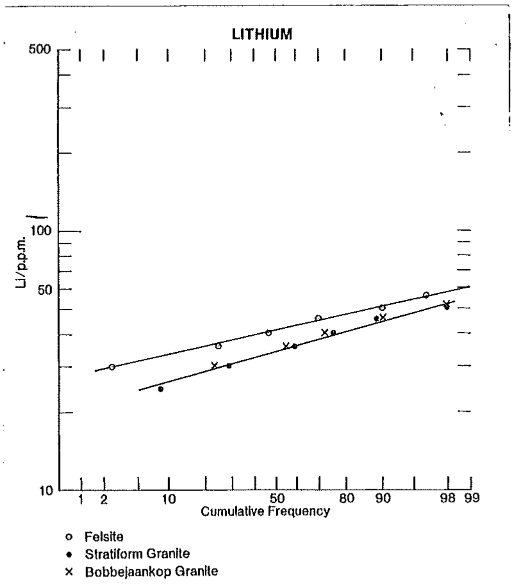

Figure 22 : *Cumulative frequency distribution (log-scale) of Li in all rock-types.*

The niobium content of the stratiform granites agrees with the world average for low-Ca granites (Turekian and Wedepohl, 1961) but it is considerably lower than the mean content determined for African anorogenic acid intrusives (Rooke, 1971), which was weighted by the inclusion of several Nb-rich types.

TABLE X : Means and Standard Deviations of Nb-Contents about Sample Stations

Rock-type	Mean $\bar{X}$	Standard Deviation σ	$\sigma/\bar{X}\%$
Coarse-grained granite (C6)	22	2,45	11,14
Aplitic granite (E4)	30	2,60	8,67
Feldspar porphyry (K14)	22	1,49	6,77
Bobbejaankop granite (J10A)	51	13,00	25,49
Bobbejaankop granite (H5)	111	16,61	14,96
Felsite (J17)	17	1,14	6,71

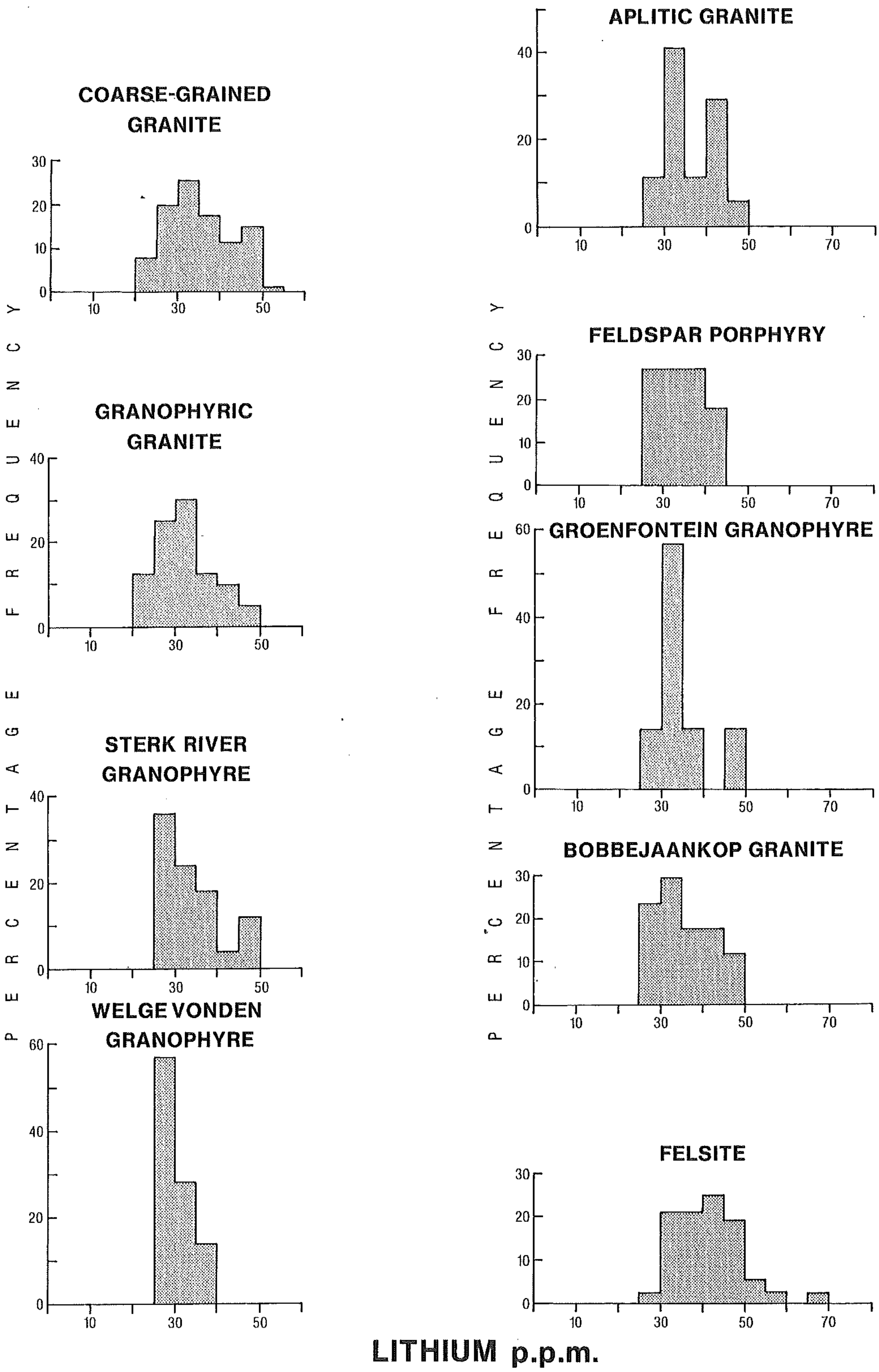

Figure 23 : *Histograms of Li distribution in different rock-types.*

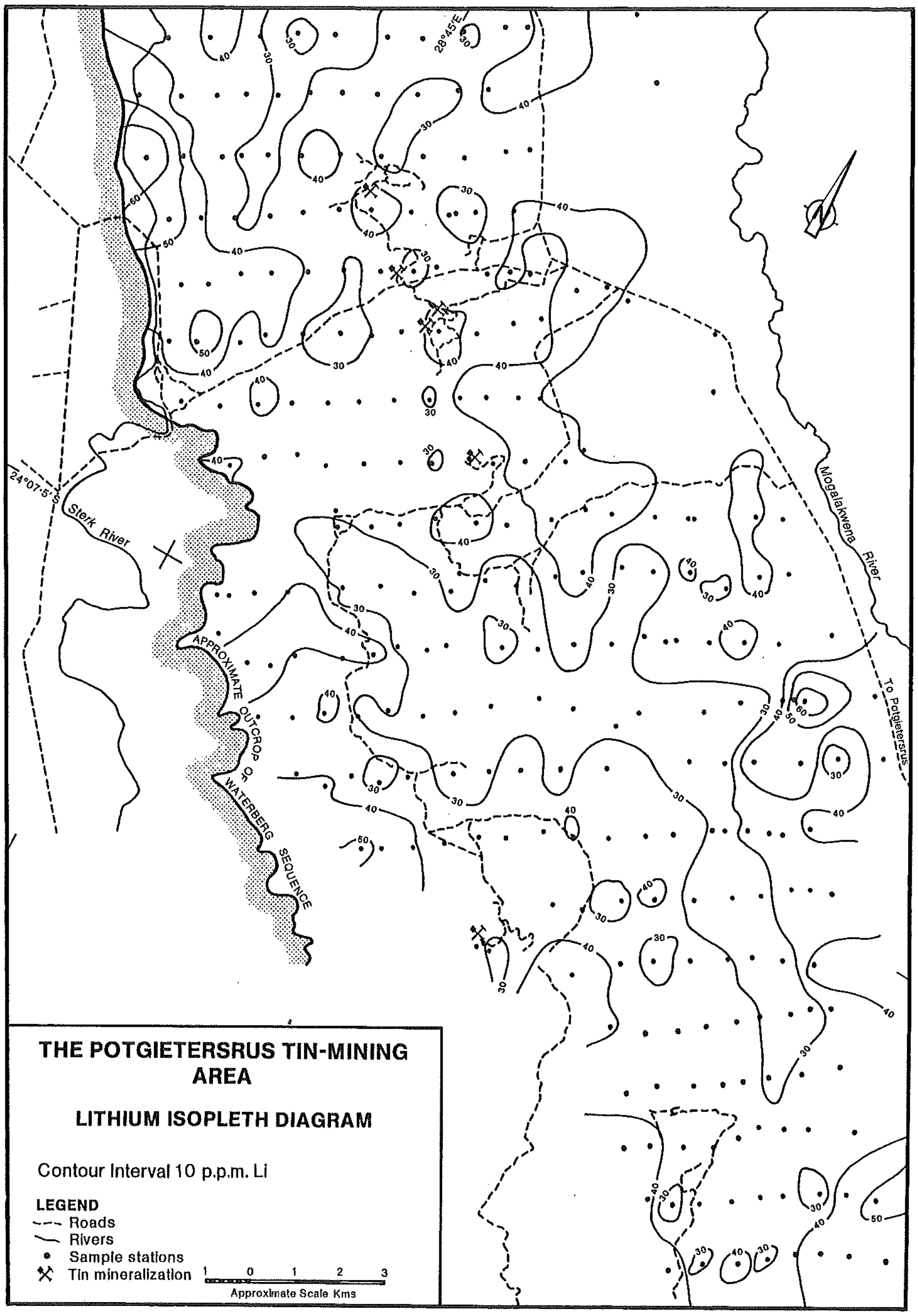

Figure 24 : *Isopleth map of Li content of all rock-types.*

Nickel was determined in only 27 samples, a maximum of 4 ppm Ni being detected in one sample. Despite the low values, the variance is large (see Table VIIIa). The mean Ni/Co ratio in the analyzed samples is 0,4 in the coarse-grained and aplitic granites, whereas it is 0,6 in the feldspar porphyry and 0,3 in the granophyric granite. The felsites have a low ratio of 0,06 and the Bobbejaankop granite a ratio of 0,4. The low concentrations of nickel, together with the low Ni/Co ratio, that is well below the normal crustal ratio of about 2,0 suggests that there has been no contamination of crustal material by meteorite impact. The postulation that the Bushveld Complex owes its origin to an impactite event (Hamilton, 1970) would be lent a measure of support if Ni-concentrations were significantly higher. The salic rocks in the Potgietersrus tin-field carry about one-quarter of the mean concentration of low-Ca granites (Turekian and Wedepohl, 1961).

Rubidium approaches a log-normal distribution in all three main rock-types (Figure 25). The granitic rocks have high concentrations of Rb, particularly the Bobbejaankop granite, that are in excess of the mean for low-Ca granites (Turekian and Wedepohl, 1961). The histograms (Figure 26) show that the coarse-grained and granophyric granites have an approximately unimodal distribution pattern, as do, but less distinctly, the Welgevonden granophyre, the feldspar porphyry, and the felsites. Bimodality is apparent in the Sterk River and Groenfontein granophyres and the aplitic granites. With the exception of these three rock-types, the coefficients of variance are low (See Tables VIb and VIc). The Bobbejaankop granite histogram suggests bimodality despite its low coefficient of variance (see Table VIb).

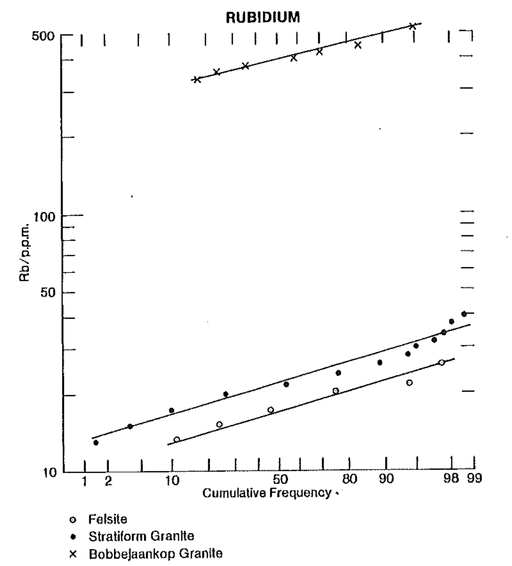

Figure 25 : *Cumulative frequency distribution (log-scale) of Rb in all rock-types.*

There is a slight increase in Rb-concentration from the base of the stratiform granites stratigraphically upwards to the feldspar porphyry. The Rb-isopleth diagram (Figure 27) illustrates the fact that the Bobbejaankop granite can be moderately well defined by the Rb = 300 ppm contour and that Rb-concentrations, in general, show little variation, except for high Rb-contents in Samples L15 (Sterk River granophyre) and K5 (aplitic granite).

The K/Rb ratios (Table VII) show that all the salic rocks, with the exception of the Bobbejaankop granite, fall within the limits of the 'normal' ratios. Certain of the aplitic granites also have low K/Rb ratios. Large-scale fractionation is necessary to account for this enrichment in Rb, for there is no significant change in the K_2O-content.

Scandium distributions have high coefficients of variance in the three main salic units (see Tables VIb, VIc, and VIIIa), that is not obvious from the isopleth diagram (Figure 30), which is contoured at intervals of 5 ppm. The 10 ppm-Sc contour approximately defines the base of the felsite succession in the northern and central parts of the map-area, but, in the south, the 5 ppm contour is close to the base of the felsites. The Bobbejaankop granite has two samples with a Sc-concentration >5 ppm and one with 5 ppm Sc. Sc^{3+} can substitute for Sn^{4+} in cassiterite, but it is not known whether these higher Sc-concentrations in the Bobbejaankop granite can be attributed to this substitution. An anomalously-high Sc-content of 49 ppm occurs in a meta-sedimentary rock at the base of the stratiform granite sheet, and the higher concentrations in the southeastern corner of the map-area are associated with hornfels and other metasediments.

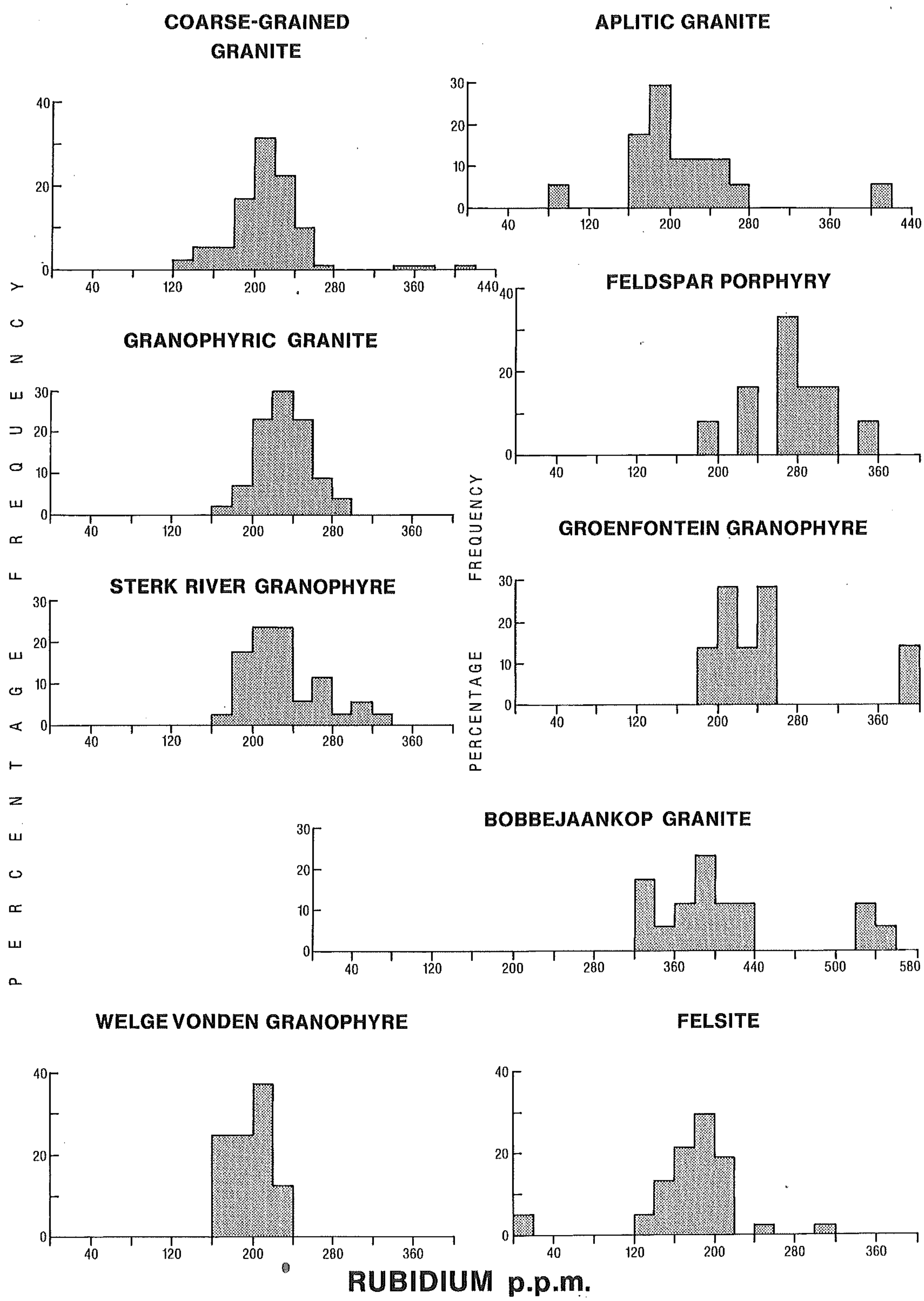

Figure 26 : *Histograms of Rb distribution in different rock-types.*

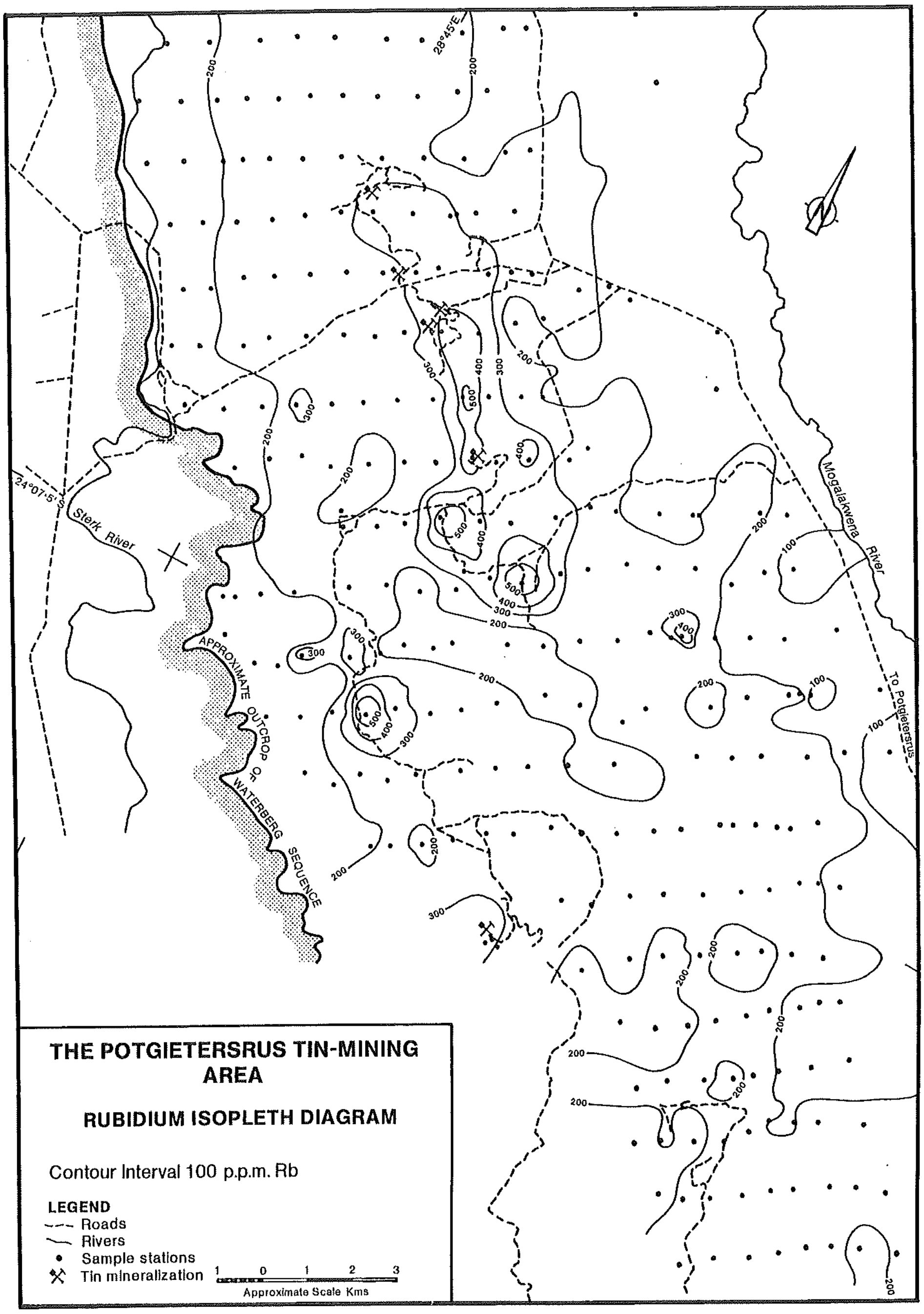

Figure 27 : *Isopleth map of Rb content of all rock-types.*

In both the felsites and stratiform granites, Sc has a log-normal distribution, except below the 10th and above the 90th percentiles, respectively. The Bobbejaankop granite has a distribution that only very crudely approaches log-normal (Figure 28). The histograms (Figure 29) reflect a general unimodal pattern, with the exception of the Bobbejaankop granite and the felsites. There is distinct negative skewness in respect to the Sc-distribution in the Welgevonden granophyre.

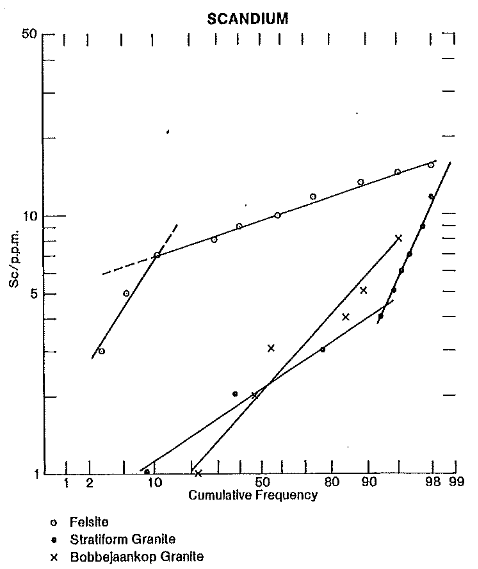

Figure 28 : *Cumulative frequency distribution (log-scale) of Sc in all rock-types.*

There is a good linear relationship between Fe and Sc based on Fourie's (1969) data (Hunter, 1973) in the felsites and stratiform granites, but the Bobbejaankop granite displays erratic concentrations of Fe relative to Sc.

The mean content of 2 ppm Sc in both the stratiform and Bobbejaankop granites is significantly lower than the mean for low-Ca granites (Turekian and Wedepohl, 1961), while the mean for the felsites exceeds this value.

Strontium is approximately log-normal in its distribution in the stratiform and Bobbejaankop granites, but the felsites show a distinct inflection at the 70th percentile (Figure 31). The histograms (Figure 32) illustrate the complex pattern of distribution of Sr in the felsites and suggest that they can be divided into three and, possibly, four distinct groups, on the basis of their Sr-concentrations. The felsites with high Sr-contents (mean 110 ppm Sr) are located, without exception, along the base of the volcanic pile. The aplitic granites again show a bimodal distribution, with two samples having Sr-concentrations in excess of 100 ppm. A trend towards bimodality is apparent in the Sterk River granophyre and the coarse-grained granite. In the latter rock-type, the samples with high Sr-contents are located in close proximity to metasediments near the upper contact of the mafic phase. The unimodal, positively skewed distribution in the feldspar porphyry is distinct. The granophyric granite has a less pronounced unimodal distribution and also includes one sample with 545 ppm Sr (Sample I13), which contributes to the high coefficient of variance in this rock-type (see Table VIb). The isopleth diagram (Figure 32) demonstrates the more erratic distribution of Sr in comparison to Rb. As Sr is mainly distributed in feldspars, apatite, and sphene, its erratic distribution may be part due to varying proportions of the accessory minerals.

Strontium decreases from 43 ppm at the base of the stratiform sheet to 19,7 ppm in the feldspar porphyry at the top. The Bobbejaankop granite is markedly impoverished in Sr (mean 6 ppm). Strontium has been reported to concentrate relative to barium in feldspars from pegmatites (Heier and Taylor, 1959). It can be seen in Figure 9 that the stratiform granites with a mean Ba/Sr ratio close to 20, have a curvilinear distribution field, wherein strontium decreases rapidly, but, as the Bobbejaankop granite field is approached, strontium is enriched relative to barium, although the mean Ba/Sr ratios increase from 22 to 41 in the feldspar porphyry (see Table VII). The Welgevonden granophyre, which, in other respects, is less fractionated than the Bobbejaankop granite, has a similar

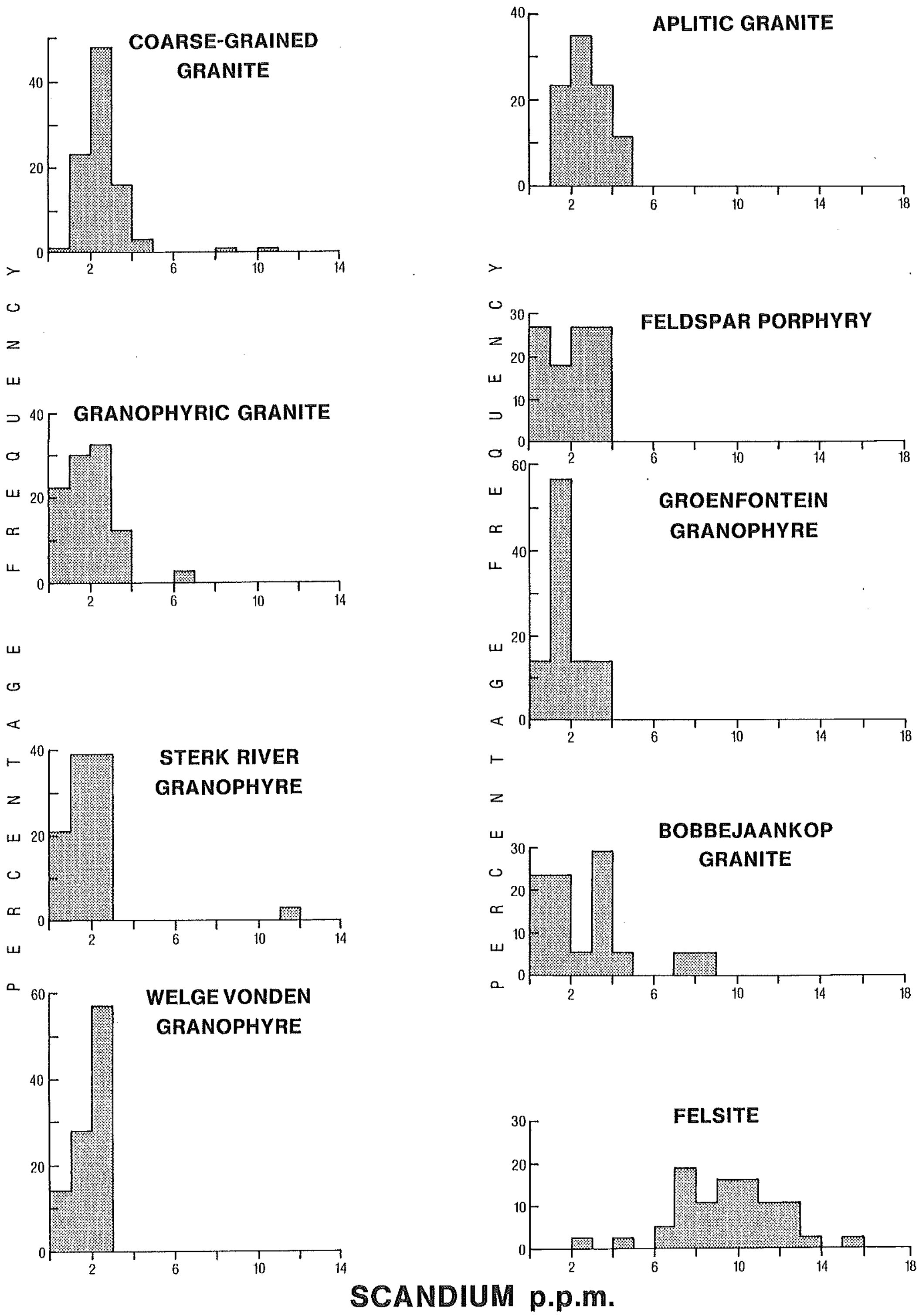

Figure 29 : *Histograms of Sc distribution in different rock-types.*

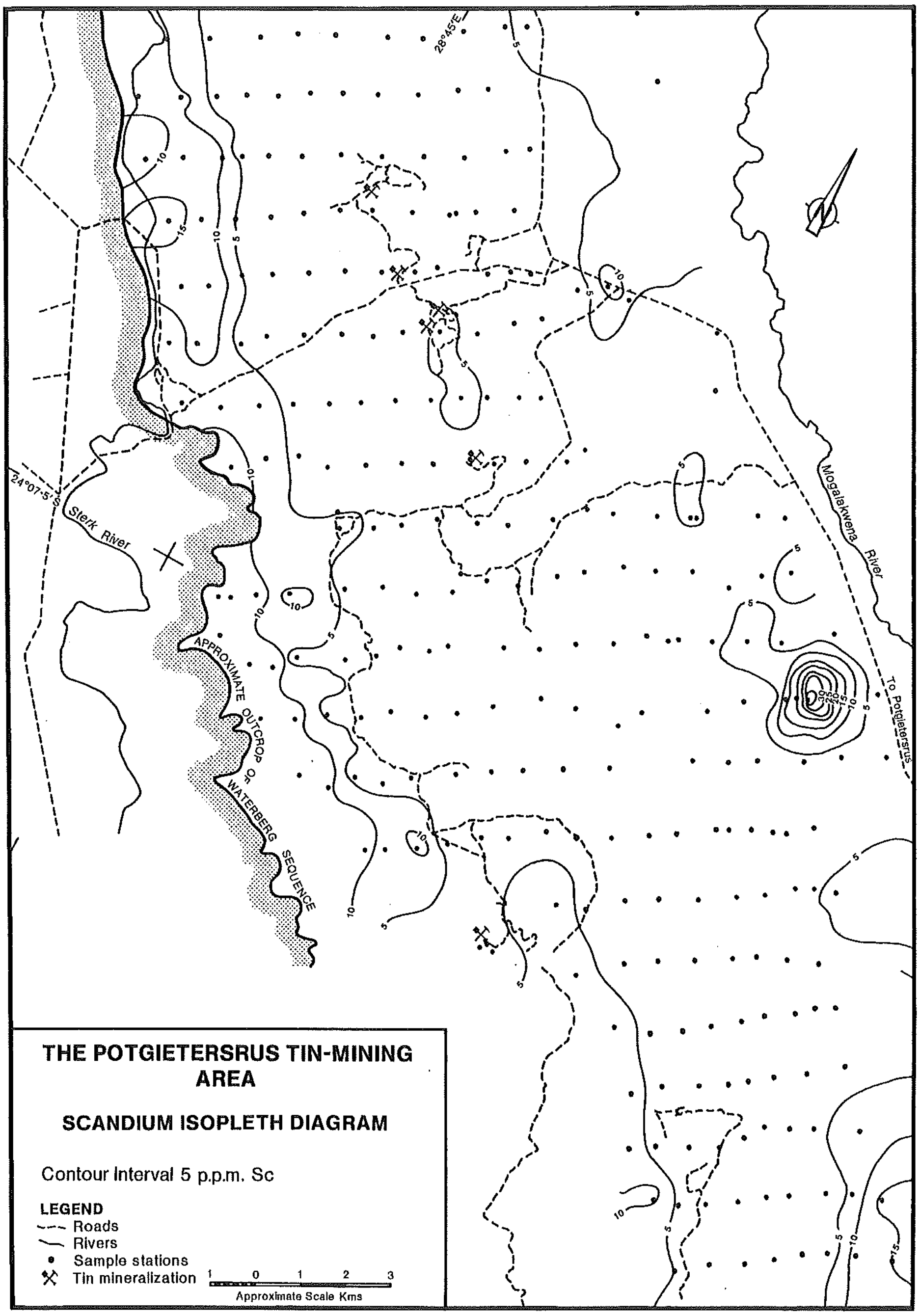

Figure 30 : *Isopleth map of Sc content of all rock-types.*

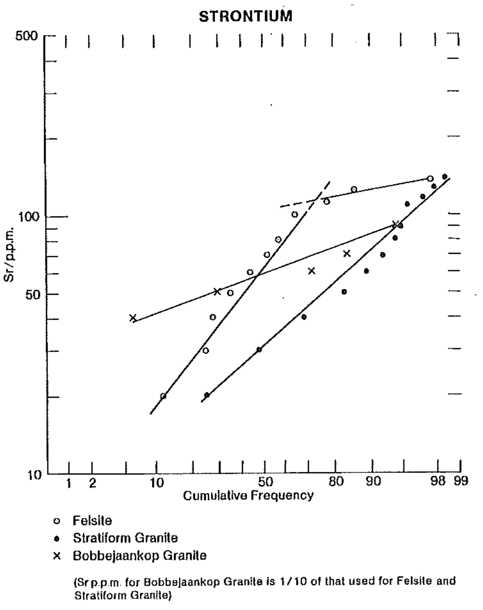

Figure 31 : *Cumulative frequency distribution (log-scale) of Sr in all rock-types.*

Ba/Sr ratio to the Bobbejaankop granite. The depletion in strontium can be provisionally attributed to its entering K sites in company with Ba^{2+}, so that the residual liquid is depleted in barium and strontium. As the Bushveld granites lie close to the ternary minimum in the system SiO_2-$NaAlSiO_4$-$KAlSiO_4$, it is suggested that strontium is concentrated relative to barium in the first crystallization products in a manner similar to that observed in feldspars of pegmatites.

Tin in the stratiform granites of the Potgietersrus tin-field has a median concentration of 6,5 ppm and in the Bobbejaankop granite this value rises to 9 ppm. The mean concentration is hence 2 and 3 times greater than the world-wide average for granitic rocks. Within the economically exploitable ore-bodies in the Bobbejaankop granite, the concentration factor is several hundred times. Sn^{4+} is closest in size to Fe^{3+} and Ti^{4+} and is similar in size to Nb^{5+}, Ta^{5+}, Mo^{4+}, W^{4+}, V^{3+}, Zr^{4+}, and Hf^{4+}. This similarity in size to several cations implies that it can be expected to have a complex behavior. Formation of $(SnO_4)^{4-}$ in silicate melts results from the high ionic potential of Sn^{4+}, which will tend to concentrate in residual melts. Sn^{4+} also substitutes for Ti^{4+} in biotite and sphene, the latter mineral and ilmenite being enriched by factors of 134 and 31 times, respectively, relative to the enrichment in biotite (Lyakhovich and Balanova, 1969). In the Kalba intrusive, it was found that 80 per cent of the tin was held isomorphously in the biotite lattice (Barsukov and Pavelenko, 1956 ; Barsukov, 1957). Hesp (1971) demonstrated that the ability of biotite to accommodate Sn^{4+} in its lattice is proportional to its Li^{+} content and inversely proportional to its content of Mg^{2+}, Ti^{4+}, and Mn^{2+}. Contrary to the findings of Barsukov and Pavelenko (1956), Hesp (1971) found that less than 45 per cent of the total tin content in granitic rocks is held in the biotite, and, in high-tin granites, only 10 to 20 per cent of the tin is carried in the biotite lattice. There are, as yet, no data on the geochemistry of the constituent minerals of the Bushveld salic rocks, so that it is not possible to apportion the whole-rock tin-content. Tin is known, however, to occur as discrete cassiterite grains in ore-bodies of the Bobbejaankop granite.

Tin in the salic rocks of the Potgietersrus tin-field has a log-normal distribution in the stratiform granites and the felsites (Figure 34). Tin in the Bobbejaankop granite is log-normally distributed to the 90th percentile, at which point there is an inflection in the curve. The histograms (Figure 35) reveal that, with the exception of the Bobbejaankop granite and the Groenfontein granophyre, tin distribution has positive skewness in the remaining rock-types. Bimodality is apparent in distribution in the Groenfontein granophyre, and there is a suggestion of this in the feldspar porphyry and the Sterk River granophyre. High coefficients of variance are a feature of the distribution (see Table VIb and C), the highest coefficient being in the Bobbejaankop granite.

The isopleth diagram (Figure 36) picks out two peak-areas of concentration within the Bobbejaankop granite but does not define the mineralization at the Groenfontein mine. Patches of

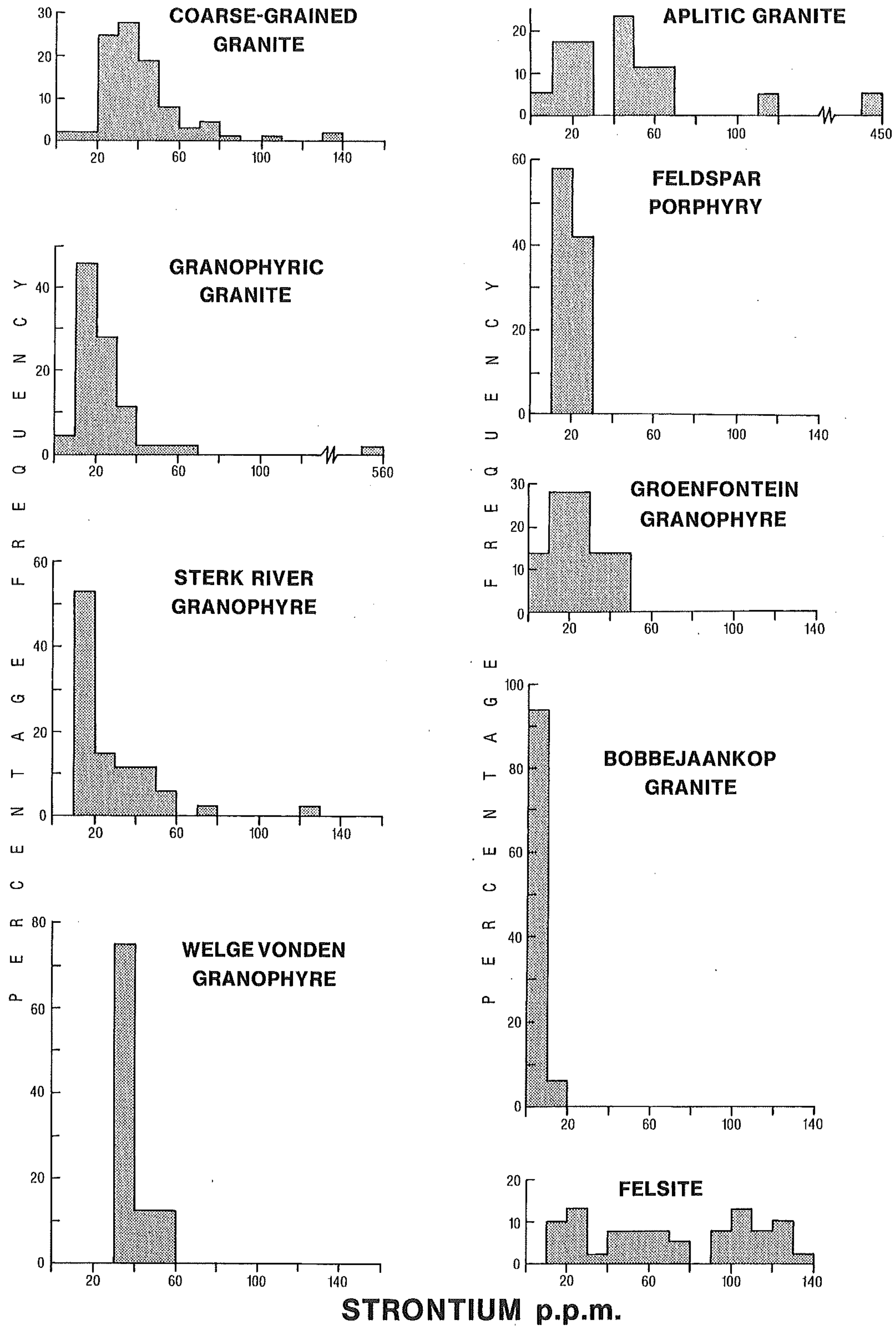

Figure 32 : *Histograms of Sr distribution in different rock-types.*

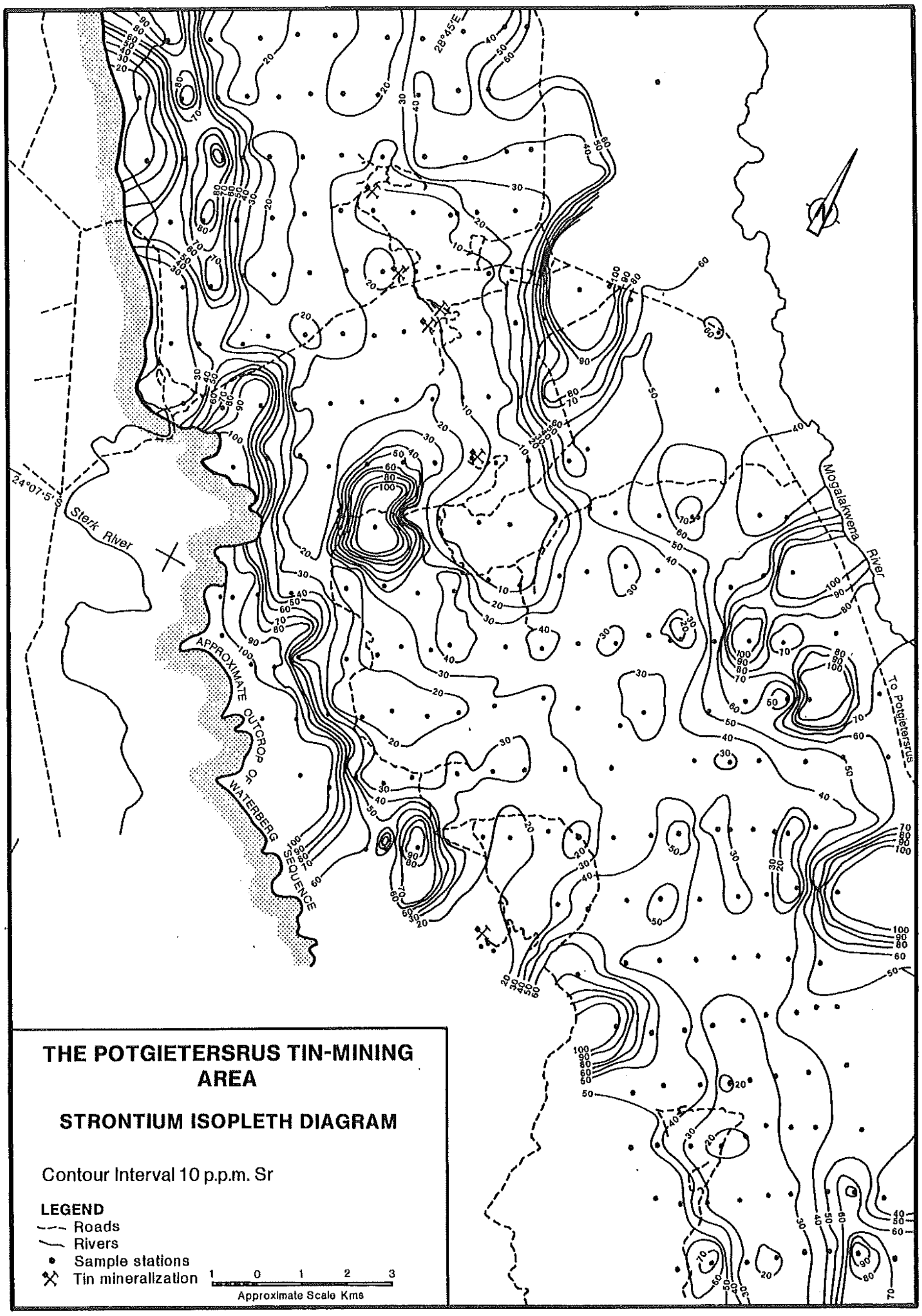

Figure 33 : *Isopleth map of Sr content of all rock-types.*

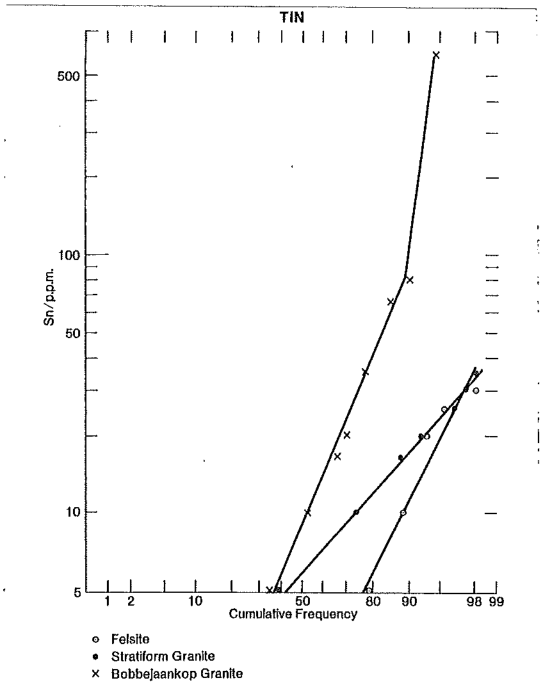

Figure 34 : *Cumulative frequency distribution (log-scale) of Sn in all rock-types.*

higher values are recorded in the feldspar porphyry, while, in the south, there is a band of values >10 ppm within the stratiform granite. One sample with a concentration of 65 ppm was found in the Sterk River granophyre, in the extreme south.

The percentage frequency of occurrence of tin concentrations is listed in Table XI, in which it can be seen that the distribution of values in the Bobbejaankop granite is similar to that in the stratiform granites. It is worth noting that approximately the same percentage of samples of the Bobbejaankop granite have <5 ppm Sn as does the percentage of the stratiform granites. In the granophyric granite, however, only 11,9 per cent of the samples contain <5 ppm. These results indicate that analysis of samples for tin, alone, will not necessarily assist the search for mineralized granites. This is further illustrated by the Sn-concentrations reported from the samples collected about Station H5, where 1242 ppm Sn was recorded. The additional samples about this station had contents that ranged from 13 to 1123 ppm.

There is no clear-cut relation between high concentrations of tin and any other particular element. However, it is apparent that higher tin-contents may be expected in those granites that are impoverished in Ba, Sr, and Ti, and enriched in Rb, F, and Nb. Fourie's (1969) data point to enrichment in Th being an additional factor, that is supported by the high gamma radiation recorded over the Bobbejaankop granite during the present study.

Titanium is log-normally distributed in the stratiform granites but shows a tendency towards a double log-normal distribution in the felsites and the Bobbejaankop granite (Figure 37). The coefficients of variance (Table VIb and c) are highest in the aplitic and Bobbejaankop granites. The high variance in the coarse-grained granite can be attributed largely to contamination at the base of the stratiform sheet, where the meta-sedimentary relics occur. In the other rock-types, the titanium content varies within narrow limits. The histograms (Figure 38) of the aplitic granites illustrate the complexity of the titanium distribution in these rocks. The Groenfontein granophyre has a more complex pattern than the other members of the stratiform granites (with the exception of the aplitic granites).

The isopleth diagram (Figure 39) shows the increase in titanium as the felsites are approached, together with the more erratic high values associated with the base of the stratiform granite sheet.

Figure 40 shows the linear relationship between Zr and Ti in the stratiform and Bobbejaankop granites. The marginal phase of the latter (i.e. the Lease microgranite) shows an increase in Zr, relative to Ti. Theoretically, the Ti/Zr ratio should increase with fractionation for, when Zr^{4+} substitutes for Ti^{4+}, it forms a more ionic bond and should thus substitute for titanium in early formed

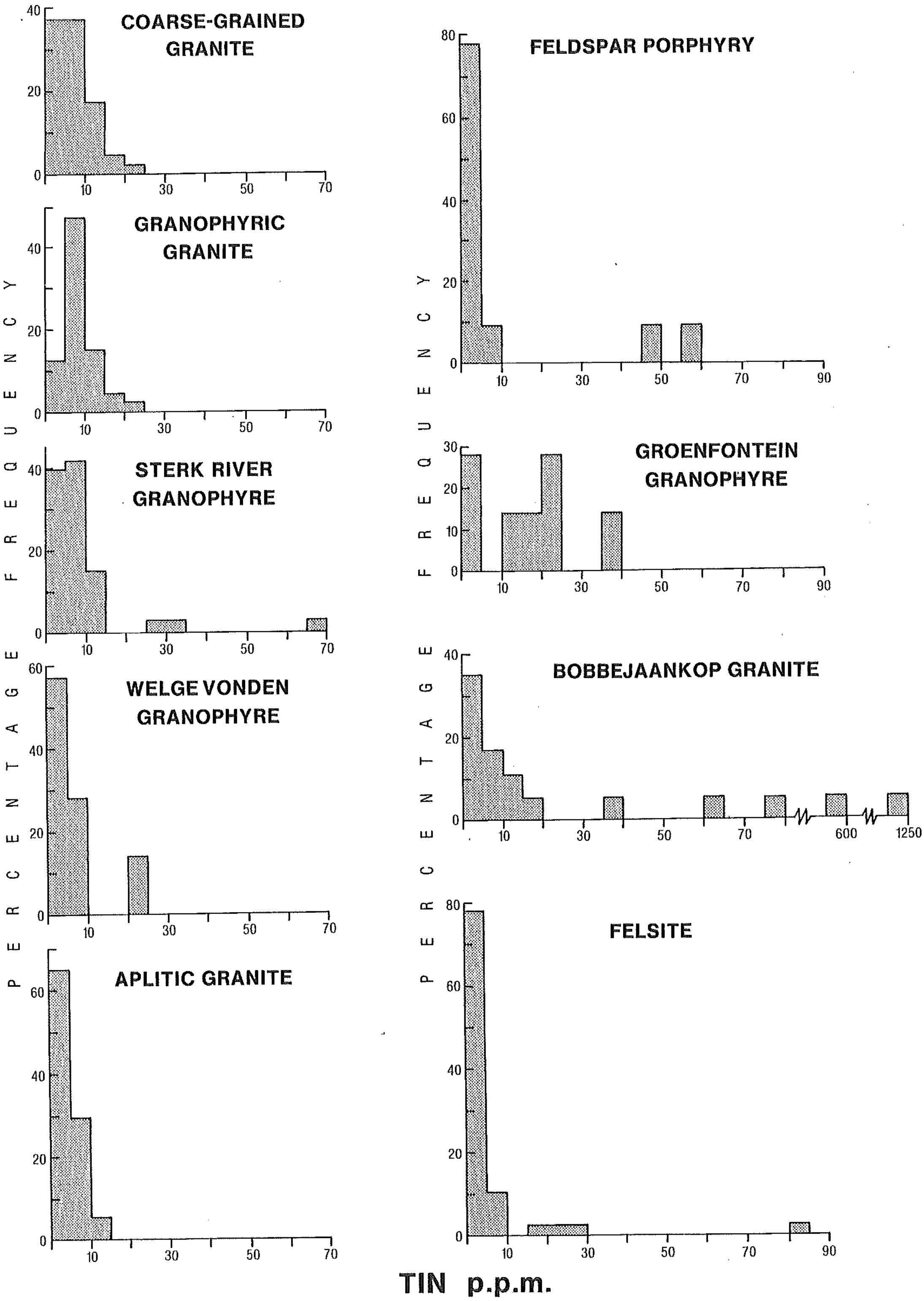

Figure 35 : *Histograms of Sn distribution in different rock-types.*

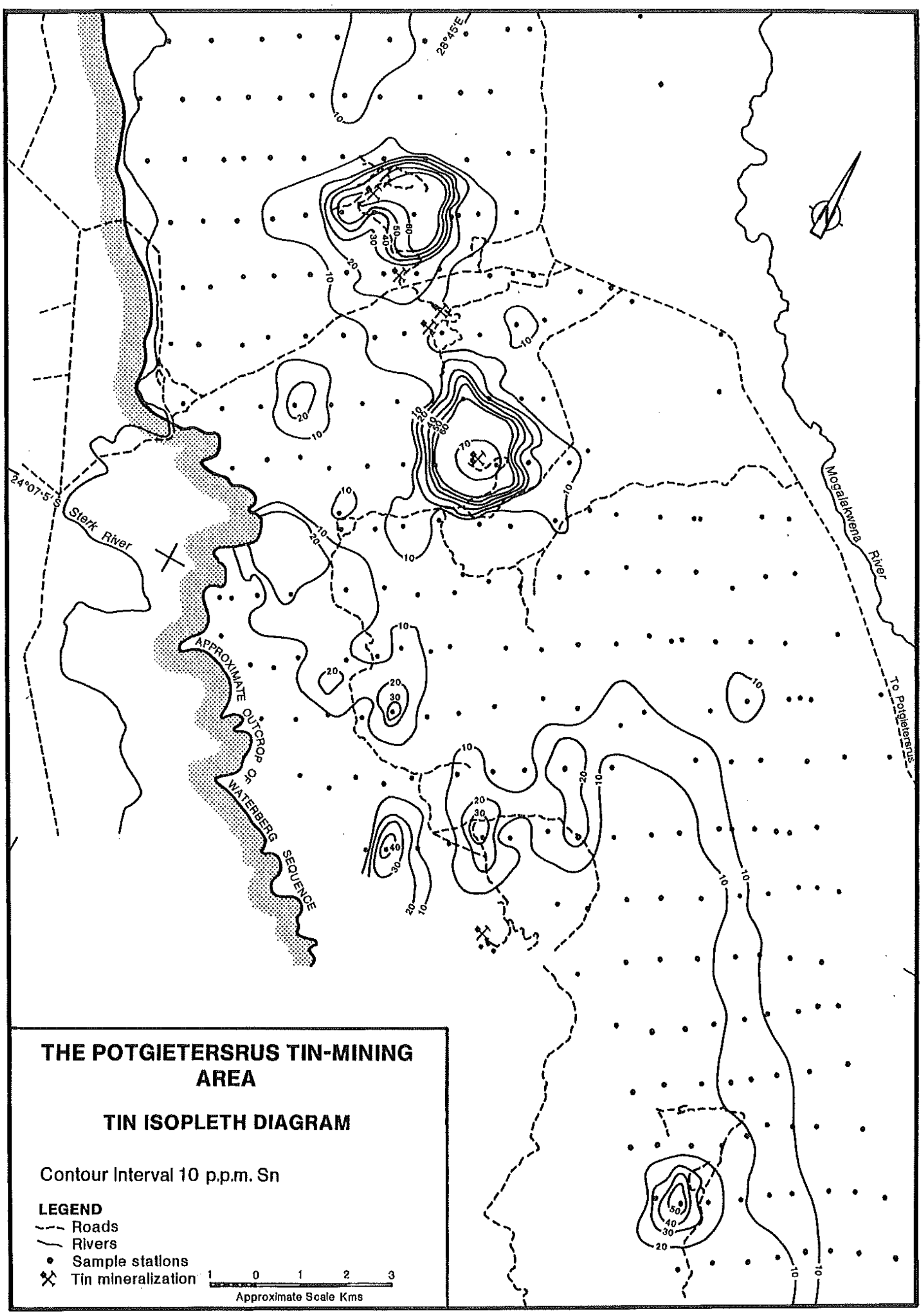

Figure 36 : *Isopleth map of Sn content of all rock-types.*

TABLE XI : Frequency of Occurrence of Tin (in ppm) in the Field-Map Units of the Acid Phase of the Bushveld Complex in the Zaaiplaats Tin-Mining Area

Sn (ppm)	Coarse Grey Granite		Bobbejaankop Granite		Rooiberg Felsites		Aplites and Porphyritic Granite		Granophyric	
	% of Samples	Cumulative %	% of Samples	Cumulative %	% of Samples	Cumulative %	% of Samples	Cumulative %	% of Samples	Cumulative %
>5	37,5	37,5	29,4	29,4	78,4	78,4	70,6	70,6	11,9	11,9
5- 9	36,9	72,6	23,5	52,9	10,8	89,2	23,5	94,1	50,0	61,9
10- 14	19,0	91,6	11,7	64,6			5,9	100,0	16,7	78,6
15- 19	6,0	97,6	5,9	70,5					11,9	90,5
20- 24	2,4	100,0			5,4	94,6			2,4	92,9
25- 29					2,7	97,3			4,7	97,6
30- 34			5,9	76,4						
50- 59									2,4	100,0
60- 64			5,9	82,3	2,7	100,0				
75- 79			5,9	88,2						
585- 589			5,9	94,1						
1240-1244			5,9	100,0						

Sn (ppm)	Sterk River Granophyre		Groenfontein Granophyre		Feldspar Porphyry		Welgevenden Granophyre		Blinkwater Granophyre and Welgevonden Metasediments	
	% of Samples	Cumulative %	% of Samples	Cumulative %	% of Samples	Cumulative %	% of Samples	Cumulative %	% of Samples	Cumulative %
>5	34,3	34,3	28,6	28,6			50,0	50,0	100,0	100,0
5- 9	42,9	77,2			75,0	75,0	37,8	87,8		
10-14	14,3	91,5	14,3	42,9	8,4	83,4				
15-19			14,3	57,2						
20-24			28,6	85,8			12,2	100,0		
25-29	2,8	94,3								
30-34	2,8	97,1								
35-39			14,2	100,0						
45-49					8,3	91,7				
60-64	2,9	100,0			8,3	100,0				

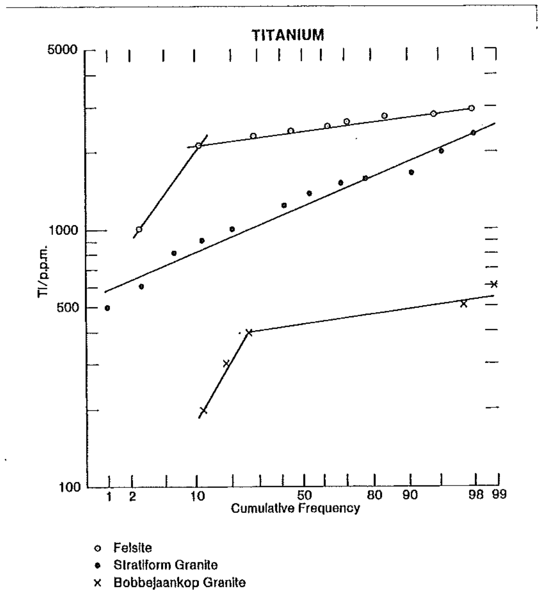

Figure 37 : *Cumulative frequency distribution (log-scale) of Ti in all rock-types.*

phases. However, an analysis, by Dr. G. Hornung, of cassiterite from the Zaaiplaats tin mine, at the northern end of the Bobbejaankop granite pluton, reveals that its Zr-content is 538 ppm. It is thus probable that the presence of cassiterite, with high concentrations of zirconium, could mask the theoretically expected trend of fractionation.

The impoverishment in Ti by a factor of 3 in the Bobbejaankop granite, relative to the stratiform granites, is marked. The marginal facies of the Bobbejaankop granite is impoverished even more, by a factor of 5. The mean Ti-concentration in the stratiform granites is in close accord with that for low-Ca granites (Turekian and Wedepohl, 1961).

Yttrium was determined in 46 samples and displays a progressive enrichment from the felsites to the Bobbejaankop granites. Coefficients of variance (Table VIIIa) are low in the felsites and the Bobbejaankop granite and intermediate in the stratiform granites, the higher coefficients of variance in the latter group being attributable to the more erratic distribution of Y in the aplitic granites and the felspar porphyry. Variance about sample stations is low in all rock-types, except in the marginal facies of the Bobbejaankop granite and the feldspar porphyry (Table XII).

TABLE XII : Means and Standard Deviations of Yttrium about Sample Stations and of Yttrium in Coarse-grained Granite, Granophyric Granite, and Aplitic Granite

Rock-type	Mean $\bar{x}$	Standard Deviation σ	$\sigma/\bar{x}\%$
Coarse-grained granite (C6)	92	11,66	12,67
Aplitic granite (E4)	128	12,69	9,91
Feldspar porphyry (K14)	112	31,67	28,28
Bobbejaankop granite (H5)	145	36,02	28,84
Bobbejaankop granite (J10A)	161	23,90	14,84
Felsite (J17)	61	2,96	4,85
Coarse-grained granite (regional)	97,4	19,46	20,00
Granophyric granite (regional)	84	10,65	12,67
Aplitic granites (regional)	126	65,75	52,18
Felsite (regional)	56,5	7,04	12,4

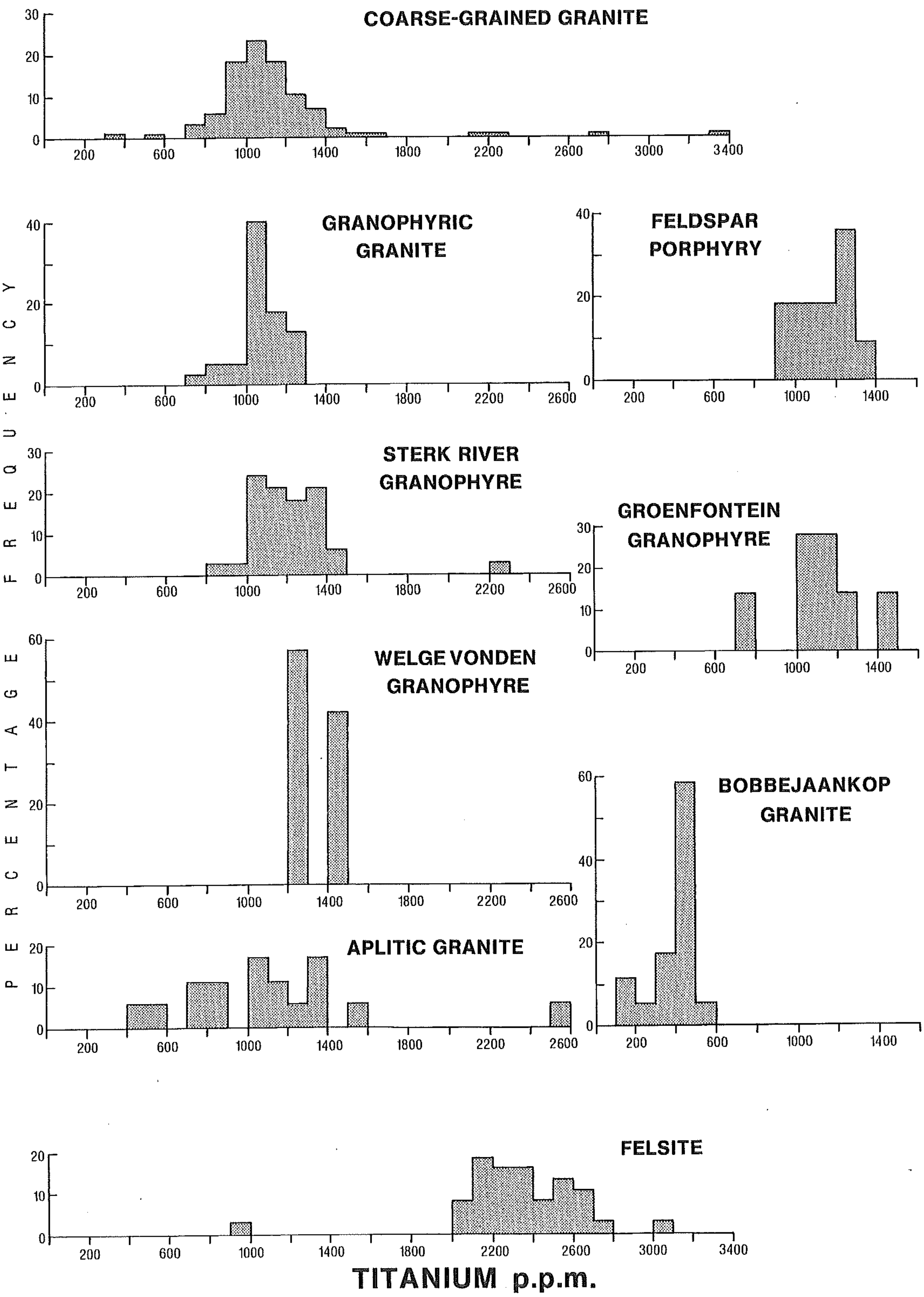

Figure 38 : *Histograms of Ti distribution in different rock-types.*

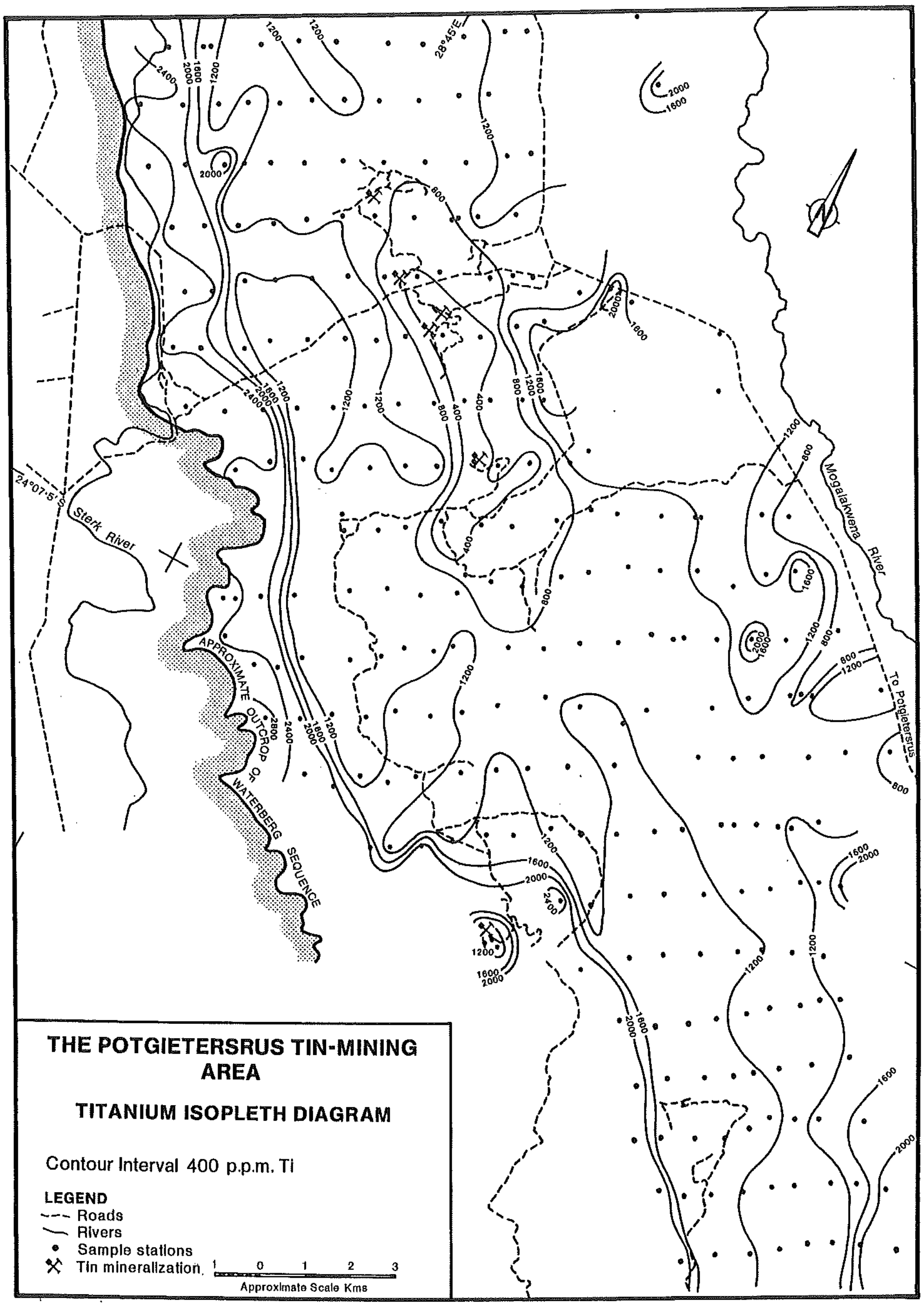

Figure 39 : *Isopleth map of Ti content of all rock-types.*

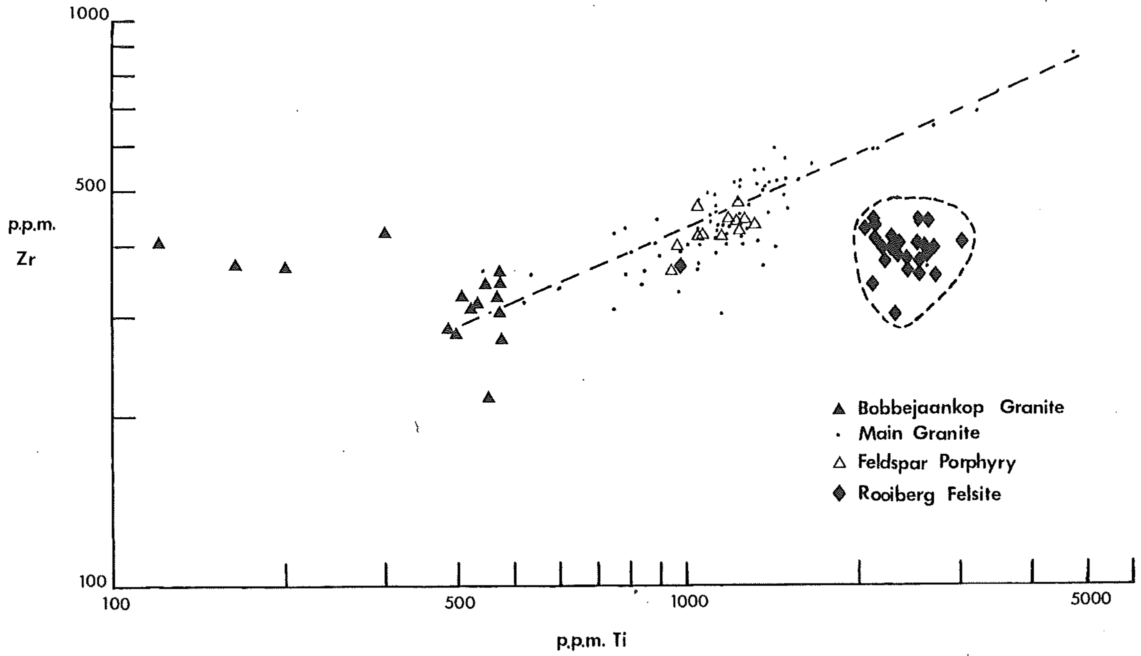

Figure 40 : *Scatter-diagram of Zr vs. Ti for the granitic rocks and felsites*

Y^{3+}, being closest in size to Ca^{2+} among the major cations, would be expected to be captured in early calcium positions. However, together with the lanthanides, yttrium is concentrated in the late-phase Bobbejaankop granite. It is possible that their concentration is due to the more covalent character of the RE-O bonds, compared to Ca-O bonds (Taylor, 1965).

Zinc is log-normally distributed in the felsites and approaches a log-normal distribution in the stratiform granites, although there is a slight inflection at about the 40th percentile (Figure 41).

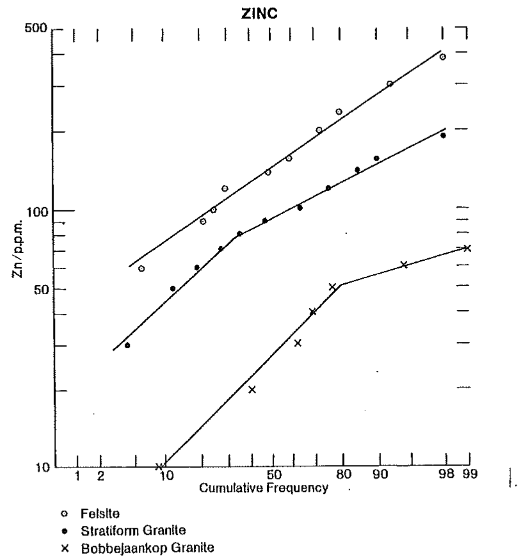

Figure 41 : *Cumulative frequency distribution (log-scale) of Zn in all rock-types.*

The Bobbejaankop granite distribution has a marked inflection at the 80th percentile. High coefficients of variance characterize the granophyric and Bobbejaankop granites and the felsites, as compared to the variance in the coarse-grained granite, Sterk River granophyre and feldspar porphyry. The histograms (Figure 42) suggest a complex distribution pattern for zinc, there being in the felsites seven analyses with values >250 ppm Zn. Two analyses of a similar order of magnitude were reported in the Sterk River granophyre and granophyric granite, the samples being from stations adjacent to each other. The possibility of a relation between mineralization and the fracture pattern has been discussed previously, and the isopleth diagram (Figure 43) indicates that, in the felsites, particularly, stratigraphic levels also may be preferentially enriched in Zn. An analysis of Fourie's (1969) results shows that felsites impoverished in Ca, Na, and Sr and enriched in Rb and K carry higher concentrations of Zn, but this pattern was not identified as being consistent in the present data. The distribution and relation of Zn concentration in the felsites requires further investigation, particularly as three of the high-Zn felsites in this area also have Sn concentration >20 ppm. The zinc content of the stratiform granites is significantly higher than in the world mean for low-Ca granites (Turekian and Wedepohl, 1961), while the Bobbejaankop granite is impoverished.

Zirconium is log-normally distributed in the three main groups of salic rocks, there being a close correspondence between the felsites and the stratiform granites. The Bobbejaankop granite is slightly impoverished in Zr, relative to the other rock-types (Figure 44). The uniformity in the distribution of Zr is reflected in the low coefficients of variance (Table VIa and b). Both the Sterk River granophyre and the aplitic granites display polymodality in the histograms (Figure 45). The salic rocks are enriched by a factor of two, relative to the low-Ca granites (Turekian and Wedepohl, 1961), but the felsites have lower concentrations of Zr than those reported in African anorogenic acid extrusives (Rooke, 1971). The isopleth diagram (Figure 46) again reflects the regular distribution of Zr.

Potassium and Sodium are the only major cations, other than calcium, for which analytical data are available. Potassium has a uniform distribution in the granitic rocks, as shown by the coefficients of variance (Table VIb and c). The felsites display a slightly greater variance, that is reflected in the histograms (Figure 47), and, which may be due to devitrification following their extrusion. The potassium content of the granitic rocks is in accord with that determined for low-Ca granites.

Sodium has higher coefficients of variance than potassium, the histograms (Figure 48) indicating bimodality in the feldspar porphyry, Sterk River granophyre, aplitic granites, Bobbejaankop granite, and the felsites. The isopleth diagram (Figure 49) illustrates the tendency for the lower part of the granite sheet to carry slightly higher concentrations of Na, due largely to contamination by metasedimentary remnants. The felsites have a mean concentration of Na that is slightly less than the granites, but the mean K/Na ratio remains nearly constant in all three main groups.

The K_2O:Na_2O ratios of the various granites and felsites (Figures 50 and 51) show a clustering about 1,5. A group of felsites impoverished in Na_2O plot along the K_2O ordinate. These samples are also significantly depleted in Sr (mean 19 ppm) and Ca, and depleted in Ba by a factor of 1/5, relative to the mean concentration in felsites. In two of the samples, Rb is enriched by a factor of two. Low-Na felsites have also been reported (Fourie, 1969) from other areas within the Bushveld Complex. Crockett (1971) has shown low sodium-contents in Ventersdorp acid volcanics from Botswana, to which he attributed an origin due to gas-fluxing. He found evidence for sodium-impoverishment and enrichment in K and Si across a gas-blasted fissure. The low-Na felsites in the Potgietersrus tin-field cannot be definitely accounted for due to proximity to such a fissure, but, significantly, the samples were gathered from areas which have maximum, or close to maximum, fracture densities. Fourie (1969) has reported one major element analysis of a Na-poor felsite that is enriched in silica and is strongly peraluminous, both of which characteristics were noted by Crockett (1971) in Botswana. Coetzee (1970) has commented on the low-Na quartz-feldspar porphyry from the Swaershoek area north of Nylstroom, suggesting that, in the absence of evidence for widespread hydrothermal activity, water generated by the devitrification of volcanic glass was the agent in forming illite and chlorite from the volcanic matrix. The abnormal character of these acid volcanics results in the wide scatter of felsite plots on Q-Ab-Or diagrams, that have led to suggestions that the felsites did not have normal magmatic crystallization history.

Gamma flux density, although not a geochemical parameter, can be conveniently considered at this point. Figure 52 demonstrates the generally uniform nature of the level of radioactivity in the stratiform granites and the felsites. However, the Bobbejaankop granite is clearly defined. Fourie's data (1969) show that the Th concentration in this granite has a mean of 49,5 ppm, which represents a twofold increase relative to the stratiform granites. It is concluded that the higher gamma radiation in the Bobbejaankop granite can be attributed to the greater concentration of Th. No data are presently available concerning the content of U in this granite, nor in which minerals these radioactive elements are located.

(iii) Blinkwater Granophyre and Associated Metasedimentary Rocks

This group of rock-types has not been considered in the preceding account, except to draw attention to their presence as to the cause of the perturbation of the isopleth contours at the base of the stratiform granite sheet. As might be expected, the concentrations of the different elements show

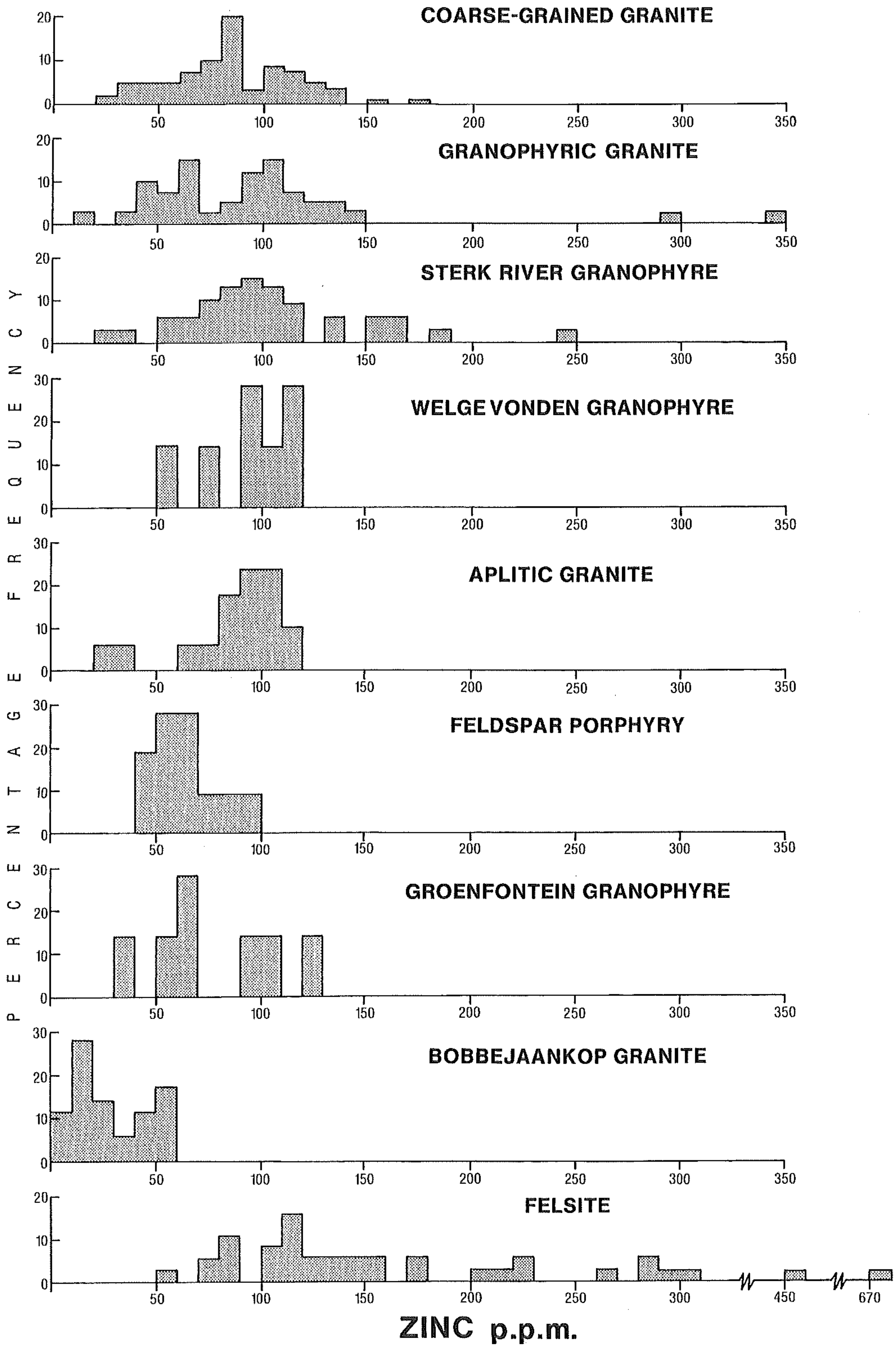

Figure 42 : *Histograms of Zn distribution in different rock-types.*

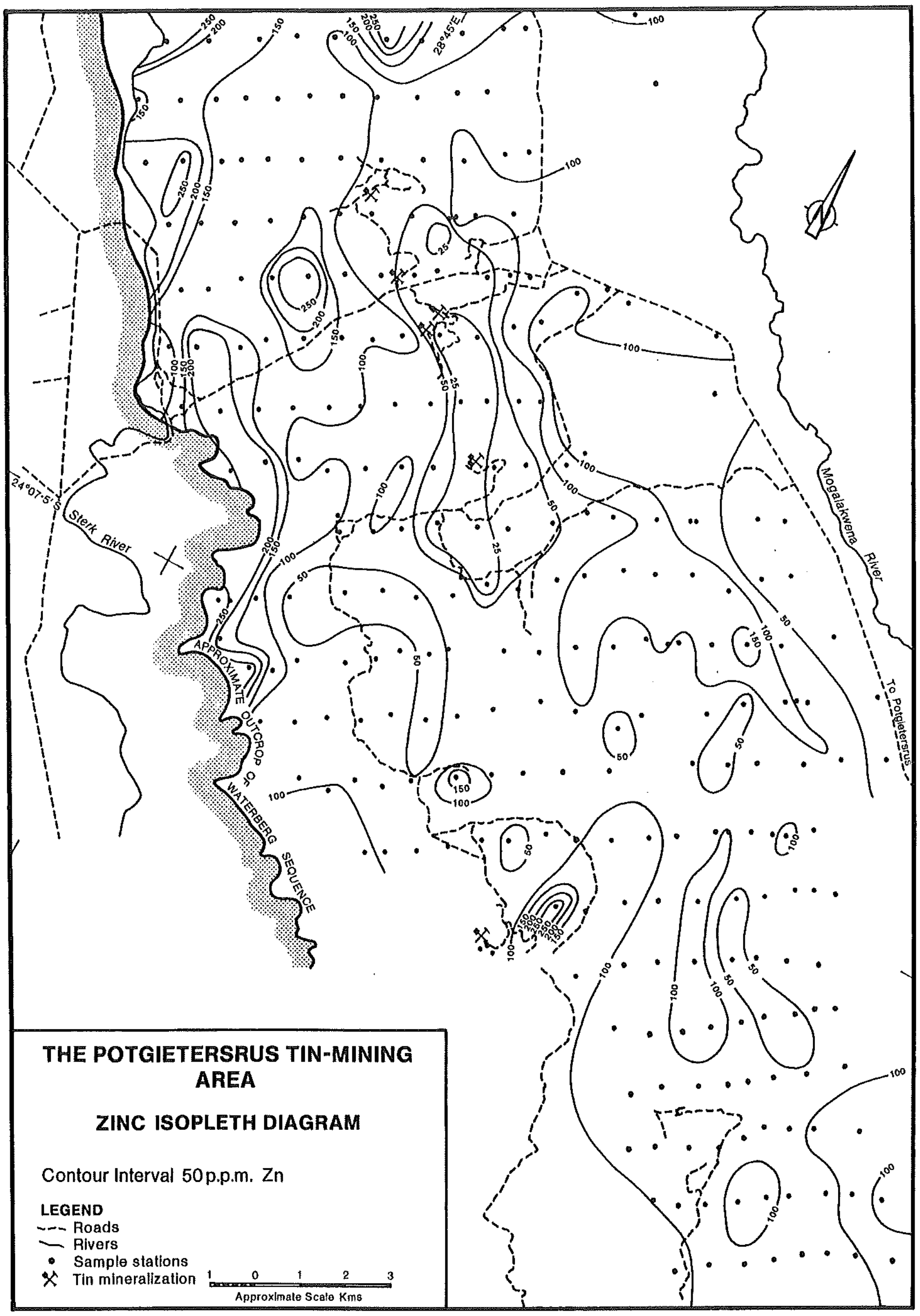

Figure 43 : *Isopleth map of Zn content of all rock-types.*

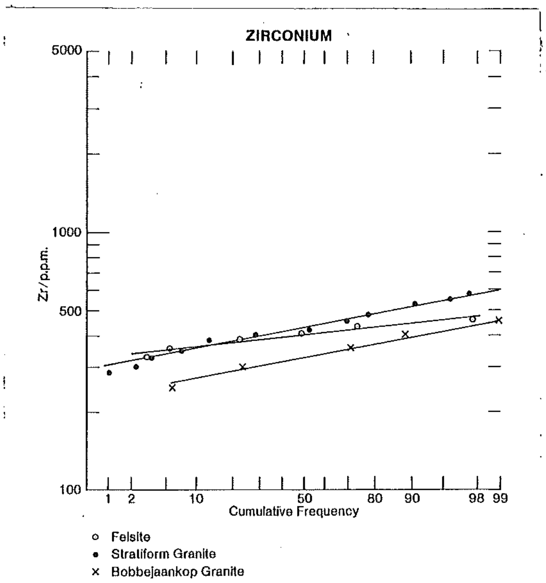

Figure 44 : *Cumulative frequency distribution (log-scale) of Zr in all rock-types.*

wide ranges reflecting the diversity of rock-types included in this group. Twelve samples were analyzed, of which two are granophyric. Feldspathic quartzites constitute the main rock-type analyzed and these display wide variations in all the elements. The coefficients of variance (Table XIII) illustrate the erratic distribution of the elements and places a major constraint on theories proposing that the stratiform granites were derived by the recrystallization of sedimentary rocks.

TABLE XIII : Means, Standard Deviations, and Coefficients of Variance in the Metasedimentary Rocks and Their Mobilized Equivalents

	Ba	Ca	Co	La	Li	Rb	Sc	Sn	Sr	Ti	Zn	Zr	K_2O%	Na_2O%
$\bar{x}$	982	13186	14	72	41	146	10	3	82	2153	98	436	4,14	3,36
σ	610	15835	8	40	11	77	12	1	55	1632	40	169	1,7	0,88
$\sigma/\bar{x}$%	62	120	58	56	27	53	120	33	67	76	41	39	42	26

(iv) Geochemical Variations in the Bobbejaankop Granite

In the foregoing discussion, the Bobbejaankop granite has been treated as a single unit. Strauss (1954) recognized a finer-grained marginal facies, to which he applied the name Lease microgranite. So far, in this account, this microgranite, although recognized as a distinct facies, has not been specifically distinguished. Of the seventeen samples of Bobbejaankop granite collected, only four belong to this marginal phase. Statistically, this distribution is inadequate to draw firm conclusions, in view of the fact that coefficients of variance of element distribution are known to be high in the Bobbejaankop granite. Bearing this constraint in mind, the mean concentrations of major and trace elements for which analytical data are available show (Table XIV) that the marginal facies is enriched in Ca, Li, Rb, Sc, Sr, and Zr and depleted in Ba, Co, La, Ti, and Zn. The apparent enrichment in Sn in the marginal phase is due to the very high Sn-concentration in one sample and may not be valid. This seems to be borne out by the fact that the economically exploited ore-bodies occur in the Bobbejaankop granite at the Zaaiplaats mine. No samples of the granite that carries disseminated cassiterite have been analyzed, so that it is not possible to discuss the distribution of economically viable concentrations of cassiterite at this stage.

The analyses for Ce, Nb, Ni, and Y, provided by Dr. Hornung, have not been used in the tabulation because only one sample, plus nine samples about this station, were analyzed. The results suggest that Ce, Y, and Ni are depleted in the marginal zone, whereas Nb is enriched, a finding that is supported in respect to Ce and Nb by Fourie (1969).

The finer-grained facies of the Bobbejaankop granite has a mean K_2O content of 4,91 per cent compared to 4,86 per cent in the main phase. Conversely, the marginal phase shows a decrease in Na_2O from 3,03 per cent in the coarse-grained Bobbejaankop granite to 2,45 per cent, which results in an increase of K_2O:Na_2O ratio from 1,6 to 2,0.

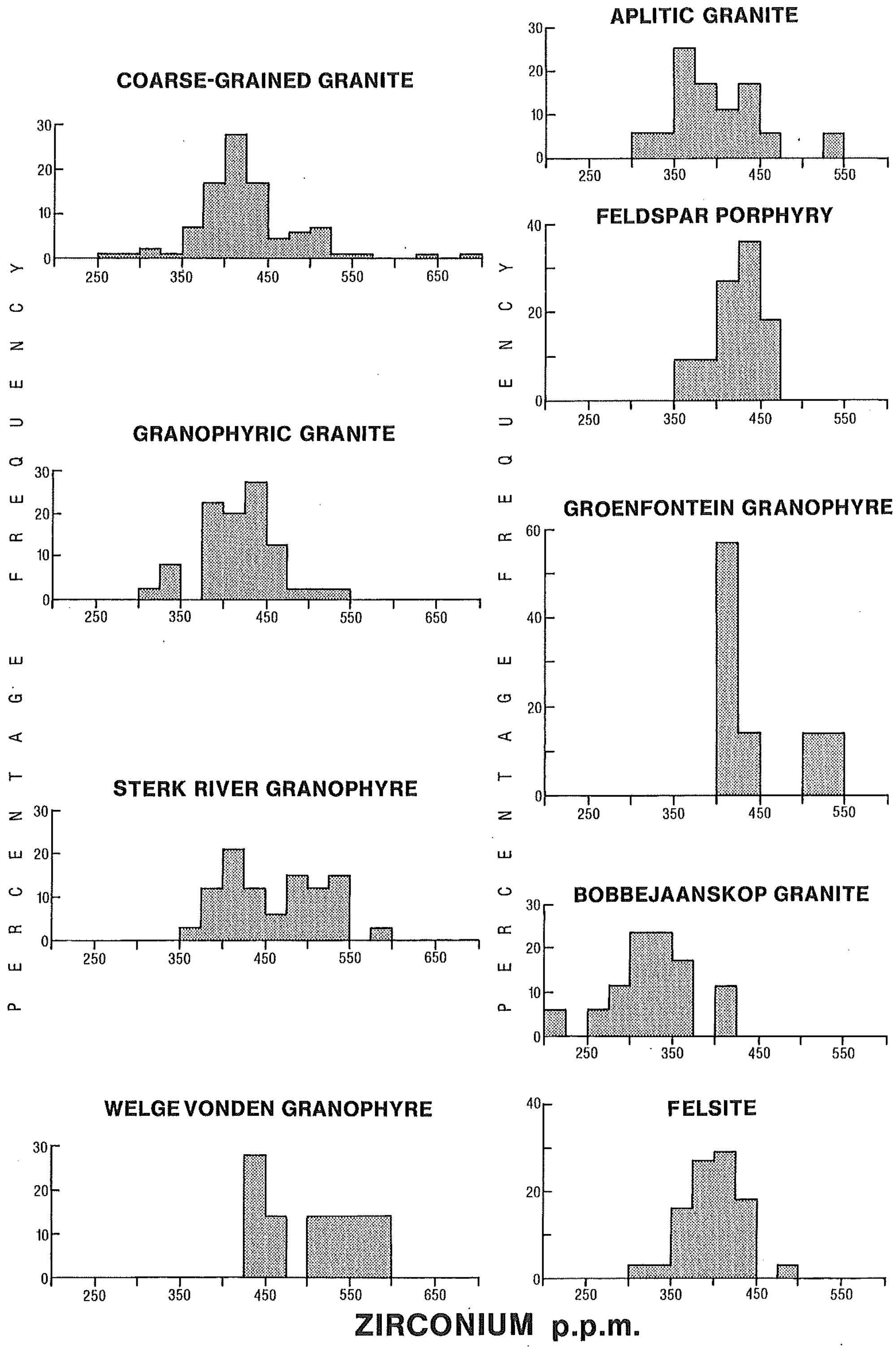

Figure 45 : *Histograms of Zr distribution in different rock-types.*

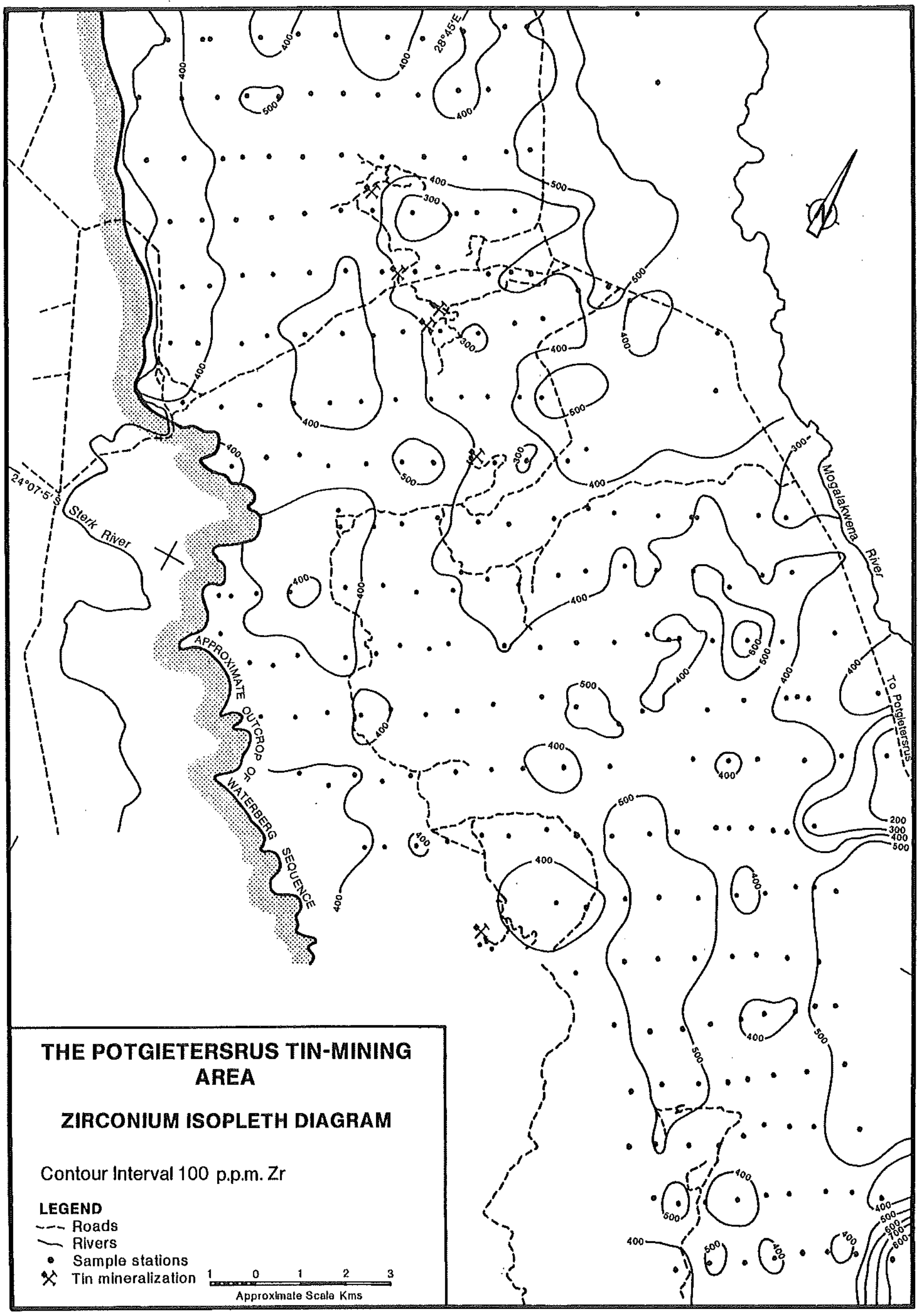

Figure 46 : *Isopleth map of Zr content of all rock-types.*

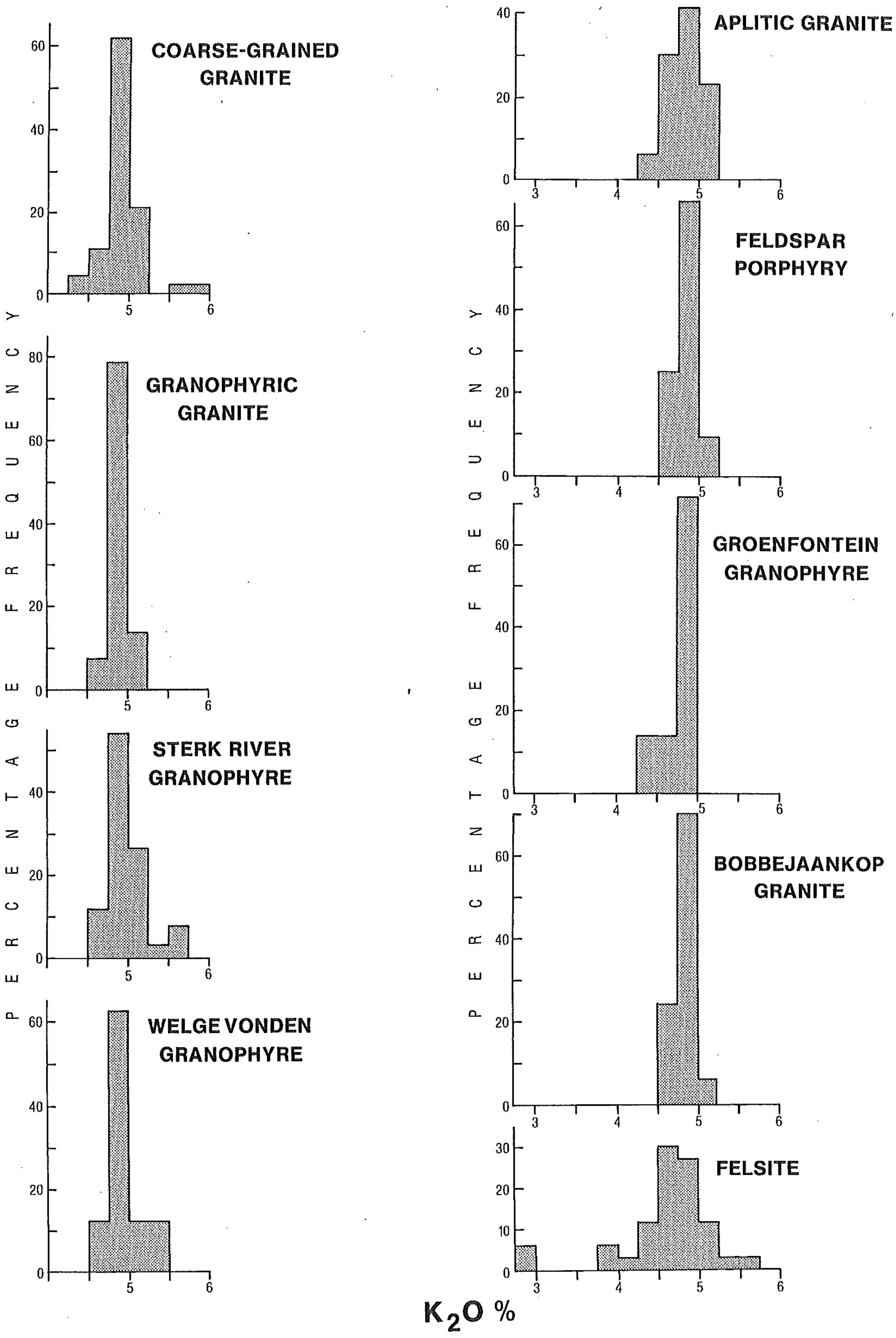

Figure 47 : *Histograms of K distribution in different rock-types.*

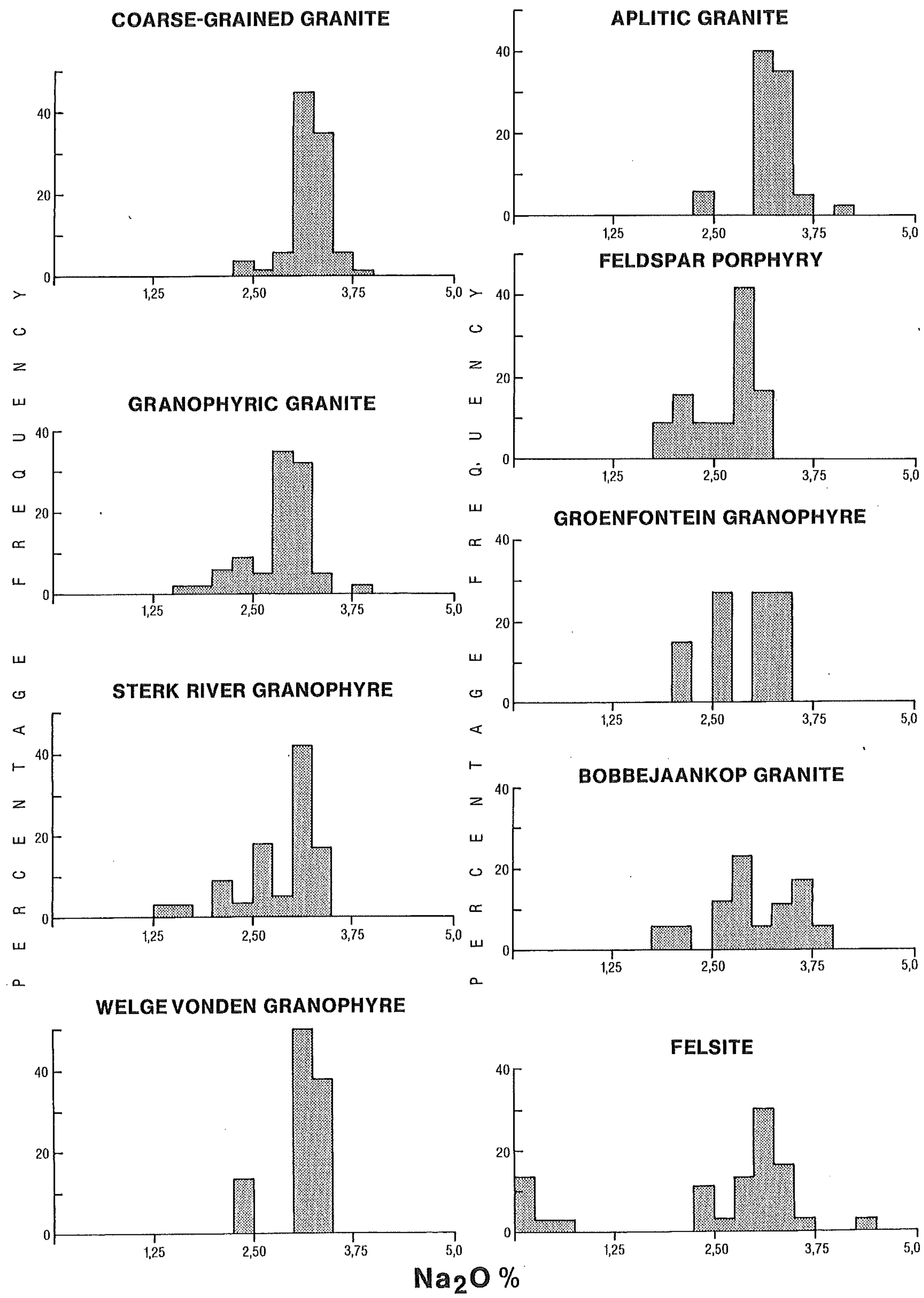

Figure 48 : *Histograms of Na distribution in different rock-types.*

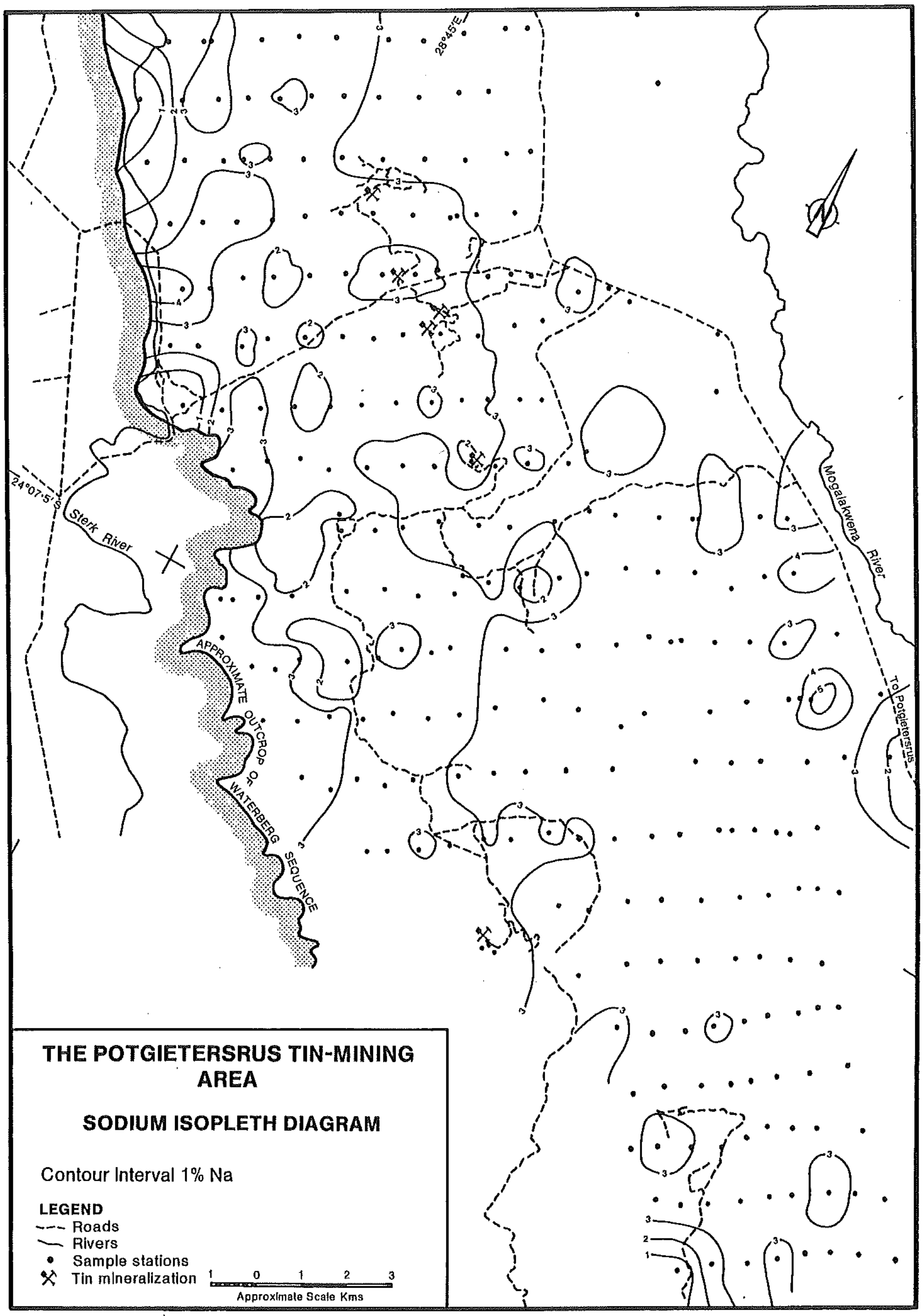

Figure 49 : *Isopleth map of Na content of all rock-types.*

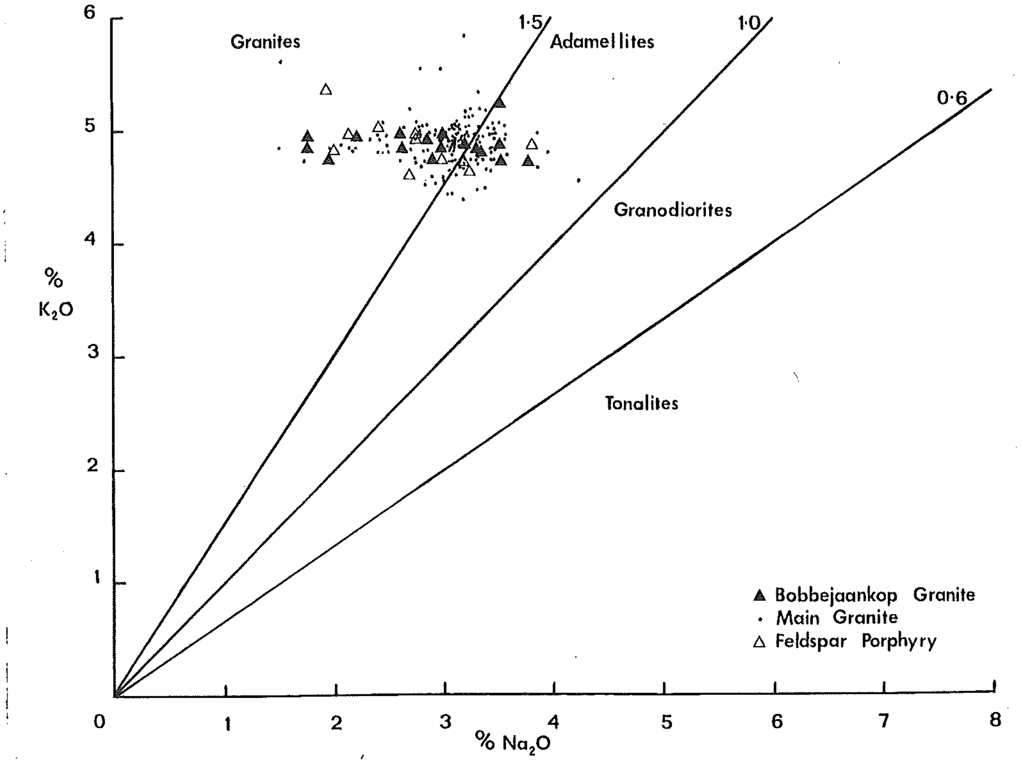

Figure 50 : *Scatter-diagram of K_2O vs. Na_2O for the granitic rocks.*

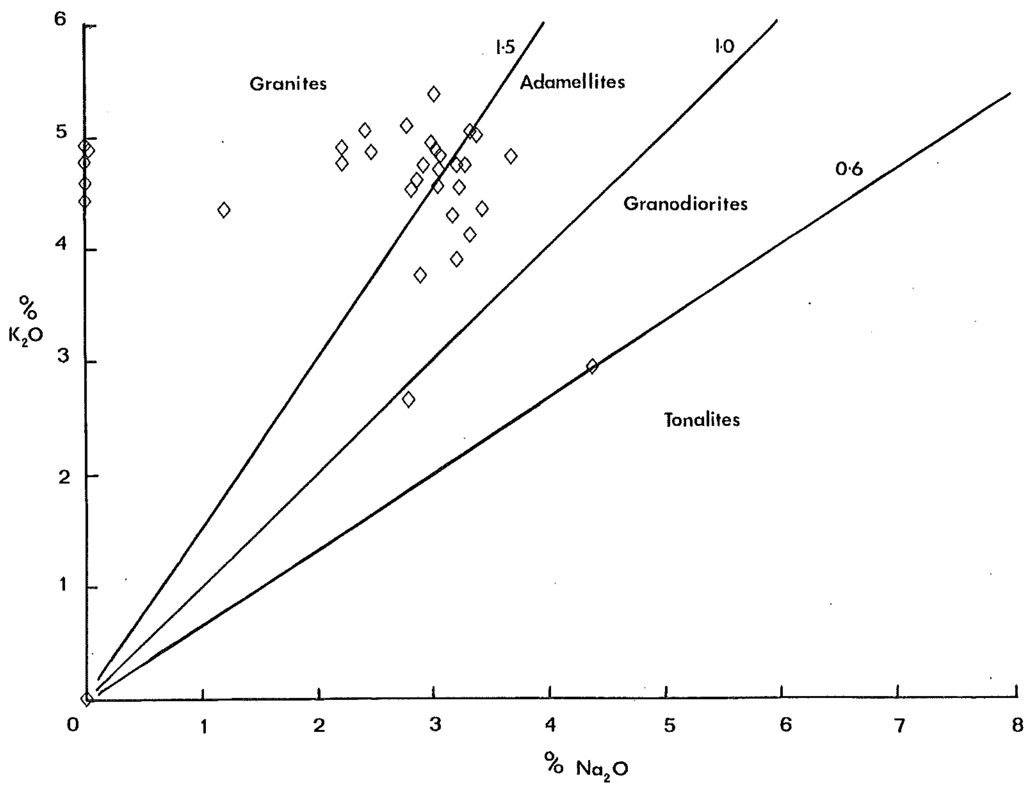

Figure 51 : *Scatter-diagram of K_2O vs. Na_2O for the felsites.*

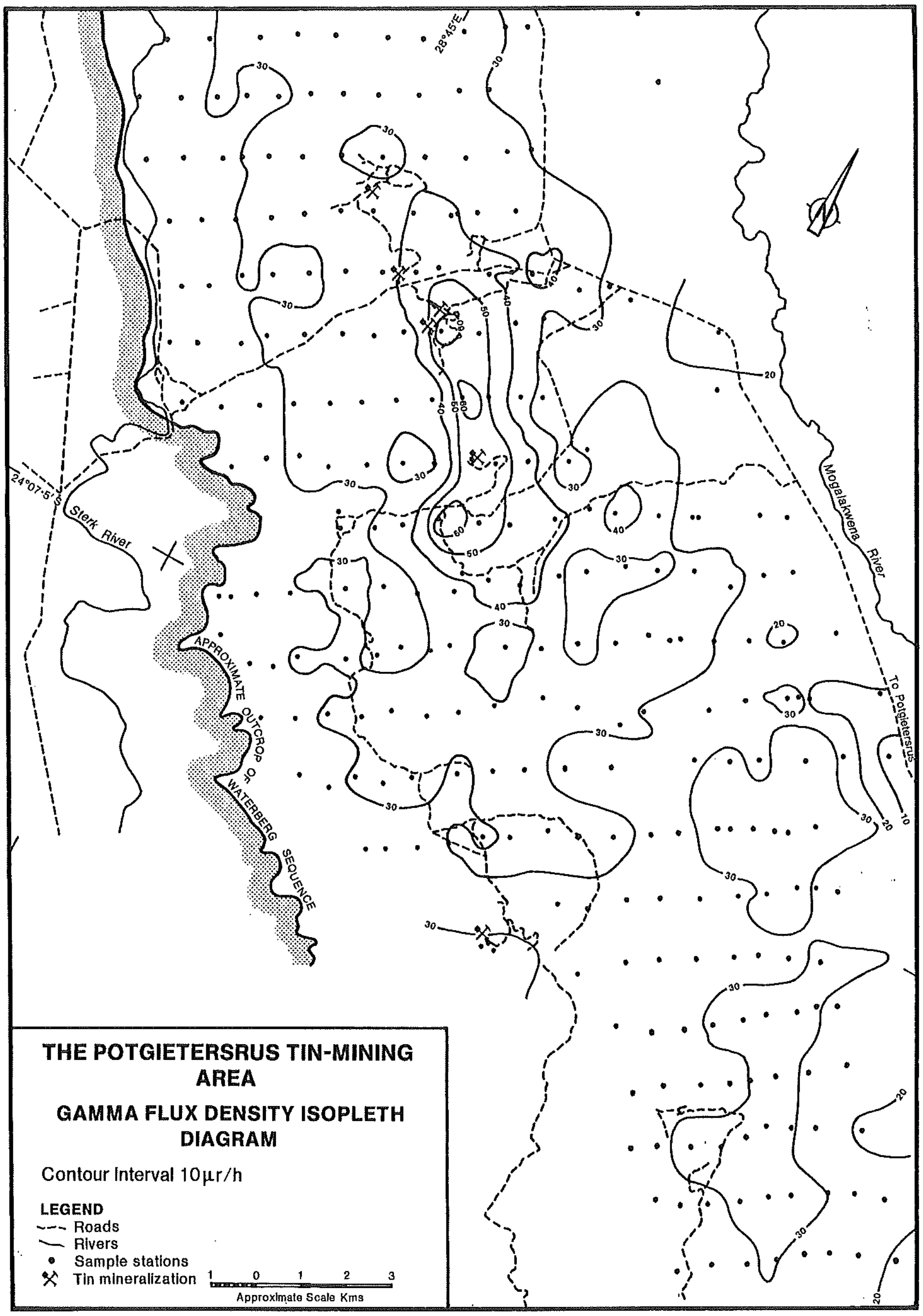

Figure 52 : *Isopleth map of gamma-flux density over all rock-types.*

TABLE XIV : Mean Concentrations of Major and Trace Elements in the Bobbejaankop Granite

	Ba	Ca	Co	La	Li	Rb	Sc	Sn	Sr	Ti	Zn	Zr
Marginal facies	211	17381	1,5	73,5	42	485	5,25	328	10	196	14,5	376
Main facies	238	6193	2,3	132,6	33,5	385	2,75	63	6	441	30,7	303

	K/Rb	Rb/Sr	Ba/Sr	Ba/Rb	Ti/Zr	K/Ba	Sc/Ti
Marginal facies	88	48,5	21,1	0,43	0,52	192,7	0,026
Main facies	106	63,1	39,7	0,62	1,12	171,4	0,006

N.B. : Co data from Leeds University analyses.

The microgranite displays, in respect to its low K/Rb, Ba/Sr, and Ba/Rb ratios, features that are suggestive of extreme fractionation. Fourie (1969) showed that the Ti/Nb, Zr/Nb, K/Cs, and Ba/Cs ratios decreased in the microgranite. The rare earth elements lanthanum and cerium, together with yttrium, are present in lower concentrations than in the main mass of the Bobbejaankop. The total rare earth element concentration decreases in the microgranite and is, in fact, close to the total in the stratiform granites (Fourie, 1969). The increase in Zr in the marginal granites may be due to the increased content of cassiterite that has been shown to carry significant concentrations of this element and is therefore a sampling bias, due to the random selection of more stanniferous microgranite samples.

Ringwood (1955) proposed that the concentration of scandium in pegmatites and residual melts is due to the presence of excess anions permitting Sc^{3+} to form $(ScO_4)^{5-}$ tetrahedra, the large size of which prevents their inclusion in silicates. Scandium can also substitute for Sn^{4+} in cassiterite and this may also influence the concentration in the microgranite. Until the geochemistry of individual minerals has been investigated, more definitive reasons for the apparently abherrant distribution of certain trace elements cannot be discussed. It is clear, however, that the weight of evidence favours the view that the microgranite crystallized from a residual liquid, even more fractionated than the main mass of the Bobbejaankop granite.

The enrichment in calcium in the marginal phase can probably be related to the presence of carbonate and fluorite, but there are not adequate data as yet to demonstrate this conclusively.

(v) Mean Compositions of the Main Rock Types

In Tables VIa, VIc, and VIIIa, the mean compositions of the various rock-types are given. It has also been shown that the analytical results from this investigation are in good accord with those previously obtained by Fourie (1969), except insofar as the Co- and Ce-concentrations are concerned. In the former case, the Co-values obtained by Fourie (1969) and Hornung are accepted, but it has not been found possible to resolve the contrast between the high Ce-values reported by Leeds and the lower values of Fourie (1969). As a first approximation in estimating the mean compositions, the values given by Fourie (1969) are accepted. It should, however, be noted that Edge and Ahrens (1962) report a cerium-concentration in Bobbejaankop granite that is of the same order of magnitude as that given in the Leeds analyses.

In Table XV, the mean compositions of the felsites, the stratiform granites, and the Bobbejaankop granites have been calculated from the new analytical data presented and from those of Fourie (1969) and Strauss (1954).

Tables XV and XVI illustrate the fact that, although there are similarities in major element chemistry between the stratiform granites and the mean for low-Ca granites, there are significant differences in the ratios, particularly in respect to K/Rb, Ba/Sr, Ti/Zr, Sc/Ti, Nb/Zr, and Rb/Sr. The significantly higher Ca/Sr ratio reflects the abundance of fluorite and/or carbonates in the stratiform granites, as well as its impoverishment in Sr.

The high content of Cs in the felsites (Fourie, 1969) is unexpected and requires explanation by more detailed study of its distribution in the constituent minerals of the felsite.

TABLE XV : Mean Composition of Felsite, Stratiform Granite, and Bobbejaankop Granite in the Potgietersrus Tin-Field Compared to Low-Ca Granites (Turekian and Wedepohl, 1961) and Anorogenic Acid Intrusives and Extrusives (Rooke, 1971)

	Felsite	Stratiform Granites	Bobbejaankop Granite	Low-Ca Granites	Anorogenic Acid Intrusives	Anorogenic Acid Extrusives
Si%	33,75	35,42	35,32	34,70	33,98	33,10
Ti%	0,23	0,11	0,04	0,12	0,16	0,18
Al%	6,36	6,42	6,62	7,20	6,62	6,72
Fe^{3+}%	3,06	1,32	0,90	1,42*1	1,19	2,31
Fe^{2+}%	1,82	0,96	0,78		1,33	0,83
Mn%	0,10	0,04	0,02	0,04	0,06	0,10
Mg%	0,22	0,18	0,14	0,16	0,16	0,16
Ca%	0,70	0,50	0,82	0,61	0,69	0,51
Na%	1,97	2,19	2,13	2,58	3,16	3,56
K%	3,59	4,08	4,03	4,20	4,15	3,75
P%	0,03	0,01	0,01	0,06	0,04	0,03
CO_2%	-	0,15	0,45	-	-	-
F%	-	0,30	0,54	0,09	0,21	0,14
Ba ppm	1100	830	220	840	420	590
Ce ppm	100	139	150	92	-	-
Co ppm	4,50	1,50	1,50	1	<10	<10
Cs ppm	6,70	2,70	6,30	4	-	-
Hg ppm	6	6	8,60	3,90	-	-
La ppm	60	90	105	55	160	155
Li ppm	40	34	35	40	66	20
Nb ppm	18	24	56	21	100	175
Ni ppm	0	1	1	4,50	<10	<10
Rb ppm	180	220	400	170	255	120
Sc ppm	9,60	2	2	7	<10	<10
Sn ppm	<5*2	6,50*2	9*2	3	-	-
Sr ppm	70	40	6	100	71	69
Th ppm	16	22,50	49,50	17	-	-
Y ppm	58	97	146	40	130	99
Zn ppm	125	95	24	39	-	-
Zr ppm	400	400	310	175	460	610

*1 Total Fe *2 Median value.

(vi) Geochemistry of Cassiterite in Zaaiplaats Mine

One sample of cassiterite obtained from the mine workings at Zaaiplaats, by countesy of the mine management, was analyzed by Dr. Hornung, with the following result (in ppm, except for Sn) :

Ce	Co	La	Nb	Ni	Rb	Sc	Sn	Sr	Y	Zn	Zr
697	0	486	240	5	2	2	71%	4	129	3	538

Although only one sample was analyzed, it does represent a mean for the composition of cassiterite in the Zaaiplaats area, because the sample was obtained from the mine mill. This also

TABLE XVI : Ratios of Elements in Felsite, Stratiform Granite, and Bobbejaankop Granite Compared to Low-Ca Granites (Turekian and Wedepohl, 1961) and African Anorogenic Acid Intrusives and Extrusives (Rooke, 1971)

	Felsite	Stratiform Granite	Bobbejaankop Granite	Low-Ca Granites	Anorogenic Acid Intrusives	Anorogenic Acid Extrusives
K/Rb	200	185	100	247	162	310
K/Ba	32,60	49	173	50	100	63,50
Ba/Rb	6,10	3,80	0,55	5	1,60	5
Ba/Sr	15,70	21	36,70	8,40	6	8,50
Ca/Sr	100	125	1366	51	86	100
Ti/Zr	5,75	2,75	1,30	6,80	3,40	3
$Sc x 10^4/Ti$	41,70	18,10	50	58	-	-
$Nb x 10^3/Ti$	7,80	21,80	140	17,30	62,50	97
$Nb x 10^3/Zr$	45	60	180	120	217	287
K/Cs	5360	15100	6400	10500	-	-
Zr/Hf	66,70	66,70	36	45	-	-
$Th x 10^4/K$	4,40	5,50	12,30	4	-	-
Rb/Sr	2,60	5,50	66,70	1,70	3,60	1,70
K/Na	1,82	1,86	1,89	1,60	1,30	1,05
Ba/Cs	164	306	35	210	-	-

places a constraint on the interpretation of the analytical data, in that a small percentage of impurity may have been present. However, the high percentage of Sn indicates that the cassiterite was essentially free of impurities.

Comparison of the Nb and Sc data, the only common trace elements, from Zaaiplaats with those from Siberia indicates that the Zaaiplaats cassiterite has Nb concentrations that are higher than might be expected, in view of the low Sc-content. The tin mineralization in the Bobbejaankop granite is associated with arsenopyrite, chalcopyrite, pyrite, sphalerite, bornite, molybdenite, and galena. Consequently, it might be expected that the cassiterite would have low concentrations of Nb, in keeping with the Siberian sulphide-cassiterite deposits.

TABLE XVII : Average Contents of Nb, Ta, Sc, Be, and Ti (in ppm) in Cassiterites from Tin Deposits in Siberia (after Dudykina, 1959, quoted from Leube and Stumpfl, 1963)

Genetic Type of Deposit	Nb	Ta	Sc	Be	Ti
A. Tin-bearing pegmatites	6000	5300	650	10	4100
B. Quartz-cassiterite					
(i) Gneisses, quartz-feldspar veins	5200	1570	580	20	7500
(ii) Quartz veins	600	150	400	10	3500
(iii) Transitional deposits	30	-	140	50	4000
C. Sulphide-cassiterite deposits	20	-	4	10	1700

The Zaaiplaats cassiterite, obtained from ore-bodies within the Bobbejaankop granite, has a high content of La and Ce, that is in keeping with the higher concentrations of these elements in the whole rock samples. Söhnge (1944) recognized allanite and parisite (Ce, La, Ca fluo-carbonate) in the Zaaiplaats ore-bodies. Partridge (1936) also identified bastnaesite, although the presence of this mineral was not confirmed by Söhnge (1944). The high content of rare earth elements in the Bobbejaankop granite is apparently distributed through a number of minerals.

Strauss (1954) reported that spectrographic examination of cassiterite from Zaaiplaats showed that Nb was absent or negligible. Schröcke's (1955) spectrographic analysis of Zaaiplaats cassiterite yielded traces of Nb, Ta, Sc, and Ti, in addition to Bi, Mn, Cr, W, Fe, and Ca. These findings are in conflict with the present data, in respect to Nb. Söhnge (1944) was of the opinion that cassiterite metallization occurred through the late pegmatitic into the hydrothermal stages. It is possible, therefore, that the composite sample may reflect a mixture of cassiterite won from different environments, although it would be expected, in this case, that Sc would show higher values. Disseminated cassiterite is found in the Bobbejaankop granite, and this might be expected to have a different geochemistry from the cassiterite in the pipes and pods of mineralization. Leube and Stumpfl (1963) found that the cassiterite from the A mine at Rooiberg carried low concentrations of Nb (mean 15 ppm), Sc (mean 33 ppm), and Be (mean 41 ppm) with considerable variation in the Ti content, which these authors attributed to the variable presence of rutile, although they did not exclude the possibility that small amounts of Ti do occur in the cassiterite lattice. Pyrite, associated with the A mine cassiterite, contains comparatively low Ni- and Co-contents (means 370 and 420 ppm, respectively). Higher concentrations of Nb (mean 40 ppm), Sc (mean 130 ppm), and Be (up to 100 ppm) were found in cassiterite from the B and C mines at Rooiberg (Leube and Stumpfl, 1963), and the associated pyrite is rich in Ni and Co (500 to 3 000 and 300 to 5 000 ppm, respectively), although considerable changes in the content of Ni and Co were noted in different lodes in the same mine. Spectrographic examination did not reveal the presence of Ni or Co at Zaaiplaats (Strauss, 1954). This observation is not considered conclusive by Leube and Stumpfl (1963), who suggest that small, but significant, amounts of Nb and Sc, Ni, and Co may be present in the cassiterites and pyrite, respectively, that escaped detection. The weight of evidence suggests that these elements are present in only small amounts, and it may be provisionally concluded that the endogranitic deposits were formed at low temperatures, possibly similar to the exogranitic deposits at the Rooiberg A mine. If this is the case, the higher temperatures suggested by the analytical data from the exogranitic deposits at the Rooiberg B and C mines relative to the endogranitic deposits requires explanation. It is clear that more studies are required before any firm conclusions can be drawn.

CRYSTALLIZATION AND GENESIS OF THE ACID ROCKS

The Salic Phase of the Bushveld Complex consists of an assemblage of acid effusives, known as the Rooiberg felsites, that locally attain thicknesses in excess of 4 km, and a composite sheet of granites, into which small plutons of red granite, genetically associated with economically viable deposits of tin, are intrusive.

The mineralogically uniform, stratiform granitic rocks, intruded more-or-less concordantly beneath the overlying felsites and above the underlying metasedimentary rocks of the Transvaal Supergroup and the Mafic Phase of the Bushveld Complex, owe their pseudo-stratified appearance to the lithological gradation from coarse-grained, locally rapakivitic, granite at the base to fine-grained granophyric varieties beneath the felsite roof, that is accompanied by a progressive change in colour from grey to red. Granophyric textures are developed in these granitic rocks, either by direct crystallization or by re-crystallization consequent upon the intrusion of later granite or diabase. Aplitic granites build sheet-like bodies within the stratiform granite, the field evidence suggesting that their emplacement was a multi-phase event. The early-formed aplitic granites have a more irregular geometry and tend to be pod-like, with diffuse boundaries with the enveloping granite. The later aplitic granites are more regular in shape and have sharp contacts. Some of the aplitic granites are porphyritic. The red, mineralized, Bobbejaankop granite forms small plutons that have microgranite developed along the upper contacts.

The major element geochemistry of the granitic rocks is extremely homogeneous, the bulk of the analyses plotting about the 0,5 kb ternary minimum (Figure 53). The felsites display a much wider scatter (Figure 54), the abherrant plots reflecting the presence of felsites that are depleted in sodium and potassium. The reasons for this depletion have not been fully investigated but are probably attributable to devitrification and possibly gas-fluxing adjacent to fissures. A large number of the plots overlap the granite field. Individual studies, using two- and three-variable scatter-plot diagrams, have met with varying degrees of success in differentiating between individual components of the Salic Phase. When the number of samples plotted on such diagrams is increased to statistically significant levels, the apparent differences in major element chemistry between individual components become obliterated by large population overlaps that result from the increased data. Pronounced major element homogeneity is apparent when all the variables are considered simultaneously, using multivariate analytical techniques (Lenthall, 1973). Cluster analysis of the data indicates that such differences as do exist in major element chemistry between the various components are within the range of analytical precision and the expected "within-sample" variation (Lenthall, 1973).

The homogeneity of the major element chemistry of the components of the Salic Phase has led to much debate concerning the origin of the rocks. The hypothesis that the granitic rocks represent the acid differentiate of the Bushveld Complex has been criticized on the grounds that the volume of acid rocks far exceeds the theoretical predicted quantity. Furthermore, if differentiation had been operative, it would be reasonable to expect that there would be less homogeneity in the acid rocks reflecting the various stages of differentiation. Isotope geochemistry (Davies and others, 1970) is not unequivocal but has been interpreted as favouring the view that the granitic rocks represent the products of partial melting of sialic crust. A third alternative has been suggested that envisages the

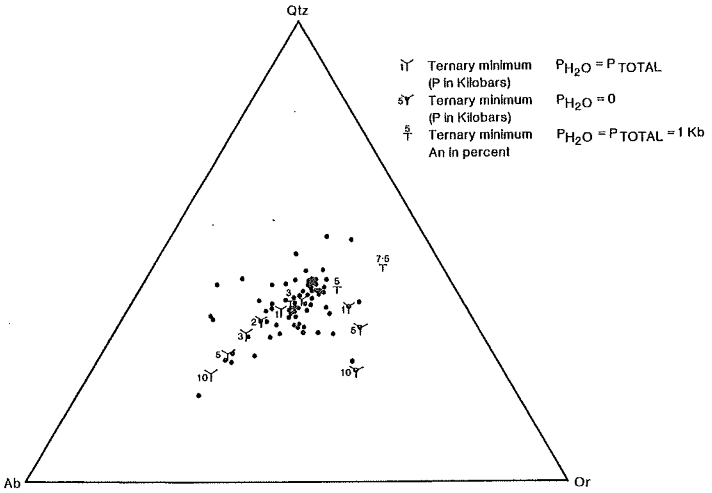

Figure 53 : *Ternary Qz-Ab-Or diagram for published analyses of Bushveld granites throughout the whole of the Complex, together with the ternary minima for* $P_{H_2O} = P_{Total}$ *at various pressures.*

production of rocks of granitic appearance by recrystallization of felsites and granite porphyries, following the intrusion of the Mafic Phase of the Bushveld Complex (de Waal, 1972). A similar but more tentative proposal has been made that the granitic rocks represent metasomatised sedimentary rocks.

On the basis of the statistical treatment of the trace element data, the acid rocks in the Potgietersrus tin-field can be divided into three distinct units :

(1) the acid effusives or Rooiberg felsites,

(2) the stratiform granites and their associated granophyric textural modifications, and

(3) the Bobbejaankop granite and its microgranitic hood facies.

Figure 54 : *Ternary Qz-Ab-Or diagram for the published analyses of felsites throughout the whole area of the Complex, together with the ternary minima for* $P_{H_2O} = P_{Total}$ *at various pressures.*

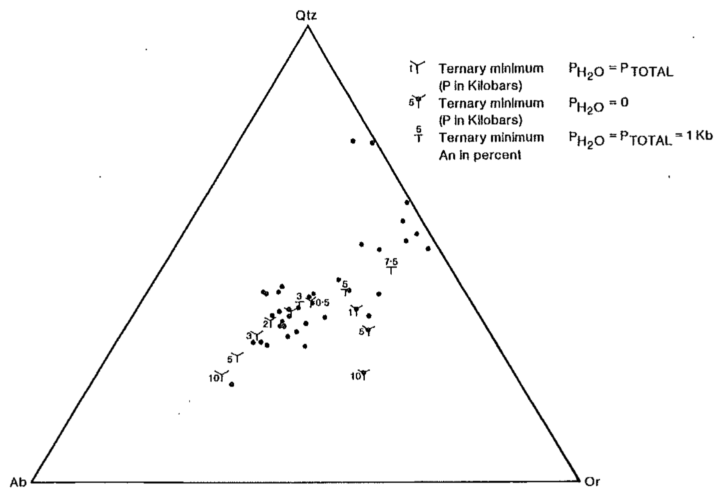

The acid effusives are distinguished by their trace element geochemistry from the granites on account of :

(1) significantly higher concentrations of Ba, Zn, Ti, Sc, Co, and Sr,

(2) significantly lower concentrations of Rb and Y, and

(3) marginally lower concentrations of La and Nb.

The Bobbejaankop granite differs from the stratiform granites by virtue of :

(1) lower concentrations of Ba, Zn, Ti, and Sr, and

(2) higher concentrations of Ca, Nb, and Rb.

The higher Ca-content of the Bobbejaankop granite does not imply an increase in the anorthite content of the granite but reflects the greater abundance of fluorite and carbonates.

Despite the identification of these three main groups by statistical methods, the variation diagrams (see Figures 5 to 8) show that all the plots lie along curves that are consistent with those expected during fractional crystallization. The Ti/Zr plot (Figure 40), however, demonstrates that, in some cases, the felsites plot in a field that does not lie on the fractionation curve. If, in fact, the felsites do represent the least fractionated acid phase, the question of the age relationships is pertinent.

In the eastern Transvaal, it has been argued that the effusive felsites pre-dated the emplacement of the Mafic Phase of the Bushveld Complex (von Gruenewaldt, 1972) and that both were subsequently intruded by the Bushveld granites. It is not possible to establish the relative ages of felsite and Mafic Phase in the Potgietersrus tin-field, because the stratiform granites intervene between them. However, if the felsites were derived from the same magma-source as the granitic rocks, can it be assumed that the processes of fractionation and emplacement of the acid rocks could have been separated by a hiatus, during which the Mafic Phase of the Complex was intruded? This question requires to be resolved before a complete model for the genesis and crystallization history of the acid rocks can be formulated. This problem places a constraint on a full discussion of the genesis of the acid rocks in the Complex, as a whole, and it is emphasized that the following account refers specifically to the data available from the Potgietersrus tin-field.

In essence, the intrusive granites and the acid effusives have similar major element chemistry, and both are close to the low-temperature trough of the quartz-orthoclase-albite system. Their trace element abundances are distinct, the granitic rocks displaying trends consistent with those produced during fractional crystallization. The felsites show no such trends, although their plots tend to overlap onto the least-differentiated portion of the granitic field.

The Bushveld granites are assumed to have been emplaced at relatively shallow depths. This is borne out by the Qz-Or-Ab plots (Figure 53) and by the field relations that demonstrate emplacement beneath the Rooiberg felsites, which have a preserved maximum thickness of about 4 000 m. It is not possible to estimate what thickness of felsites may have been removed by erosion prior to the deposition of the Waterberg sediments, but the absence of a major angular unconformity between the Waterberg rocks and the Rooiberg felsites suggests that the amount was probably small.

The Bushveld granites have a mean An content close to 5 (with Ab+Or+An+Q calculated as 100), and Figure 53 shows that the majority of the Bushveld granites plot in the plagioclase field. Exceptions are an aplite from the Olifants tin-field near Marble Hall, that lies in the orthoclase field and plots of the microgranitic marginal facies of the Bobbejaankop granite, a granite from the Olifants tin-field, and a granite from the Steelpoort Park granite, intruding the mafic phase of the Complex west of Lydenburg all of which fall in the quartz field. The presence of rapakivitic textures in some of the Bushveld granites might be taken to imply that potash feldspar and quartz crystallized first, on the basis of experimental granite systems that omit the influence of the An content. Stewart (1959) demonstrated that rapakivitic textures develop in magmas where plagioclase is the first to crystallize, when equilibrium is not maintained on cooling through the incomplete reaction of crystals and liquid, so that plagioclase, formerly in the five-phase field with alkali feldspar, quartz, and aqueous fluid, is less potassic, at temperatures of ±680°C and at H_2O pressures of 2 kb, than it would be if equilibrium were maintained. Accordingly, alkali feldspar is resorbed into the liquid, and plagioclase crystallizes either on existing plagioclase crystals or on some of the alkali feldspar, to form mantles.

The presence of miarolitic cavities in the Bobbejaankop granite and the high concentration of fluorine in the stratiform granites points to the fact that they crystallized from melts rich in volatiles. The Bushveld granites have high contents of SiO_2 and K_2O and relatively low contents of MgO, CaO, and Al_2O_3. This indicates an excess of alkalis that are concentrated with volatiles in the liquid phase during crystallization. Investigation (Tuttle and Bowen, 1958) of the system K_2O-Al_2O_3-SiO_2-H_2O in the presence of water vapour at a pressure of 1 000 kg/cm^2 showed that the orthoclase-quartz eutectic appears in the system as a maximum on the boundary between the quartz and orthoclase fields at 760°C. The boundary between the quartz and orthoclase fields falls on the potassium side to temperatures below 400°C and reaches compositions of nearly pure potassium silicate, the liquid probably containing more than 30 per cent water. Tuttle and Bowen (1958) consider that the system Na_2O-Al_2O_3-SiO_2-H_2O is probably similar and, in the presence of water, will give rise to very low-melting mixtures, if more sodium is present than is required to combine with all the alumina to form albite.

The production of a hydrous liquid, that would continue to crystallize at temperatures below 400°C, is theoretically possible from a magma of the composition of the Bushveld granites. This hydrous liquid would be able to produce autometasomatic processes in the granite itself and metasomatic processes in the country rocks (e.g. see Strauss, 1947). The micrographic intergrowth of quartz with orthoclase in the granophyric granites and adjacent to the Bobbejaankop granite pluton is a further manifestation of this process.

Figure 53 demonstrates that the Bushveld granites were close to saturation, for the plots lie near the trend of the hydrous ternary minima. It is clear that the magma became saturated as it crystallized, there being both alteration of the ferromagnesian minerals and the alkali feldspars in the upper parts of the stratiform granite sheet and in the Bobbejaankop granite. These feldspars are red due to the oxidation of dispersed iron under water-saturated conditions.

The rare earth element data (Fourie, 1969) shows a Cu-negative anomaly in the stratiform granites, that becomes more marked in the Bobbejaankop granite. Low K/Rb and Sr/Ba ratios, taken in conjunction with the R.E.E. data, suggest that the magma that produced the Bushveld granites was generated at relatively shallow crustal depths, where plagioclase and amphibole were present in the residuum.

The emplacement of the Bushveld granites was preceded by the intrusion of basaltic magma that is now represented by the Mafic Phase of the Bushveld Complex. This basaltic magma was injected into a sialic crust largely composed of tonalitic gneisses, interlayered with plagioclase-amphibolites and various potassic granites. The tonalitic gneisses include metamorphites of amphibolite grade exposed at the present level of erosion, and it is probable that the deepest portions of this gneiss terrane attain the granulite grade. It is suggested that the basaltic magma reacted with, and partially melted, this sialic crust. It would be expected that reaction-melting between basaltic magmas and country-rocks of the granulite facies (probably composed of feldspars, pyroxenes, garnets, and other minerals stable at high temperatures) would produce ferro-gabbros, diorites, and quartz syenitic liquids. The apparent absence of the latter as a constituent of the Bushveld Complex may be due to (i) further reaction-melting between this liquid and the more granitic country rocks in the intermediate crust, to form more granitic liquid, or (ii) the injection of the basaltic magma directly into higher, and more granitic, crustal levels, where reaction-melting between this magma and the country-rocks produced granitic liquids in one stage. The proposal made here for the genesis of the Bushveld granites is not susceptible to proof on the basis of the data available from the Potgietersrus tin-field, but it is in keeping with the conclusions (Davies and others, 1970) based on isotope geochemistry.

The negative slope of the granite melting curve under saturated conditions places a constraint on the vertical distance through which a wet granitic magma can rise. To reach a high crustal level, the Bushveld granite must have been essentially dry, initially. However, as crystallization proceeded, the residual liquids would become progressively more saturated with water and volatiles, that would move down temperature and pressure gradients, to collect in lower-temperature and pressure regimes. Accumulation would preferentially select domical irregularities at or near the roof of the granite mass. Any cations (e.g. Sn, Zn, Rb) incompatible within the lattices of the crystallizing mineral phases would be caught up by the volatiles and accumulate with them. Where small volumes of volatile-rich aqueous solutions collected, the granite would suffer a general discoloration from grey to red, caused by the oxidation of iron. The ferromagnesian minerals, hornblende and biotite, would be chloritized and exsolution perthites and granophyric intergrowths would develop. The presence of the volatiles would influence the degree of ordering in the potassium feldspars. The bulk composition of the alkali feldspar can regulate the Al/Si ordering, which takes place more readily in Or-rich alkali feldspar than in feldspars containing significant amounts of Ab. No data are available concerning any compositional variations that may exist in the potassium feldspars through the stratiform granite sheet, but the correlation between the increasing effects of the presence of volatiles with the higher degree of Al/Si ordering suggests that, in this case, the major influence was the presence of volatiles.

Where larger volumes of volatiles collected, the melting point of the granite magma was depressed to below, or just below, the ambient temperature, initiating remobilization. The extent to which the melting point is depressed would determine the degree of remobilization and the amount of movement of the remobilized material permitted. Intrusive contacts as seen at the margins of the Bobbejaankop stock at Zaaiplaats would represent a condition of maximum movement of the remobilized magma. However, the presence of excess volatiles would not permit the magma to move any great distance vertically before it re-crossed the melting curve and solidified. Inherent in this concept of the generation of the Bobbejaankop-type granite is the conclusion that the stock will be rootless. It follows that, if subsequent erosion has proceeded deep below the roof-zone in which the volatiles collected, no granites of Bobbejaankop-type can be expected. The search for further stocks of stanniferous Bobbejaankop-type granite should be confined to preserved roof-zones, particularly where domical irregularities in the configuration of the original roof are developed.

If the intrusion of the magma has fractured the country rocks forming the roof, it seems logical to suppose that some of the volatiles will escape, to give rise to exogranitic veins. Similarly, the presence of suitable rock-types at the contact will encourage metasomatic activity (e.g. see Strauss, 1947).

The concentration of volatile-rich phases towards the roof of the stratiform granite sheet provides an explanation for the apparent greater degree of trace element fractionation in the granophyric granites and granophyre of the Sterk River-type.

The aplitic granites that in the field and in their geochemistry reflect the existence of two populations can be attributed to the broad temperature range over which the stratiform granites crystallized. The older, irregularly-shaped aplitic granite bodies, with geochemical characteristics similar to the basal stratiform granites, are viewed as the crystallization products of magma intruded into joints and other planes of discontinuity developing in a quasi-solid crystal mush. Any slight disturbance within this mush would deform these aplitic granite bodies. The aplitic granites displaying a greater degree of fractionation are envisaged as the crystallization products of residual magma, that were intruded into near-horizontally-disposed joints towards the close of the crystallization sequence.

The lack of Al/Si ordering in the grey Bushveld granite at the base of the stratiform sheet suggests that, when the temperature dropped low enough for orthoclase-microcline inversion, the rock was already solidified. The lack of discoloration of the alkali feldspars and of chloritization of the ferromagnesian minerals imply that most of the volatiles had escaped before this stage, so that the ordering of the potash feldspar was sluggish.

The feldspar porphyry sheet at the roof of the stratiform granite has a trace element chemistry that is similar to that of the stratiform granites in many respects, but it has lower K/Rb and Sr/Ba ratios that are suggestive of fractionation. The presence of micrographic intergrowth between alkali feldspar and quartz and its occasional reddish discoloration suggest that this marginal facies has been affected by volatiles. In some places, the fine-grained groundmass is devoid of granophyric intergrowths. The fine grain-size of the rock, together with the fact that the phenocrysts are built of quartz and plagioclase, precluded the determination of the degree of Al/Si ordering in the alkali feldspar. It is proposed that the feldspar porphyry represents a remnant of the original roof of the granite that was disrupted locally by later pulses of magma. The spherulitic groundmass orthoclase is assumed to have been produced by rapid crystallization.

Wagner (1929) regarded the microgranitic margin of the Bobbejaankop granite as its chill phase. Strauss and Truter (1944) discounted this possibility on the grounds that numerous veins of the microgranite cut the main mass of the Bobbejaankop granite and that it is confined to arches in the roof of the Bobbejaankop pluton. These authors favoured an origin whereby the microgranite was formed by reconstitution of Bobbejaankop granite, consequent upon the concentration of volatiles in domical arches. They further considered that portions of the overlying granophyric granite was similarly altered *in situ* to Lease microgranite. The restriction of the microgranite to apical parts of the roof of the Bobbejaankop pluton was taken as evidence that the microgranite was not a later intrusion. The concept of a late intrusive phase does not account for the reported reconstitution of xenoliths of stratiform granite in the Bobbejaankop granite to Lease microgranite. The geochemical data support Strauss's and Truter's (1944) contention. The availability of hydrous liquid would promote autometasomatic processes in the Bobbejaankop granite and metasomatism of its country-rocks. The concepts described above are illustrated diagrammatically in Figure 55.

The genesis of the felsites cannot be treated completely with the presently available data. Plots on the Q-Or-Ab diagram (Figure 54) tend to concentrate in the same low-temperature trough as the granitic rocks, but there is a considerable scatter of points that may be attributable to devitrification, gas-fluxing, or loss of fluid phases. The trace element chemistry of the felsites show smaller degrees of variance than do the granites. More detailed investigation of the chemistry of individual flows or eruptive events is required before attempting to discuss the trace element distributions. The overlap of the felsite geochemistry with some of the granites suggests that the felsites are consanguinous with the granites. The felsites show evidence of fractional crystallization. It is provisionally suggested that the felsite magmas have a similar origin as do the granitic magmas. However, the felsites are assumed to have been explosively extruded, while the granites reflect fractional crystallization of magmas that moved more slowly upwards in quiescent conditions.

The provisional model therefore envisages the production of magmas of granitic composition consequent upon reaction-melting between intrusive basaltic magma and sialic crust. A fraction of this magma is explosively extruded, while the remainder moves upwards under quiet anorogenic conditions. As crystallization proceeds, the residual liquids become progressively more hydrous. The extreme products of the fractionation process collect in apical areas of the magma chamber, causing changes in the already crystallized portions and, locally, attaining such concentrations that they are able to remobilize existing granitic rocks. In the case of the Bobbejaankop granite, remobilization, in fact, led to limited mobility, so that intrusive contacts developed. Cations not accepted in silicate lattices were swept along with the volatiles and collected with them. Economically, the most important of those elements carried by the volatiles is tin that was deposited when the residual fluids crystallized.

The Bushveld granites in Zaaiplaats area, with a mean Sn-content of 6,5 ppm, are enriched in that element by a factor of 2, compared to the world-wide mean for granitic rocks. It has been suggested in the preceeding discussion that Sn was concentrated in the volatile phases of the Bushveld granite during stable anorogenic conditions. If the Bushveld granite magma was produced as a result of reaction-melting between sialic crust and basaltic magma, the question arises whether the stanniferous nature of the granite magma reflects the melting of salic rocks that were themselves stanniferous. Tin-bearing pegmatites are known in the Archean basement in Swaziland and near Klein Letaba in the northern Transvaal. It is not known what the content of Sn is in minerals such as biotite, hornblende, sphene, etc. in these Archean rocks, that might also have contributed to the tin content of the Bushveld magma. It seems likely that, if the Bushveld granite magma owes its origin to reaction-melting, its stanniferous nature may result from the involvement of tin-bearing rocks in the reaction-melting process.

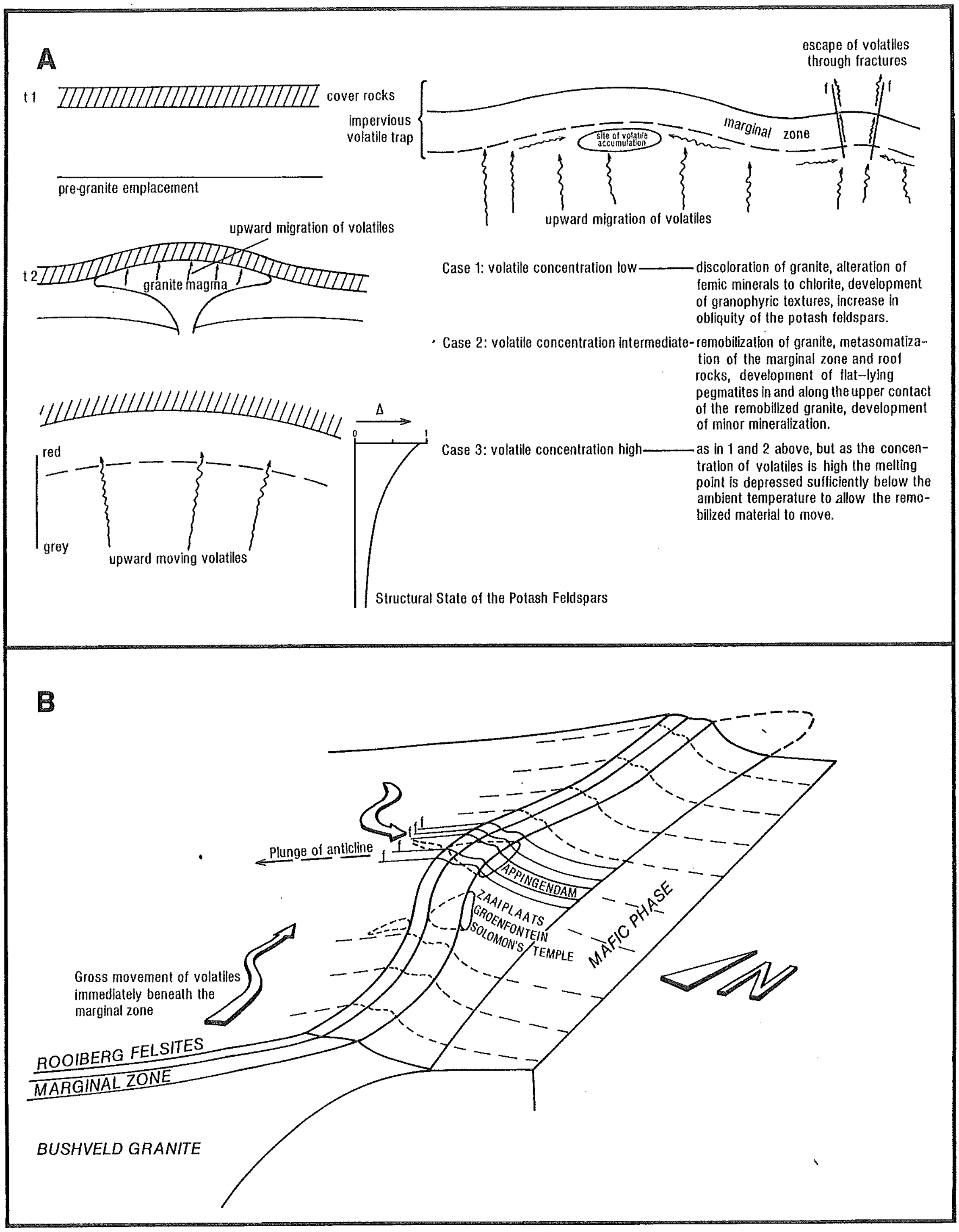

Figure 55 : *(A) Diagrammatic representation of the conceptual model for the formation of tin-bearing granites in the Bushveld Complex. At time t_1, the granite has been emplaced and volatiles are beginning to collect. Enlargements of part of the roof-zone are shown in the other sections of the diagram, together with a graphical representation of the increasing obliquity values for potassium feldspars in the stratiform granites.*

(B) A conceptual model for the concentration of volatiles at Zaaiplaats, based on Figure 55A. The large arrows indicate the directions in which the volatiles move to collect in an antiformal structure.

An alternative explanation may be that the volatiles scavenged Sn from the Bushveld magma. The mean Sn-content of 17 samples of Bushveld granite from the Sekhukhuni plateau is 3,9 ppm, but reliable information is lacking from other areas of the Complex.

While it is possible to propose a model for the concentration of tin within particular phases of the Bushveld granite, there is not yet sufficient data to establish the processes that gave rise to the original stanniferous nature of the Bushveld granite in the Zaaiplaats area or whether this area is geochemically distinct from other developments of Bushveld granite.

ACKNOWLEDGEMENTS

The analytical data determined by Dr. G. Hornung, Leeds University, is gratefully acknowledged. This assistance from Dr. Hornung added considerably to the evaluation of the geochemical parameters.

The co-operation received from Dr. D.M. Biggy, Nuclear Physics Research Unit, University of the Witwatersrand, in obtaining provisional F determination was of great help in assessing the significance of the Ca-concentrations.

Mr. T.S. McCarthy provided valuable advice during the K_2O, Rb, and Sr analyses and willingly made available his computer programme.

REFERENCES

Barsukov, V.L. (1957). The Geochemistry of Tin : Geochemistry, Vol. 1, pp. 41-51.

Barsukov, V.L. and Pavelenko, L.I. (1956). Distribution of Tin in Granitic Rocks. Doklady, Akad. Nauk, SSSR, Vol. 109, pp. 589-592.

Carr, M.H. and Turekian, K.K. (1961). The Geochemistry of Cobalt. Geochim. et Cosmochim. Acta, Vol. 23, pp. 9-60.

Coetzee, G.L. (1970). The Rooiberg Felsite Series North of Nylstroom. Geol. Soc. S. Afr., Spec. Pub. No. 1, pp. 312-325.

Crockett, R.N. (1971). The Rocks of the Ventersdorp System of the Lobatse and Ramotswa areas, Republic of Botswana : Their Possible Origins and Regional Correlations. Trans. geol. Soc. S. Afr., Vol. 74, pp. 1-24.

Davies, R.D., Allsopp, H.L., Erlank, A.J. and Manton, W.I. (1970). Sr-Isotopic Studies on Various Layered Mafic Intrusions in Southern Africa. Geol. Soc. S. Afr., Spec. Pub. No. 1, pp. 576-593.

de Waal, S.A. (1972). The Bushveld Granites in the Zaaiplaats Area. Trans. geol. Soc. S. Afr., Vol. 75, pp. 135-147.

Edge, R.A. and Ahrens, L.H. (1962). Studies on the Trace Element Content of Some South African Rocks. Trans. geol. Soc. S. Afr., Vol. 65, Part 1, pp. 113-124.

Fourie, P.J. (1969). Die Geochemie van Granitiese Gesteentes van die Bosveldstollingskompleks. Unpub. D.Sc. Thesis, University of Pretoria, Pretoria.

Goldschmidt, V.M. (1937). The Principles of Distribution of Chemical Elements in Minerals and Rocks. J. Chem. Soc., pp. 655-673.

Goldschmidt, V.M. (1944). Crystal Chemistry and Geochemistry. Chemical Products, Vol. 7, pp. 29-34.

Hamilton, W. (1970). Bushveld Complex - Product of Impacts? Geol. Soc. S. Afr., Spec. Pub. No. 1, pp. 367-374.

Heier, F. and Taylor, S.R. (1959). Distribution of Ca, Sr, and Ba in Southern Norwegian Precambrian Alkali Feldspar. Geochim. et Cosmochim. Acta, Vol. 17, pp. 286-304.

Hesp, W.R. (1971). Correlations Between the Tin Content of Granitic Rocks and Their Chemical and Mineralogical Composition. Reprinted by Division of Mineral Chemistry, C.S.I.R.O. Australia, from Can. Inst. Min., Spec. Vol. No. 11, "Geochemical Exploration", 15 pp.

Hunter, D.R. (1973). Geochemistry of Granitic and Associated Rocks in the Kaapvaal Craton. Inf. Circular No. 81, Econ. Geol. Research Unit, Univ. Witwatersrand, 67 pp.

Kolbe, P. (1966). Geochemical Investigation of the Cape Granite South-Western Cape Province, South Africa. Trans. geol. Soc. S. Afr., Vol. 69, pp. 161-199.

Lenthall, D.H. (1973). The Application of Discriminatory and Cluster Analysis as an Aid to the Understanding of the Acid Phase of the Bushveld Complex. Inf. Circ. No. 72, Econ. Geol. Research Unit, Univ. Witwatersrand, 33 pp.

Leube, A. and Stumpfl, E.F. (1963). The Rooiberg and Leeuwpoort Tin Mines, Transvaal, South Africa. Econ. Geol., Vol. 58, pp. 391-418 and pp. 527-557.

Lyakhovich, V.V. and Balanova, T.T. (1969). Mean Contents of W, Mo, Sn, Ta, Nb, and Zn in Sphene and Ilmenite from Granites. Geokhimiya, No. 3, pp. 322-327.

Menge, G.F.W. (1963). The Cassiterite Deposits on Doornhoek 342 KR and Vicinity, West of Naboomspruit, Transvaal. Unpub. M.Sc. Thesis, University of Pretoria, Pretoria.

Nockolds, S.R. and Mitchell, R.L. (1948). The Geochemistry of Some Caledonian Plutonic Rocks : a Study in the Relationship Between the Major and the Trace Elements of Igneous Rocks and Their Minerals. Trans. Roy. Soc. Edinburgh, Vol. 61, pp. 533-575.

Partridge, F.C. (1936). A Contribution to the Mineralogy of the Potgietersrust Tinfields. Trans. geol. Soc. S. Afr., Vol. 39, pp. 461-464.

Pretorius, D.A. (1970). The Quantitative Hydrogeological Mapping of Zebedelia Estates, Central Transvaal. Unpub. Ph.D. Thesis, University of the Witwatersrand, Johannesburg.

Ringwood, A.E. (1955). The Principles Governing Trace Element Distribution During Magmatic Crystallization. Part I, The Influence of Electronegativity, Geochim. et Cosmochim. Acta., Vol. 7, pp. 189-202; Part II, The Role of Complex Formation, Geochim. et Cosmochim. Acta, Vol. 7, pp. 242-254.

Rooke, J.M. (1971). Geochemical Variations in African Granitic Rocks, and Their Structural Implications. In Clifford, T.N. and Gass, I.G. (Editors), African Magmatism and Tectonics, Oliver and Boyd, Edinburgh, pp. 355-417.

Schröcke, H. (1955). Zur Geochemie Erzgebirgischer Zinnerzlagerstätten. Neues. Jb. Mineral., Vol. 87, pp. 416-456.

Söhnge, P.G. (1944). The Structure, Ore Genesis, and Mineral Sequence of the Cassiterite Deposits in the Zaaiplaats Tin Mine, Potgietersrust District, Transvaal. Trans. geol. Soc. S. Afr., Vol. 47, pp. 157-181.

Stewart, D.B. (1959). Rapakivi Granite from Eastern Penobscot Bay, Maine. Proc., 20th Intern. Geol. Cong., Mexico, Vol. 11A, pp. 293-320.

Strauss, C.A. (1947). Granitization and Rheomorphism Associated with the Granite Near the Leeuwpoort Tin Mine. Trans. geol. Soc. S. Afr., Vol. 50, pp. 161-170.

Strauss, C.A. (1954). The Geology and Mineral Resources of the Potgietersrus Tin-Fields. Memoir 46, Geol. Surv. S. Afr., 241 pp.

Strauss, C.A. and Truter, F.C. (1944). The Bushveld Granites of the Zaaiplaats Tin-Mining Area. Trans. geol. Soc. S. Afr., Vol. 47, pp. 47-78.

Taylor, S.R. (1965). The Application of Trace Element Data to Problems in Petrology. Phys. Chem. Earth. Vol. 6, pp. 133-213.

Turekian, K.K. and Wedepohl, K.H. (1961). Distribution of the Elements in Some Major Units of the Earth's Crust. Bull. geol. Soc. Amer., Vol. 72, pp. 175-192.

Tuttle, O.F. and Bowen, N.L. (1958). Origin of Granite in the Light of Experimental Studies in the System $NaAlSi_3O_8$-$KAlSi_3O_8$- SiO_2-H_2O. Memoir 74, Geol. Soc. Amer., 153 pp.

von Gruenewaldt, G. (1972). The Origin of the Roof-Rocks of the Bushveld Complex Between Tauteshoogte and Paardekop in the Eastern Transvaal. Trans. geol. Soc. S. Afr., Vol. 75, pp. 121-134.

Vorma, A. (1971). Alkali Feldspars of the Wiborg Rapakivi Massif in Southeastern Finland. Bull. 246, Comm. Geol. Finlande, 72 pp.

Wagner, P.A. (1929). In Handbuch der Regional Geologie Heft. VII, Bd 7.A., The Union of South Africa (Rogers, A.W.; Hall, A.L.; Wagner, P.A. and Haughton, S.H.), pp. 194-195.

* *

APPENDIX I

(a) Instrumental Conditions and Selection of Standards for Ba, Ca, Co, La, Sc, Sn, Ti, Zn, and Zr Determinations by X-Ray Fluorescence Analysis

[*General Superintendence Co. (S.A.) (Pty.) Ltd.*]

Element	Analysis Line	Tube Target	Excitation Power mA x KV	Crystal	Collimeter	°2θ Analysis Line	°2θ Background
Ba	L-β1	Cr	30 x 60	LiF 200	480 μ	79,19	81
Ca	K-∝	Cr	15 x 50	LiF 200	480 μ	113,08	B
Co	K-∝	Au	30 x 60	LiF 220	160 μ	77,93	B
La	L-∝1	Cr	30 x 60	LiF 200	480 μ	82,86	81,50
Sc	K-∝	Cr	30 x 60	LiF 200	480 μ	97,67	96,00
Sn	K-∝	Au	30 x 60	LiF 200	160 μ	19,90	19,00
Ti	K-∝	Cr	30 x 60	LiF 200	160 μ	86,08	B
Zn	K-∝	Au	30 x 60	LiF 220	160 μ	60,60	59,40
Zr	K-∝	Au	30 x 60	LiF 220	160 μ	32,12	B

B = synthetic blank (see selection of background).

In all cases, pulse height selection was used to reduce the background intensity and the possibility of harmonic overlap. For all elements where the analysis line had $\lambda > 1.8 Å$, a flow proportional counter was used. The scintillation counter was used in all other cases. Only the first-order reflections were used in all cases.

The background in each case, where it was used, was determined by slowly scanning through an angular range which included the peak of the element. The scan was carried out on the standard containing the highest concentration of the element, as well as on a large number of samples picked at random. The background angle was then selected as close as possible to the peak, without getting overlap from the peak. Special corrections were made in the cases where the peak was superimposed on a sloping background.

A synthetic blank was prepared, using analytical reagent-quality chemicals, containing all the major elements, except the element being analyzed. The concentrations of these elements were based on the values given for the U.S.G.S. Standard G-2. Where the blank was used, scans were done on the blank and a large number of samples through an angular range which included the peak of the element being analyzed. A comparison was made between the background of the blank and the background of the samples. In all cases, the background intensity of the blank corresponded closely to that of the samples. The blank was used where it was difficult to obtain a precise background angle due to peaks close to the peak being analyzed and pseudo-reflections from the crystal. No corrections were found necessary for overlaps of peaks adjacent to those being analyzed.

The standards were prepared by the method of internal standard, same element (spiking). A composite of the samples was made. This composite was thoroughly homogenized and then split into three portions. Each portion was then spiked with a specific group of elements. The elements were also divided into three groups, such that there would be no interference between two elements in the same spike.

The following tabulation shows the amount of element added to each portion of the composite, as well as elements added to the three portions of the composite. In each case, where the oxide of the element was available in a stable form, it was used. In addition, for Ca and Ti, a number of samples were picked at random and analyzed for the two elements by wet chemical methods. The values so obtained were incorporated in the calculations.

The U.S.G.S. Standard G-2 was used as a control throughout. Graphs of the concentrations versus the intensity of the spikes were plotted for each of the elements analyzed. The graphs were found to be linear for all elements in the working range of the spikes. Regression analysis was used to determine the points which gave the best coefficient of correlation. The slope factor obtained from these points was used in the calculations.

Group I

Element	1 ppm	2 ppm	3 ppm	4 ppm	5 ppm	6 ppm	7 ppm	8 ppm
Co	1	2	5	8	12	20	30	50
Sc	1	2	4	6	8	10	15	20
Sn	1	2	4	6	8	10	15	20
Ti	1900	2400	2900	3400	3900	4400	4900	5400
Zn	5	10	30	50	80	110	140	180
Zr	100	150	200	250	300	350	400	450
Group II								
Ca	1000	5000	10000	15000	20000	25000	30000	35000
La	10	30	60	100	120	140	180	210
Group III								
Ba	700	1000	1300	1600	2000	2400	2800	3200

Mass absorption coefficients were not, as such, determined. Inter-element effects were minimized by preparing spiked standards in a composite matrix of the samples themselves and applying the (P-B)/B correction.

(b) Instrumental Conditions for Na_2O Determinations (National Institute for Metallurgy, Johannesburg)

Pulse height selection was employed for the Na determinations.

Analysis Line	Tube Target	Excitation Power mA x K.V.	Crystal	Collimeter	°2θ Analysis Line	°2θ Background
K-α	Cr	50 x 53	RbAp	480 μ	54,20	52,00 and 60,00

The background used was determined by slowly scanning through the angular range which included the sodium peak. The background angle was then related as close as possible to the peak without getting overlap from the peak.

The U.S.G.S. Standard G-2 was used to calibrate the instrument and the Standards GSP-1 and NIM-G were determined at frequent intervals.

(c) Instrumental Conditions for K_2O, Rb, and Sr Determinations

Pulse selection height was employed for the K_2O, Rb, and Sr determinations.

Element	Analysis Line	Tube Target	Excitation Power mA x K.V.	Crystal	Collimeter	°2θ Analysis Line	°2θ Background
K_2O	K	Cr	18 x 50	PET	160	51,40	-
Rb	K	Mo	40 x 65	LiF 220	160	37,94	37,00 39,85
Sr	K	Mo	40 x 65	LiF 220	160	35,81	35,00 37,00

For the K_2O determinations, the following standards were used in the calibration of the working curves :

(i) the French Standards GA, GR, and GH

(ii) the U.S.G.S. Standard GSP-1, and

(iii) the National Institute for Metallurgy Standard NIM-G.

An excellent, straight-line working curve could be constructed for the international standards, the values of which corresponded favourably with published data. No background readings were measured, nor were any mass absorption corrections made during the K_2O determinations.

The background positions for Rb and Sr were determined by slowly scanning through the angular range of the peaks of the elements. Background positions were selected above, below, and between the two peaks, and these points were then used to extrapolate background values beneath the two peaks. The standards used for calibration included the U.S.G.S. Standards G-1, G-2, and W-1 and the internal standard of the Bernard Price Institute of Geophysical Research, University of the Witwatersrand. Mass absorption coefficients were calculated by Reynold's (1967) method using the Mo Compton peak.

Calculations of the Rb and Sr concentrations were carried out on the IBM 360/50 computer of the University of the Witwatersrand, using the programme prepared by Mr. T.S. McCarthy, Department of Geology, University of the Witwatersrand.

* *

APPENDIX II

Analytical Data for All Samples from Original Stations (Analysts : General Superintendence, National Institute for Metallurgy, and Senior Author)

In Appendix II, hidden duplicate samples were analyzed to check precision. The following are duplicate samples :

J15 = duplicate of N11
M 6 = duplicate of D 4
M 7 = duplicate of G13
R 9 = duplicate of A 2
Q 9 = duplicate of S 2
U 9 = duplicate of B 9

Key to Analytical Data According to the Classification Adopted in This Paper

Coarse-Grained Granite

A 1, 2, 4, 5	H 1, 2, 3, 8	O 1, 2, 3, 4
B 1, 2, 3, 4	I 5, 6, 7, 8	P 1, 2, 3, 4
C 2, 3, 4, 6	J 2, 4, 5, 6, 7, 8, 11	Q 1A, 2, 3, 4, 9
D 2, 3, 8	K 1, 3, 4, 5A, 6, 7, 8, 9, 10	R 2, 3, 4, 9
E 2, 5, 6	L 4, 7	S 1, 2, 3, 4, 5
F 2	M 2A, 3, 4, 5, 10, 12	T 2, 3, 4, 5, 6, 7
G 2	N 1, 2, 2A, 3, 4, 5	U 3, 4

Bobbejaankop Granite

D 4, 5	H 4, 5
E 7, 8	I 9, 10, 11
F 4, 5	J 9, 10, 10A
G 4, 5	M 6

Rooiberg Felsite

A 11	H 11, 12	O 8, 9
B 11, 12	J 17, 18, 18A	P 8
C 10, 11, 12	K 17, 18, 18A	Q 8
D 11, 12	L 17, 18	R 8
E 14, 15	M 7	S 9
F 12, 13	M 16, 17	T 9
G 11, 12, 13	N 16	U 8

Aplitic Granite

A 3	F 1, 3	L 3
C 1	G 1	L 6
D 1	I 2, 3, 4	M 2
E 1, 3, 4	K 5	O 2A

Granophyric Granite

A 6, 7, 8	G 3, 6, 7, 8, 9	N 9, 10, 11
B 5, 6, 7	H 9	O 6
C 5, 7, 8	I 13, 14, 14A	Q 5
D 7, 9	J 12, 13, 14, 15	R 5
E 10, 11	L 5, 10, 11	S 6
F 8, 9	M 9, 11	U 5, 6

Sterk River Granophyre

A 9, 10	H 10	P 6, 7
B 8, 9, 10	J 16	Q 6, 7
C 9	K 12	R 7
D 10	K 13, 16	S 7, 8
E 12, 13	L 12, 14, 15, 16	T 8
F 10, 11	N 8, 14	U 7, 9
G 10	O 7	

Groenfontein Granophyre

D 6	H 6, 7
E 9	I 12
F 6, 7	

Feldspar Porphyry

K 14, 15	N 12, 13, 15
L 13,	WG 1, 2, 3
M 13, 14, 15	

Welgevonden Granophyre

K 11	N 6, 7
L 8, 9	O 5
M 8	P 5

Blinkwater Granophyre and Associated Metasediments

I 1	L 1, 2	R 1
J 1, 3.	M 1	T 1
K 2	Q 1	U 1, 2

* *

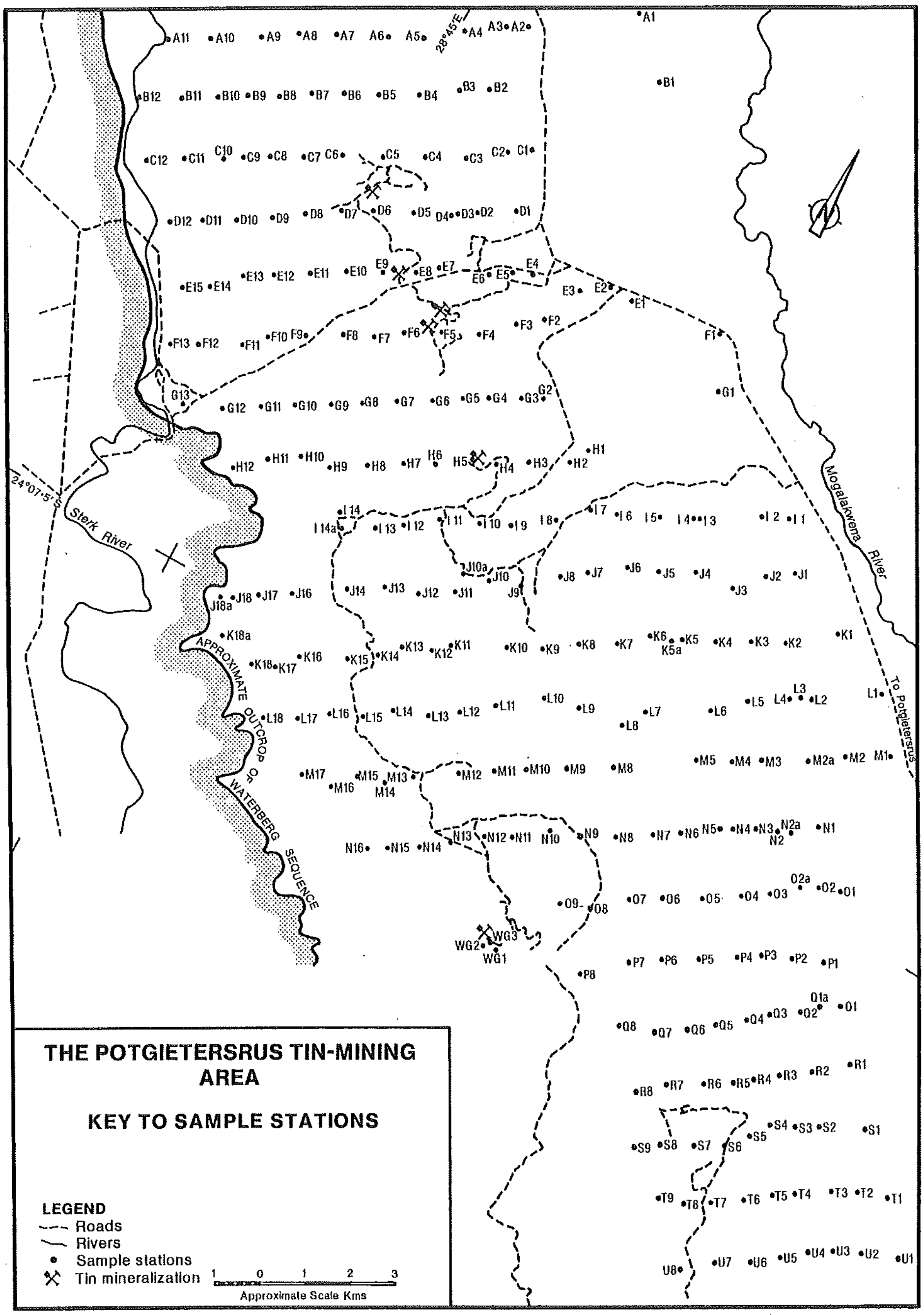

Figure 56 : *Location of sample sites.*

APPENDIX III

Analytical Data of Samples Collected About Sample Stations

Sample No.	Ba	Ce	Co	La	Nb	Rb	Sc	Sn	Sr	Ti	Y	Zn	Zr
(a) Coarse-Grained Granite at Station C6													
C6	748	258	2	71	22	240	3	5	27	1302	99	121	374
C6.1	713	290	2	85	24	214	2	3	32	1253	114	155	420
C6.2	740	279	2	82	25	229	5	8	29	1245	99	148	377
C6.3	756	271	2	77	23	229	3	6	27	1248	89	137	367
C6.4	864	212	3	55	20	241	2	11	24	1337	77	105	338
C6.5	681	281	3	81	25	233	0	9	21	1200	97	130	406
C6.6	752	209	2	51	18	236	1	11	21	1256	80	96	356
C6.7	644	256	2	75	23	230	0	8	22	1229	96	127	44
C6.8	796	274	3	71	22	260	0	12	23	1291	91	93	412
C6.9	780	211	2	54	18	237	2	10	22	1400	73	105	316
$\bar{x}$	747	254	2,3	70	22	235	1,8	8,3	25	1276	92	122	371
σ	57,84	30,00	0,46	11,86	2,45	11,10	1,54	2,76	3,57	55,4	11,66	20,43	32,3
$\sigma/\bar{x}$%	7,74	11,81	20,00	16,89	11,14	4,72	85,56	33,25	14,28	4,3	12,67	16,75	8,71
(b) Granophyric Granite at Station J14													
J14.1	600	-	-	153	-	-	-	-	-	1120	-	26	352
J14.2	395	-	-	121	-	-	-	-	-	969	-	82	372
J14.3	498	-	-	357	-	-	-	-	-	1076	-	58	370
J14.4	576	-	-	150	-	-	-	-	-	1216	-	52	356
J14.5	693	-	-	269	-	-	-	-	-	1170	-	31	354
J14.6	609	-	-	125	-	-	-	-	-	1130	-	30	355
J14.7	575	-	-	168	-	-	-	-	-	1079	-	34	377
J14.8	565	-	-	148	-	-	-	-	-	1216	-	50	353
J14.9	526	-	-	138	-	-	-	-	-	1141	-	27	336
J14.10	589	-	-	152	-	-	-	-	-	1144	-	26	347
$\bar{x}$	563	-	-	178	-	-	-	-	-	1126	-	42	357
σ	74,3	-	-	71,4	-	-	-	-	-	69,3	-	17,6	11,8
$\sigma/\bar{x}$%	13,2	-	-	40,1	-	-	-	-	-	6,1	-	41,9	3,3
(c) Sterk River Granophyre at Station J16													
J16.1	573	-	-	120	-	-	-	-	-	998	-	38	417
J16.2	439	-	-	140	-	-	-	-	-	975	-	53	388
J16.3	386	-	-	129	-	-	-	-	-	925	-	98	344
J16.4	344	-	-	129	-	-	-	-	-	951	-	43	408
J16.5	373	-	-	115	-	-	-	-	-	1015	-	80	379
J16.6	413	-	-	164	-	-	-	-	-	987	-	82	363
J16.7	462	-	-	878	-	-	-	-	-	928	-	67	379
J16.8	425	-	-	217	-	-	-	-	-	1002	-	94	369
J16.9	580	-	-	881	-	-	-	-	-	981	-	30	379
J16.10	374	-	-	114	-	-	-	-	-	989	-	78	368
$\bar{x}$	437	-	-	289	-	-	-	-	-	975	-	66	379
σ	77,2	-	-	296,8	-	-	-	-	-	29,2	-	22,8	20,2
$\sigma/\bar{x}$%	15,3	-	-	102,7	-	-	-	-	-	3,3	-	34,5	5,3

APPENDIX III (Continued)

Sample No.	Ba	Ce	Co	La	Nb	Rb	Sc	Sn	Sr	Ti	Y	Zn	Zr
(d) Feldspar Porphyry at Station K14													
K14	1000	440	2	200	20	213	2	11	27	-	173	90	394
K14.1	787	284	4	85	22	221	0	8	20	1353	82	130	370
K14.2	992	289	2	91	23	210	0	8	32	1287	92	142	418
K14.3	914	526	3	210	22	205	0	10	23	1200	118	90	396
K14.4	1286	420	2	162	25	234	2	6	34	1222	108	91	420
K14.5	866	437	2	192	22	226	0	10	21	1311	120	80	368
K14.6	857	283	2	210	20	227	2	10	28	1283	80	87	400
K14.7	859	215	2	64	22	231	0	10	21	1195	86	100	380
K14.8	747	220	5	61	24	209	2	10	24	1200	80	114	397
K14.9	940	227	3	70	24	263	0	10	19	1199	131	250	375
K14.10	1040	420	4	155	22	278	0	11	18	1314	165	127	366
$\bar{x}$	935	342	2,8	136	22	229	0,7	9,5	24	1256	112	118	389
σ	140,14	103,81	1,03	59,55	1,49	21,86	0,96	1,43	5,08	56,5	31,67	45,99	18,25
$\sigma/_{\bar{x}}\%$	14,99	30,35	36,52	43,79	6,77	9,55	131,51	15,12	21,16	4,5	28,28	38,97	4,69
(e) Aplitic Granite at Station E4													
E4	122	258	2	63	27	267	1	3	14	-	127	115	311
E4.1	168	281	0	75	32	263	0	7	10	951	120	125	299
E4.2	143	256	1	73	31	300	1	6	16	927	141	102	344
E4.3	160	239	3	67	25	282	1	6	11	1007	137	107	301
E4.4	123	301	2	94	32	294	1	7	11	932	159	120	332
E4.5	106	282	1	92	34	280	0	6	13	857	132	104	322
E4.6	148	301	2	97	34	273	1	5	13	894	118	113	353
E4.7	125	268	1	80	30	276	1	6	15	885	117	94	328
E4.8	125	260	0	75	29	284	1	4	13	880	120	120	304
E4.9	149	260	1	82	30	264	0	4	11	979	116	90	305
E4.10	145	286	3	82	31	273	0	2	13	940	121	95	330
$\bar{x}$	138	272	1,5	80	30	278	0,6	5	13	925	128	108	321
σ	17,89	18,84	0,99	10,42	2,60	11,25	0,48	1,57	1,77	44,5	12,69	11,25	17,41
$\sigma/_{\bar{x}}\%$	12,96	6,93	66,00	13,03	8,67	4,05	75,00	30,78	13,62	4,8	9,91	10,42	5,42
(f) Bobbejaankop Granite at Station J10A													
J10A	137	241	2	82	20	402	6	13	5	-	146	53	272
J10A.1	7	336	3	124	59	400	2	24	6	513	126	35	235
J10A.2	63	300	4	97	68	417	1	24	5	566	167	41	263
J10A.3	100	352	3	126	71	460	4	10	6	613	197	50	248
J10A.4	108	262	2	92	45	456	2	9	7	608	162	31	212
J10A.5	84	227	1	74	51	420	0	12	7	548	116	34	250
J10A.6	98	225	2	75	42	441	1	8	7	493	150	31	250
J10A.7	88	202	3	64	54	425	1	10	6	593	161	32	240
J10A.8	111	360	1	130	53	425	3	15	6	619	192	46	261
J10A.9	140	273	2	89	50	460	0	17	8	582	174	44	237
J10A.10	95	248	2	78	46	416	0	10	6	543	176	38	245
$\bar{x}$	94	275	2,3	94	51	429	1,8	13,8	6,3	568	161	40	247
σ	34,6	51,95	0,86	21,99	13,0	20,86	1,8	5,43	0,86	40,9	23,90	7,45	15,43
$\sigma/_{\bar{x}}\%$	36,81	18,89	37,86	23,39	25,49	4,86	100,0	39,35	13,72	7,2	14,84	18,63	6,25

APPENDIX III (Continued)

Sample No.	Ba	Ce	Co	La	Nb	Rb	Sc	Sn	Sr	Ti	Y	Zn	Zr
(g) Bobbejaankop Granite (Lease Microgranite) at Station H5													
H5	273	39	0	3	125	430	3	776	13	-	91	23	306
H5.1	167	260	0	109	110	354	5	63	5	-	150	12	288
H5.2	267	203	0	86	119	321	3	98	12	-	145	19	297
H5.3	250	115	0	38	119	331	0	13	10	-	142	30	291
H5.4	255	169	0	59	121	388	4	21	7	-	100	45	261
H5.5	270	149	1	56	121	330	3	34	12	-	193	28	311
H5.6	230	155	0	70	115	332	1	42	12	-	214	25	292
H5.7	235	222	0	76	121	381	0	1123	9	-	161	17	309
H5.8	209	94	0	29	77	281	0	23	11	-	123	28	314
H5.9	196	442	0	171	80	363	0	31	11	-	131	21	314
$\bar{x}$	235	185	0,10	70	111	298	1,9	222	10	-	145	25	298
σ	33,41	105,03	0,37	44,19	16,61	15,56	1,81	355,13	2,40	-	36,02	8,55	15,56
$\sigma/\bar{x}\%$	14,22	56,77	370,0	63,13	14,96	5,22	95,26	159,9	24,00	-	28,84	34,48	5,22
(h) Groenfontein Granophyre at Station F6													
F6.1	805	-	-	88	-	-	-	-	-	1251	-	123	408
F6.2	778	-	-	114	-	-	-	-	-	1245	-	99	426
F6.3	778	-	-	105	-	-	-	-	-	1187	-	110	396
F6.4	781	-	-	93	-	-	-	-	-	1223	-	124	385
F6.5	782	-	-	114	-	-	-	-	-	1290	-	102	447
F6.6	822	-	-	94	-	-	-	-	-	1216	-	183	413
F6.7	852	-	-	101	-	-	-	-	-	1315	-	156	415
F6.8	847	-	-	92	-	-	-	-	-	1206	-	211	413
F6.9	803	-	-	93	-	-	-	-	-	1281	-	164	427
F6.10	806	-	-	104	-	-	-	-	-	1249	-	166	430
$\bar{x}$	805	-	-	100	-	-	-	-	-	1246	-	144	416
σ	26,13	-	-	8,81	-	-	-	-	-	38,03	-	35,81	16,82
$\sigma/\bar{x}\%$	3,2	-	-	8,81	-	-	-	-	-	3,05	-	24,86	4,04
(i) Welgevonden Granophyre at Station K11													
K11.1	919	-	-	137	-	-	-	-	-	1164	-	105	408
K11.2	898	-	-	124	-	-	-	-	-	1136	-	100	426
K11.3	917	-	-	81	-	-	-	-	-	1272	-	131	396
K11.4	925	-	-	134	-	-	-	-	-	1125	-	89	385
K11.5	877	-	-	99	-	-	-	-	-	1131	-	104	447
K11.6	861	-	-	129	-	-	-	-	-	1218	-	107	413
K11.7	852	-	-	114	-	-	-	-	-	1113	-	71	415
K11.8	898	-	-	120	-	-	-	-	-	1184	-	84	413
K11.9	890	-	-	116	-	-	-	-	-	1222	-	91	427
K11.10	879	-	-	126	-	-	-	-	-	1216	-	90	430
$\bar{x}$	892	-	-	118	-	-	-	-	-	1178	-	97	416
σ	23,39	-	-	16,10	-	-	-	-	-	50,05	-	15,40	16,80
$\sigma/\bar{x}\%$	2,62	-	-	13,64	-	-	-	-	-	4,24	-	15,88	4,02

APPENDIX III (Continued)

Sample No.	Ba	Ce	Co	La	Nb	Rb	Sc	Sn	Sr	Ti	Y	Zn	Zr
(j) Felsite at Station J17													
J17	1148	227	1	61	16	148	7	4	94	-	55	126	416
J17.1	1160	228	8	68	15	160	9	1	102	2453	58	110	435
J17.2	1026	231	8	62	17	176	8	4	80	2482	60	104	414
J17.3	1014	214	4	62	17	166	4	3	96	2468	60	108	397
J17.4	1093	225	12	64	15	177	6	4	100	2360	62	99	429
J17.5	1141	251	12	73	16	207	10	5	97	2531	61	130	419
J17.6	1026	224	11	62	16	163	7	3	120	2404	62	88	414
J17.7	1002	242	9	73	18	165	9	4	96	2598	65	130	447
J17.8	1072	230	10	63	18	158	2	3	118	2405	65	118	431
J17.9	1088	237	8	64	18	170	8	3	121	2365	65	114	445
J17.10	1216	228	11	62	18	169	9	6	128	2310	62	100	420
$\bar{x}$	1090	231	8,5	65	17	169	7	3,6	105	2438	61	112	424
σ	66,60	9,37	3,26	4,21	1,14	14,34	2,29	1,23	14,09	82,07	2,96	12,99	14,13
$\sigma/\bar{x}\%$	6,11	4,06	38,13	6,48	6,71	8,49	31,81	33,79	13,42	3,4	4,85	11,60	3,33

Analysts : Samples about Stations C6, K14, E4, J10A, H5 and J17 analyzed by Dr. G. Hornung, Leeds University, with exception of all Ti determinations which were made by General Superintendence Company (S.A.) (Pty.) Ltd. Samples about all other stations by General Superintendence Company (S.A.) (Pty.) Ltd.

* *

APPENDIX IV

Details of Additional Analytical Data

Sample Station	Ba	Ce	Co	La	Nb	Ni	Rb	Sc	Sn	Sr	Y	Zn	Zr
(a) Coarse-Grained Granites													
C3	761	309	2	97	22	0	186	0	5	40	134	135	350
L7	790	222	4	69	24	0	243	2	10	27	78	62	391
O2	1170	277	5	95	25	2	236	0	7	62	82	72	472
S3	781	281	1	73	19	0	224	2	7	25	86	91	323
(b) Granophyric Granite													
E10	742	262	3	80	20	1	241	2	20	10	73	119	356
G8	869	326	2	102	24	0	255	0	11	14	76	106	373
L10	705	219	2	66	23	0	188	3	10	27	86	64	395
Q5	921	326	2	102	29	2	294	1	13	25	101	138	435
(c) Sterk River Granophyre													
A9	654	333	0	111	17	0	237	0	7	18	98	145	301
(d) Groenfontein Granophyre													
F7	890	334	3	118	20	1	230	2	12	16	81	104	360
(e) Bobbejaankop Granite													
D5	67	342	3	97	52	2	427	2	494	4	187	68	240
F5	82	179	3	53	113	0	441	4	8	5	137	20	312
M6	512	299	2	141	80	2	513	0	19	5	102	14	349
(f) Aplitic Granites													
A3	780	165	3	29	23	1	185	2	10	31	101	113	340
I4	1286	182	4	49	14	0	193	2	3	58	44	89	323
K5	59	182	2	44	48	0	410	2	8	8	205	34	271
(g) Blinkwater Granophyre													
J3	1250	212	3	69	23	0	190	1	5	66	86	106	450
(h) Feldspar Porphyry													
M13	965	287	3	88	28	3	260	0	11	21	84	64	443
(i) Felsite													
H11	1085	264	8	82	18	0	214	6	1	45	68	234	442
L18	756	241	1	79	20	0	363	5	32	27	50	100	446
S9	1080	210	6	54	17	0	187	6	1	101	53	81	438

All analyses by Dr. G. Hornung, Leeds University.

* *

APPENDIX V

Provisional Fluorine Determinations

	Sample Station	Fluorine (ppm)	Calcium (ppm)*
(a)	*Coarse-Grained Grey Granite*		
	A5	3300	1936
	H2	1760	5050
	J5	2390	2994
	M2A	2660	4774
	R4	2300	1731
	T2	2330	5973
(b)	*Granophyric Granite*		
	C7	2400	2685
	D7	750	5655
	E11	3680	-497
	G9	6580	1423
	I13	5490	3341
(c)	*Aplitic Granite*		
	O2A	2840	1608
(d)	*Welgevonden Granophyre*		
	N12	2200	5037
(e)	*Feldspar Porphyry*		
	F7	2780	1229
(f)	*Bobbejaankop Granite*		
	D4	2560	583
	D5 (Lease)	9750	2560
	E8	4430	149
	G5 (Lease)	8240	17258
	I11 (Lease)	2200	-328
	J10A	5820	1608

* Ca available after provision of Ca to F to form fluorite. The negative values arise from possible overestimate for F.

All analyses by Dr. D.M. Bibby, Nuclear Physics Research Unit, University of the Witwatersrand.

] [